Lancaster University

Geochemical Signals of Volcanic Unrest at the Virkisjökull Glacier Iceland

Alistair Robert McDonald

MSc Environmental Science (By Research)

Supervisors

Dr Peter Wynn

Dr Hugh Tuffen

Dr Mike James

September 2015

Declaration

“Submitted as an integral part for the degree of MSc (By Research) at Lancaster Environmental Centre, Lancaster University, September, 2015. I certify that the following work is my own and that significant academic debts and borrowings have been properly acknowledged and referenced.”

Signed:_____ Date:_____

Name:_____

Abstract

Understanding the relationship between areas of active geothermal or volcanic activity and the glaciers that overlie them remains a significant knowledge gap in the earth sciences. Using Virkisjökull glacier in south east Iceland as a case study, a geochemical approach is taken to this problem by utilising stable isotopes of water and sulphate alongside major chemistry and the noble gases. Analysis of oxygen deuterium data collected over four years revealed a hydrological system dominated by glacial meltwater and aquifer fed groundwater that varied both seasonally and spatially. Sulphate isotopes suggested that water chemistry is the result of a ternary mixing of three endmembers: precipitation, ice melt and bedrock weathering whose relative inputs varied with season. This seasonality demonstrated that prevailing weather conditions have a significant impact on the chemistry of the meltwaters. Oxygen sulphate isotopes were used as an indicator of redox status in the subglacial hydrological regime. This pointed towards a year round fully oxidized channel system operating at the glacier bed, which is in contrast to the seasonality observed at other glaciers in Iceland and around the world. Finally, noble gases were used to identify the relative contribution of basal ice melt at various sites in the sandur. Taken together these chemical indicators hint at a weak to non-existent geothermal regime operating under the Virkisjökull glacier.

Acknowledgments

First and foremost, I would like to thank my principal supervisor Peter Wynn for making this project an intellectually stimulating experience and giving me free reign to explore new ideas and hypothesises. A chance to discuss the mechanical intricacies of 1960 Fergie tractors also proved a welcome distraction. My thanks are also extended to Hugh Tuffen and Mike James for giving their insight into the volcanology side of the project. Also, to Greg Holland whose input on the noble gas side of the project proved invaluable.

I am extremely grateful to BGS for allowing us access to the chemical data that they have collected during the Virkisjökull monitoring project. In particular, my thanks are extended to Jez Everest for organising the field campaign and for his surprising excellent culinary skills and to Alan MacDonald for his input into the hydrogeology side of the project. Andrew Black from Dundee University is also thanked for supplying us with stream data from the Virkisá River.

My thanks are also extended to Montserrat Auladell-Mestre and Dave Hughes for their assistance in the labs during data analysis.

I would like to thank everyone in the office who has welcomed me over the past year but in particular to Laura Deeprose for her infectious enthusiasm for science and for her excellent home baking that frequently appeared on my desk.

I would like to thank my friends Andy and Elspeth and their family for providing me with somewhere to stay during the latter part of this thesis and for the immense hospitality and kindness they have shown me over the past year. Finally to my parents, for their never-ending love and support. Thank you all.

Table of Contents

List of Figures

List of Tables

Chapter 1: Introduction and Literature Review

1.1 Introduction

Glaciers and ice caps currently cover 10% of the Earth's land surface (Knight, 2013) and have been widely shown to be in rapid retreat since the beginning of the 20th century (Dyurgerov and Meier, 2000). This relationship between atmospheric conditions and cryospheric response has received a great deal of attention in the scientific literature (Clark et al., 2009; Rignot et al., 2008; Serreze et al., 2000). However, more recent work has demonstrated that the interaction between the cryosphere and volcanically active portions of the lithosphere is more closely related than originally thought. Work by Maclennan et al. (2002) on Icelandic glaciers has demonstrated that decreasing isostatic pressure from the melting of glaciers and ice caps at the end of the Pleistocene resulted in up to a hundred fold increase in volcanic activity. Devastating glacial outburst floods (jökulhlaups) occur in Iceland as a result of sub-glacial eruptions and have been known to cause severe damage to infrastructure and fatalities. Moreover, subglacial volcanic activity has been demonstrated to be occurring underneath the West Antarctic ice sheet (Blankenship et al., 1993; Corr and Vaughan, 2008) where any form of positive feedback between decreasing ice coverage and increasing volcanic activity has the potential to have global consequences.

Identifying sub-glacial geothermal or volcanic activity has proved problematic with most studies focusing on either airborne geophysics (Corr and Vaughan, 2008) or a mixture of chemical signals (Kristmannsdóttir et al., 2002b). However, recent work by Wynn et al. (2015) has demonstrated the potential of sulphate isotope analysis to determine the presence of seasonal geothermal activity underneath the Mýrdalsjökull ice cap in Iceland. Coupled with other chemical signatures, this has the potential to be a powerful new tool in analysing subglacial geothermal fields and eruptions. By utilising Virkisjökull glacier in south-east

Iceland, which has been monitored for over four years by the British Geological Survey (BGS), this study will attempt to understand the relationship between the ice cap, the hydrological system, and any subglacial volcanic activity. Specifically, sulphate isotopes will be analysed alongside major ion chemistry and the noble gases in order to relate the chemistry of the glacial meltwater to subglacial processes.

1.2 Statement of Objectives

1. Utilising water isotopes and major ion chemistry, a conceptual hydrological model for the Virkisjökull catchment will be produced.

2. Sulphate isotopes from sites across the Virkisjökull region will be used to identify any signal of subglacial geothermal activity (Wynn et al., 2015).

3. Noble gas concentrations (Ne through to Xe) will be analysed to understand the variable contribution of basal and surface melt throughout the year. Using noble gases to understand cryospheric processes is a relatively new and novel technique but has produced a variety of exciting and promising results in recent years (Ritz et al., 2011; Winckler and Severinghaus, 2013).

1.3 Geological History of Iceland

Iceland represents "one of the most dramatic 'geowonderlands' on Earth" (Thordarson and Hoskuldsson, 2002) being one of the few locations where a mid-ocean ridge is exposed above sea level. In addition, Iceland is the only remaining active portion of the North Atlantic Igneous Province which includes Tertiary volcanics from the Isle of Skye in Scotland to South East Greenland (Thompson, 1982; Thordarson and Hoskuldsson, 2002). Iceland formed during the mid-Tertiary as a mantle plume migrated underneath the active mid-ocean ridge (Lawver and Muller, 1994). The presence of a mantle plume is adhered to due to seismic (Wolfe et al., 1997) and numerical modelling investigations (Ito et al., 1999) with some suggesting its origin lies at the core-mantle boundary (Helmberger et al., 1998). Lawver and Muller (1994) suggest that the plume began underneath Greenland at 70Ma and has been tracking eastwards since then to its present location underneath the Vatnajokull ice cap. However, the plume hypothesis is by no means universally accepted (Foulger, 2010) but remains the most widely used model to explain Iceland's unique situation.

Iceland sits at the junction between the Reykjanes Ridge in the south and the Kolbeinsey Ridge in the north (Thordarson and Hoskuldsson, 2002) which branch out in a series of minor faults across the island that are characterized by active volcanism and earthquakes. The main volcanic zones are termed the Western, Eastern and Northern volcanic zones. The youngest geology is found towards the centre of the island and the oldest towards the western and eastern coasts, reflecting their common origin from a diverging mid-ocean ridge. The oldest surface rocks dated in Iceland are found in the north west and have been dated between 14-16Ma (McDougall et al., 1984; Moorbath et al., 1968). It is suggested therefore, that this is the time when Iceland first rose above sea level. However, this has been disputed by Foulger (2006) who stipulates that the distance between the oldest crust on either side of Iceland suggests a much earlier origin of 26–37 Ma.

The geology of Iceland is simplified into three main formations (Figure 1): The Tertiary basalt formation (16-3.3Ma); the Plio-Pleistocene formation (3.3-0.7Ma) and the Upper Pleistocene formation (<0.7Ma) (Thordarson and Hoskuldsson, 2002). The majority of rocks on Iceland are basic to acidic igneous rocks with sedimentary rocks only comprising 2% of the Tertiary and up to 50% of Quaternary deposits (Einarsson and Albertsson, 1988).

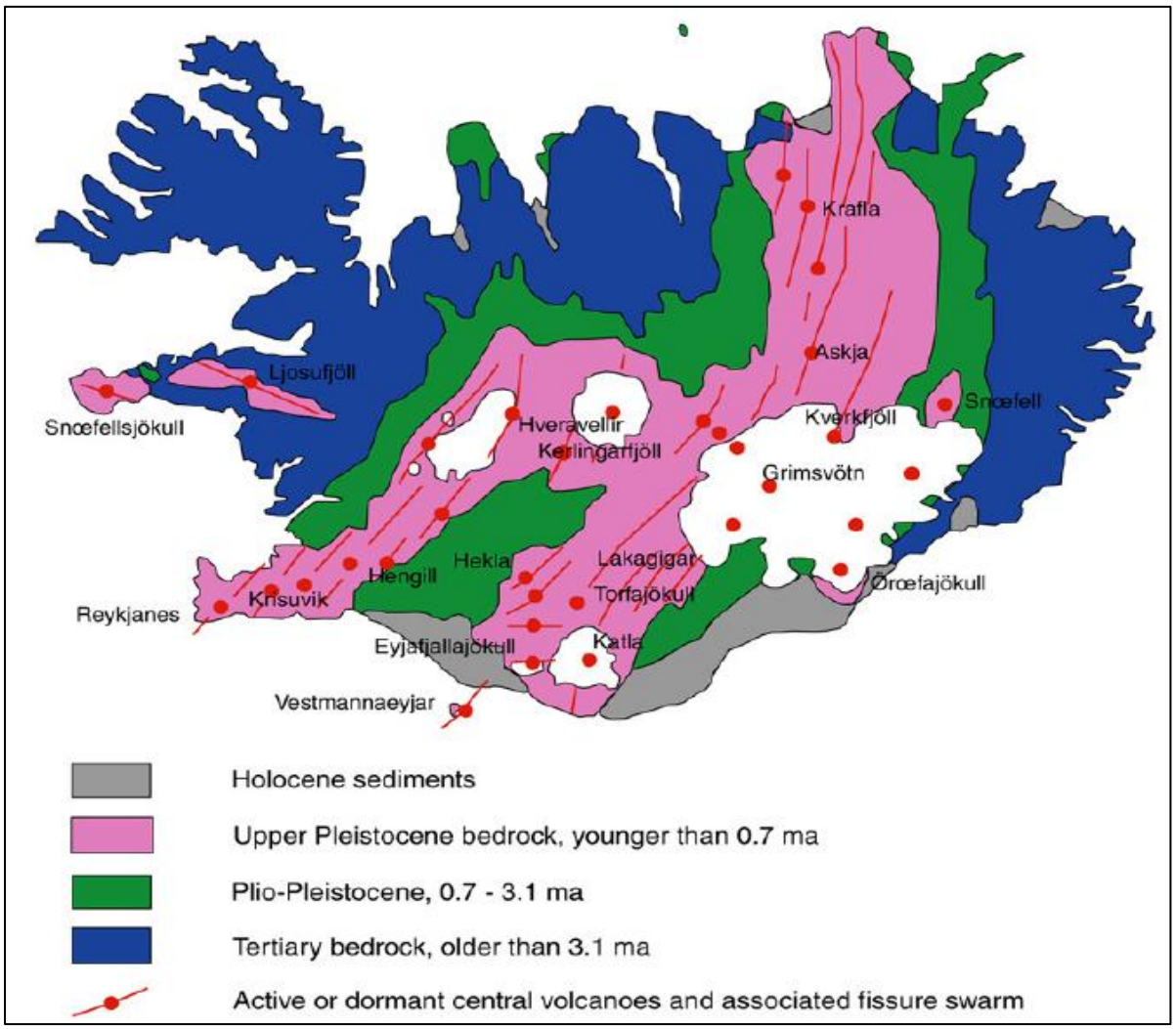

Figure 1: Simplified geological map of Iceland. Adapted from Jóhannesson and Sæmundsson (1998).

1.3.1 Glacial History

The glacial history of Iceland since the Pleistocene has proved difficult to reconstruct. Gudmundsson (1997) gives an overview of the glacial history of Iceland showing how our understanding has evolved from a relatively simple model to one of significant complexity. The first model of deglaciation was set up by Einarsson (1961) and termed the Single Advance Deglaciation, or SAD model. This was based on the assumption of age correlation between moraines on opposite sides of the island. This assumption proved incorrect and the DAD model or Double Advance Deglaciation was introduced by Einarsson (1967). Further work by Ingólfsson (1985) revealed that multiple advances have taken place bringing about the now widely accepted MAD model (Multiple Advance Deglaciation). Exactly how volatile the glaciers on Iceland have been is still unclear but Einarsson and Albertsson (1988) suggest that at least 4 glaciations have occurred in the last 0.7Ma with 15-23 glaciations in the last 3Ma. During the Last Glacial Maximum the ice sheet extended out to the continental shelf before changes in ocean currents forced its break up around 15ka (Geirsdóttir et al., 2009).

1.3.1.1 Holocene Glaciation

The glacial history of the Holocene has been reconstructed through pollen analysis; sediment records; carbon dating and historical accounts (Geirsdóttir et al., 2009). By 10.3ka the Icelandic ice sheet was undergoing rapid retreat. Associated with this retreat were a series of jökulhlaups (outburst floods) that resulted in the erosion of many glacial deposits (Geirsdóttir et al., 1997). In addition, evidence of extensive birch forests become apparent around 10ka reinforcing the case for a warming climate during the Preboreal and Boreal stages of the Holocene (Geirsdóttir et al., 2009). The Holocene thermal maximum was reached around 8ka with temperatures around 3°C higher than present and largely ice free conditions across Iceland (Geirsdóttir et al., 2009). This warm period finished around 6ka with glacial activity becoming more intense around 3-2.5ka. The Medieval warm period did not appear to accelerate deglaciation in Iceland. On the contrary, it appears that minor glacial advances took place during this time (Gudmundsson, 1997). However, the "Little Ice Age" (AD 1250-1900) caused a significant increase in glaciation associated with temperatures 1-2°C less than present resulting in the most expansive glaciation during the Holocene on Iceland (Bradwell, 2004).

Most present day Icelandic glaciers have been in retreat since the end of the Little Ice Age (1780-1900) (Bradwell et al., 2013) with accelerated retreat in the past two decades. Icelandic glaciers are particularly sensitive to small perturbations in temperature or precipitation given their large altitude range and low accumulation to ablation ratio (MacDonald et al., 2012). It appears therefore, that despite the vast number of deglaciations occurring in Iceland over the past 3Ma, the current deglaciation is one of the most rapid to date. In addition, recent research has shown that a positive feedback may exist between glacial retreat and volcanic activity (Tuffen, 2010).

1.3.2 Sub-Glacial Eruptions

The volcanoes on Iceland generally occupy topographically higher areas and are therefore overlain by glaciers. Interaction between the volcanoes and cryosphere is an inevitable and well-documented phenomenon in Iceland. The large thermal gradient generated between extrusive igneous products and the glacier bed results in the formation of distinctive rock types and features. The rapid cooling of a rising body of magma results in the formation of hydroclastite (Gudmundsson et al., 1997) which can contain distinctive features associated with rapid cooling such as pillow basalts and sideromelane tuff (Allen, 1980). On a regional scale, sub-glacial eruptions are credited with forming the iconic table mountains (or tuyas) that are found across the island (Bourgeois et al., 1998). They are the result of continual horizontal rather than vertical propagation of magma along the glacier base (Wilson and Head, 2002) resulting in the accumulation of flat lying layers of lava. In addition, thicker ice sheets are capable of containing a volcanic eruption and thus decreasing the potential hazard. However, (Tuffen, 2010) shows that the current thinning of the Icelandic ice sheets can result in dramatic pressure release and therefore increase the explosivity of an eruption.

The effect ice sheets have on the frequency and intensity of volcanic activity has only recently become clear (Tuffen, 2010). The rapid retreat of ice sheets as is being recorded in the present day leads to significant lithospheric unloading and subsequent isostatic rebound. At the end of the last glacial maximum, volcanic activity increased globally by a factor of two to six (Huybers and Langmuir, 2009) and in Iceland somewhere between 30 to 50 (Tuffen, 2010). The exact mechanism by which this occurs is still under debate (Tuffen, 2010) but it is believed that isostatic rebound causes decompression of the asthenospheric mantle, resulting in increased melt (Hardarson and Fitton, 1991). Maclennan et al. (2002) have shown the chemistry of lava flows post glaciation to be consistent with increased melt generation associated with asthenospheric decompression. Furthermore, it is clear that

increased volcanism is notable almost immediately after deglaciation (Maclennan et al., 2002). However, Tuffen (2010) concludes that further investigation is needed to understand the response times of volcanoes to glacial unloading and the associated hazard that it will pose in the near future.

1.4 Geochemistry

1.4.1 Isotopes in the Earth Sciences

Isotopes are defined as elements with different atomic masses and are employed ubiquitously in the Earth sciences. Their usefulness is derived from the way they fractionate, which is related to physical processes. The two main methods for isotopic fractionation are kinetic or equilibrium which are outlined below.

1.4.1.1 Kinetic Fractionation

Kinetic fractionation results from isotopes having the same kinetic energy but different masses and therefore velocities. This results in the lighter isotopes diffusing and evaporating more rapidly than the heavier isotope. This is clearly demonstrated in Craig's meteoric water line. Craig (1961) showed that the deuterium and oxygen isotopes in meteoric waters tend to be lightest at the poles and heaviest as the equator. It is argued that this can be explained by the heavier isotopes "raining out" over the lower latitudes and thus the isotopic composition of polar waters is relatively enriched in the lighter isotopes.

1.4.1.2 Equilibrium Fractionation

Equilibrium fractionation tends to be most prevalent at lower temperatures and is the result of the heavy isotopes going preferentially to the element with the strongest chemical bond (Clark and Fritz, 1997). Equilibrium fractionation can be explained by considering quantum mechanical effects and their relationship to an atom's mass. Isotopes that have been fractionated in this way can be used as an indicator of temperature and pressure as the process of equilibrium fractionation is governed by the laws of thermodynamics.

1.4.1.3 Oxygen deuterium isotopes

Oxygen-deuterium isotopes ($^{18}O/^{16}O$ and $^{2}H/^{1}H$) of waters, provide insight into provenance. This is most commonly done by comparing results to the global or local meteoric water line.

1.4.1.3.1 Meteoric Water Line

The meteoric water line was first described by Craig (1961) and represents a predicted relationship between oxygen and hydrogen isotope values in precipitation (Figure 2). Craig (1961) defined the "global meteoric water line" by the equation:

$$\delta D = 8\delta^{18}O + 10 \qquad \textit{Equation 1}$$

This describes linear isotopic variation with respect to latitude across the globe. This is termed the "latitude effect" whereby heavier isotopic values are observed at the equator and the lightest isotopic values are found at the poles. This linear relationship arises from a kinetic fractionation effect whereby the heaviest isotopes are "rained out" first leaving water vapour that is preferentially enriched in the lighter isotopes (Clark and Fritz, 1997).

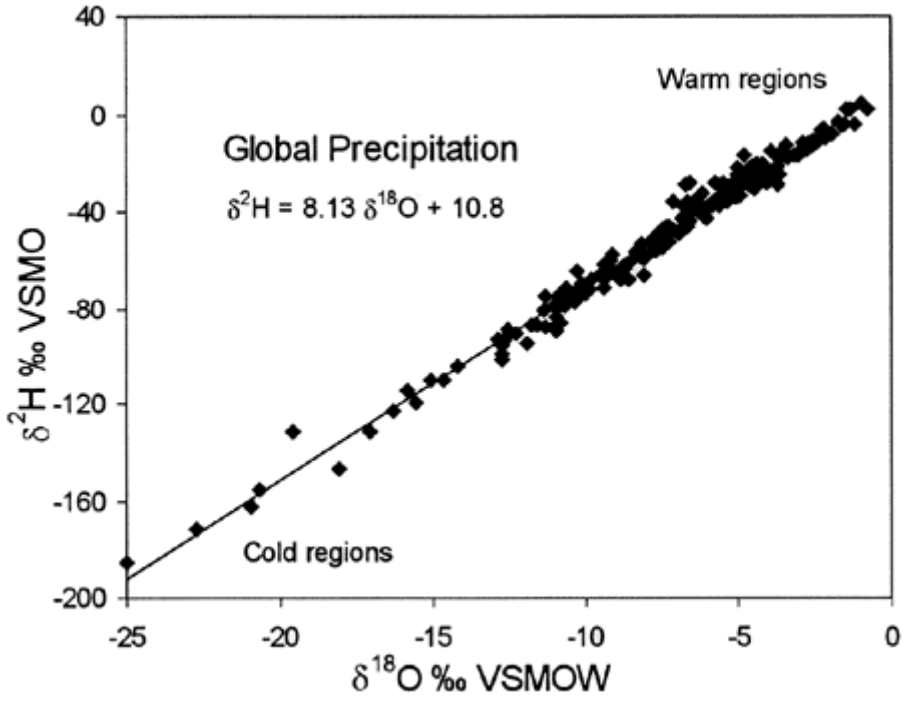

Figure 2: Global Meteoric Water line (Clark and Fritz, 1997)

In addition, to the "latitude effect" identified by Craig (1961) three other factors are known to cause kinetic fractionation in water isotopes: The continental effect, altitude effect and amount effect (Clark and Fritz, 1997). The continental effect was first described by Dansgaard (1964) and is the result of a similar kinetic fractionation that brings about the latitude effect. Precipitation of marine origin will become preferentially enriched in the lighter isotopes towards the continental interior. Moreover, a similar process is responsible for the altitude effect whereby heavier isotopes are rained out at lower altitudes (Dansgaard, 1964). This latter fractionation effect has important implications for glaciology as it allows the altitude of meltwater to be determined (e.g. Wynn et al. 2015). Finally, the "amount affect" refers to the process observed where heavy rainfall decreases the δD and $\delta^{18}O$ values of the precipitation (Clark and Fritz, 1997). This is best observed in arid regions.

1.4.1.3.2 Deuterium Excess

It became apparent soon after Craig (1961) published his landmark paper that local derivation occurred from the global meteoric water line. This led Dansgaard (1964) to introduce a new parameter termed "deuterium excess" which relates to the physical conditions present at the oceanic source (Froehlich et al., 2002). Deuterium excess is defined by the equation:

$$d = \delta D - 8 * \delta^{18}O \qquad \textit{Equation 2}$$

Deuterium excess is directly related to humidity at precipitation source (Clark and Fritz, 1997) and has been successfully employed by Petit et al. (1991) to determine the origin of Antarctic snows to be in tropical waters rather than local.

1.4.2 Sulphur isotopes

Sulphur is composed of four stable isotopes with masses of 32, 33, 34 and 36 (Seal, 2006). Of these ^{32}S and ^{34}S have relative abundances of 95.02% and 4.21% respectively and therefore are the most widely employed. Sulphur isotopes have been successfully utilized across the geosciences to understand a variety of processes including pyrite provenance (Muntean et al., 2011), snowball earth (Bao et al., 2009) and more recently as a potential indicator of subglacial geothermal activity (Wynn et al., 2015).

Sulphur is ubiquitous in geothermal and volcanic systems (Mandeville, 2010). It is most commonly present as either sulphate (SO_4) or hydrogen sulphide (H_2S) (Kristmannsdóttir et al., 2000). An Icelandic glacier will therefore have three major sulphur inputs: Atmospheric sulphur, bedrock sulphur and geothermal sulphur (Wynn et al., 2015). Atmospheric sulphur is a combination of marine derived sulphate and anthropogenic emissions with minor inputs of volcanic aerosols and continental biogenic emissions. Given Iceland's location the input from volcanic aerosols into the atmospheric inventory is likely to be elevated. The isotopic composition of marine derived sulphur is relatively fixed at +21‰ (Rees et al., 1978). Volcanic aerosols tend to have a sulphur isotope ratio of around 0‰ (Nielsen et al., 1991). Finally, anthropogenic emissions have a variable sulphur isotope composition of between -5 to 10‰ (Clark and Fritz, 1997). The effect of anthropogenic sulphur varies depending on location. In central Europe or North America anthropogenic sulphur can have a very significant effect on the atmospheric isotope composition of sulphur. However, in more isolated areas, such as Iceland, its effect is reduced.

The isotopic composition of Icelandic bedrock was measured by Torssander (1989) who showed that the sulphur isotope ratio is related to the silica content of the bedrock. Basalts

for example tend to have a sulphur isotope composition of 0‰ whereas geology of more intermediate or felsic composition can have a sulphur isotope ratio of up to +4.2‰.

Geothermal sulphur isotope ratios are difficult to constrain given the variety of geothermal gases that can be emitted. For example, hydrogen sulphide has a sulphur isotope composition of +5.8 to +6.2‰ whereas other volcanic gases and magmatic sulphide has a composition of 0‰.

1.4.2.1 Sulphate in Glacial Catchments

Sulphate is most widely employed in glacial catchments as an indicator of redox status at the glacier bed or as a tracer of the various chemical inputs into the catchment (Robinson et al., 2009b; Wynn et al., 2015). Tranter et al. (2002b) successfully used sulphate oxygen isotopes to demonstrate the seasonal variation in redox conditions at the bed of the Haut Glacier d'Arolla in Switzerland. This was furthered by Wynn et al. (2006) who demonstrated this seasonality to also occur in polar glaciers and that the "switch" from anoxic to oxic conditions was very rapid. Finally, Wynn et al. (2015) successfully used sulphate oxygen isotopes to resolve a signal of geothermal interaction at the base of Sólheimajökull glacier in Iceland. Robinson et al. (2009b) also demonstrated the potential of sulphur isotopes in Iceland as tracers of hydrochemical processes and water origin. This is due to the diagnostic sulphur isotope composition of major hydrological inputs such as marine derived precipitation (+21‰) and bedrock (0‰).

1.4.3 Glacial Chemistry

The chemical signature of glacial meltwater is the product of two sources: The atmosphere and chemical weathering of bedrock (Tranter et al., 1996). In addition, glaciers that reside in tectonically active zones may have a third chemical input from geothermal and volcanic activity (Sigvaldason, 1963). Therefore, the unique chemical signature of glacial meltwater will be a combination of the water source and any chemical weathering of local geology during its transportation to the glacier snout (Tranter et al., 1997). How much chemical weathering occurs in a glaciated basin will depend on four factors suggested by Tranter et al. (1996):

1. The reactive mineralogy
2. Reactive surface area to water ratio
3. Duration of water-rock contact
4. Availability of other chemical species (e.g.O_2, CO_2, H^+)

In addition, Hodson et al. (2000) suggest that a glacier's thermal regime will affect the rate of chemical weathering. Cold based glaciers will have very low rates of chemical denudation whereas polythermal or warm based glaciers will have much higher rates. This reflects an increase in water-rock contact when compared with cold based glaciers. Moreover, chemical weathering in polythermal glaciers may be accelerated by cold ice at the glacier margins preventing the drainage of sub-glacial runoff to the glacier snout and thus prolonging water-rock contact (Hodson et al., 2000). Chemical weathering provides the majority of base cations to glacial meltwater as well as increasing the concentration of dissolved ions such as HCO_3^- and SO_4^{2-}. The atmosphere provides sea salt, carbon dioxide, oxygen, nitrate and sulphate aerosols (Tranter et al., 1996). In addition, recent research has shown that subglacial microbial communities have the ability to influence meltwater chemistry by providing a secondary source of nitrate (Wynn et al., 2007).

Meltwater was initially believed to be composed of two endmembers: subglacial and englacial (Collins, 1977). However, Tranter et al. (1993) introduced the terminology "quick flow" and "delayed flow" to better reflect the residence time of the meltwater within the glacier. Quick flow tends to dominate at periods of highest discharge (in paradox to river systems). This reflects its rapid flow through conduits as opposed to delayed flow which utilises a series of cavity systems along the glacier bed (Tranter et al., 1993). Tranter et al. (1997) went further and subdivided glacial meltwaters from the Haut Glacier d'Arolla in Switzerland into three separate categories (Figure 3).

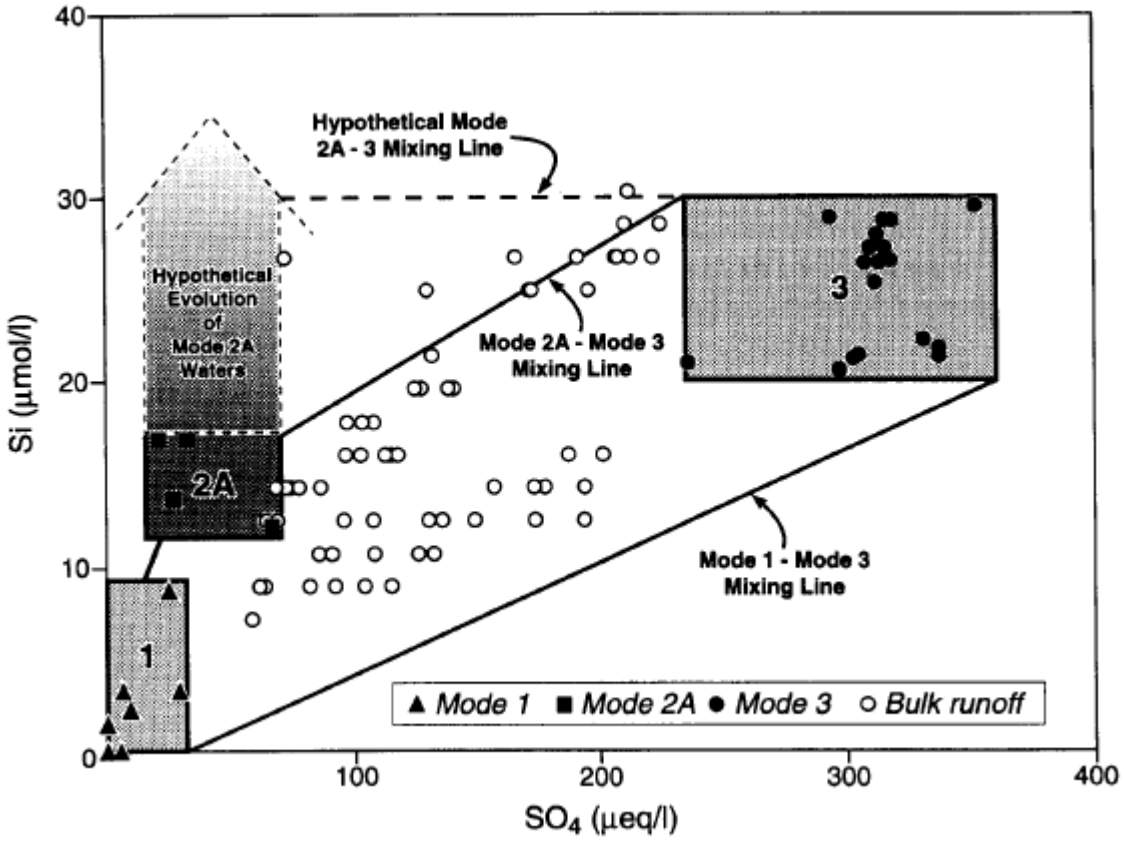

Figure 3: The geochemical relationship between different types of glacial runoff (Tranter et al., 1997)

Mode 1 represents very dilute meltwater that has undergone minimal interaction with surficial geology. Mode 2 waters are very similar to bulk runoff but with smaller concentrations of major ions. Tranter et al. (1997) suggest that this represents subglacial meltwater that exchanges with channel water on a daily basis. Finally, Mode 3 waters are significantly more concentrated in major ions than bulk runoff, particularly with regard to Ca^{2+}, HCO_3^-, SO_4^{2-} and CO_2 reflecting significant interaction with the country rock. This water type is believed to be associated with a flow path through a distributed cavity system at the glacier's base. This confirms the assumption by Tranter et al. (1996) that the flow path of meltwater will affect its chemistry.

1.4.4 Chemical Evolution

To understand how a glacier's chemistry originates requires a series of assumptions to be made (Hodson et al., 2000; Tranter et al., 1993). For example, by assuming that all Cl^- is of marine origin (Hodson et al., 2002; Hodson et al., 2000) this allows the marine component of the major cations to be calculated if the standard marine ratio to chlorine is known. This technique appears to work well in stable cratonic environments where the assumption that all chlorine is marine derived is fairly accurate. However, in regions of active volcanism such as the study area in Iceland, magmatic chlorine will be degassing as a result of active volcanism and therefore any chemical analysis derived from this assumption should be interpreted with a degree of caution.

1.4.4.1 Acquisition of Base Cations

Tranter et al. (1993) conducted one of the first series studies into the chemistry of glacial meltwater by assuming that base cations are acquired by either simple dissolution or acid hydrolysis.

Equation 3: Acid Hydrolysis

$$\underset{\text{Anorthite Feldspar}}{CaAl_2Si_2O_{8(s)}} + 2H^+_{(aq)} \leftrightarrow Ca^{2+}_{(aq)} + \underset{\text{Weathered Feldspar Surface}}{H_2Al_2Si_2O_{8(s)}}$$

Where the aqueous protons are provided by either dissociation of CO_2 or the oxidation of sulphides (Equation 4) (Tranter et al., 1993):

Equation 4: Sulphide Oxidation

$$4FeS_{2(s)} + 15O_{2(aq)} + 14H_2O_{(aq)} \leftrightarrow 16H^+_{(aq)} + 4Fe(OH)_{3(s)} + 8SO_4^{2-}{}_{(aq)}$$

Equation 3 (acid hydrolysis) assumes the breakdown of the feldspar end member anorthite. As anorthite is in solid solution with the potassium endmember albite then it is likely that albite is also undergoing acid hydrolysis and thus providing potassium.

Equation 5: Acid Hydrolysis of Albite

$$\underset{\text{Albite Feldspar}}{KAlSi_3O_{8(s)}} + H^+_{(aq)} \leftrightarrow K^+_{(aq)} + \underset{\text{Weathered Feldspar Surface}}{HAlSi_3O_{8(s)}}$$

Tranter et al. (1997) added to this model by showing that meltwater can acquire major cations and anions by carbonation reactions with glacial floor. This was expanded on by Tranter et al. (2002a) who identified the two main carbonation reactions occurring as carbonation of carbonates (Equation 6) and carbonation of silicates (Equation 7). In addition, Tranter et al. (2002a) show that these reactions are most likely to occur in warm based glaciers with channelized drainage systems allowing free access to atmospheric gases.

Equation 6: Carbonation of Carbonates

$$CaCO_{3(s)} + CO_2 + H_2O \leftrightarrow Ca^{2+}_{(aq)} + 2HCO_3^-$$

Equation 7: Carbonation of Silicates

$$CaAl_2Si_2O_8 + 2CO_2 + 2H_2O \leftrightarrow Ca^{2+}_{(aq)} + 2HCO_3^-{}_{(aq)} + H_2Al_2Si_2O_{8(s)}$$

1.4.4.2 Acquisition of Major Anions

The major anions consist of the four chemical species: Cl^-, NO_3^-, SO_4^{2-} and HCO_3^- with SO_4^{2-} and HCO_3^- being the most abundant. Both chlorine and nitrate are assumed to have only one source with all chlorine originating from sea salt and all nitrate being provided by the atmosphere (Hodson et al., 2002). However, Wynn et al. (2007) demonstrate that nitrate is also produced in the subglacial environment by the microbial assisted oxidation of ammonium and the mineralisation of organic nitrogen. Sulphate has three sources (Hodson et al., 2000): marine, atmospheric and crustal. The marine sulphate component can be calculated based on its ratio to marine chloride. Atmospheric sulphate is then deduced from the difference between snowpack sulphate and the calculated marine sulphate. The remainder is assumed to be crustal (Hodson et al., 2000). The crustal component will vary depending on the local geology but tends to make up the majority of sulphate in glacier meltwater with the snowpack only contributing 1-2% (Tranter et al., 1996). The major crustal source of SO_4^{2-} is from the oxidation of sulphides (Equation 4), also expressed as coupled sulphide oxidation – carbonate dissolution. (Equation 8).

Equation 8: Sulphate oxidation coupled with carbonate dissolution

$$4FeS_{2(s)} + CaCO_{3(s)} + 15O_{2(aq)} + 14H_2O_{(aq)} \leftrightarrow 16Ca^{2+}{}_{(aq)} + 16HCO_3^- + 4Fe(OH)_{3(s)} + 8SO_4^{2-}{}_{(aq)}$$

Hodson et al. (2002) noted that the equivalence ratio of sulphate to bicarbonate should always be 1 according to Equation 8. However, in practice, it is often significantly less, which suggests there must be other sources of bicarbonate. Hodson et al. (2002) suggest that a number of sources contribute to total bicarbonate including: carbonation of carbonates and silicates (Equations 6 and 7); acid neutralisation of snowpack nitrate by carbonates; sulphide

oxidation (Equation 4) and oxidation of organic carbon. Any bicarbonate not accounted for by these processes is assumed to be atmospheric (Hodson et al., 2000). Table 1 summarises the different sources of major anions according to Hodson et al. (2000).

Table 1: The calculations and assumptions behind major anion concentrations. Taken from Hodson et al. (2000)

Solute	Component	Provenance Calculation	Comments & Assumptions
Cl^-	All Cl^- marine	Total Cl^-	No lithogenic Cl^-, no volatilization of snowpack Cl^-
SO_4^{2-}	Sea salt SO_4^{2-}	$^{sea}(SO_4^{2-}/Cl^-)$ x $^{total}Cl^-$	Marine SO_4^{2-}/Cl^- ratio is 0.051
SO_4^{2-}	Aerosol SO_4^{2-}	$^{snowpack}(SO_4^{2-}/Cl^-)$ x $^{total}Cl^-$ ($^{seasalt}SO_4^{2-}$)	Use site specific SO_4^{2-}/Cl^-
SO_4^{2-}	Crustal SO_4^{2-}	$^{total}SO_4^{2-}$ – ($^{seasalt}SO_4^{2-}$ + $^{aerosol}SO_4^{2-}$)	Snowpack SO_4^{2-} not preferentially eluted with respect to Cl^- no volatilization of snowpack SO_4^{2-}
NO_3^-	Aerosol NO_3^-	$^{total}NO_3^-$	No crustal NO_3^- sources, no volatilization of snowpack NO_3^-
HCO_3^-	Aerosol hydrolysis HCO_3^-	$^{total}NO_3^-$ + 2($^{aerosol}SO_4^{2-}$)	Carbonates neutralise acidic snow aerosols
HCO_3^-	SO – CD $HCO3^-$	2($^{crustal}SO_4^{2-}$)	Oxidation of crustal sulphide is by carbonate dissolution
HCO_3^-	Silicate HCO_3^-	1.58[Si] or 3.4[$*Na^+$ + $*K^+$] in equivalent concentrations	
HCO_3^-	Carbonate Carbonation HCO_3^-	0.5[$^{total}HCO_3^-$ – ($^{aerosol}{}_{hydrolysis}HCO_3^-$ + $^{SO-CD}HCO_3^-$ + $^{sil}HCO_3^-$)]	Half from atmosphere half from carbonates
HCO_3^-	Atmospheric HCO_3^-	$^{silicate}HCO_3^-$ + $^{carbonate}{}_{carbonation}HCO_3^-$	Acid aerosols neutralised by carbonates only; No SO_4^{2-} from evaporates all Si, $*Na^+$ and $*K^+$ from silicate carbonation, no subglacial Si precipitation, no HCO_3^- due to oxidation of organic carbon or simple carbonate hydrolysis

SO: Sulphide Oxidation CD: Carbonate Dissolution

1.4.5 Chemical Indicators of Subglacial Geothermal Activity

Initial studies into glacial chemistry focused on Arctic and Alpine glaciers in stable tectonic environments (Hodson et al., 2002; Tranter et al., 1997a). Recently however, attention has turned to glaciers in tectonically active regions such as Iceland where a geothermal or volcanic chemical input must be considered (Galeczka et al., 2014). The danger posed by jökulhlaups resulting from subglacial geothermal activity lead Elefsen et al. (2002) to suggest for permanent monitoring stations to be set up to measure electrical conductivity and discharge. It is argued that a coupled increase in electrical conductivity and discharge is indicative of subglacial geothermal activity melting the glacier rather than increased precipitation or melting of glacier ice; which would lower conductivity. This is expanded on by Kristmannsdóttir et al. (2002a) who demonstrated that conductivity during jökulhlaups can be more than double the Icelandic average of 20-300μScm^{-1}. During jökulhlaups Kristmannsdóttir et al. (2002a) note a particular increase in hydrogen sulphide, mercury, silica and calcium, the latter most likely reflecting an increase in the weathering of bedrock by hot geothermal fluids. The association of hydrogen sulphide with subglacial geothermal activity was also noted by Lawler et al. (1996) and demonstrates the ubiquitous nature of the compound in geothermally active areas. In addition, Kristmannsdóttir et al. (2002b) argue that a significant increase in total dissolved solids will be noted in geothermally derived glacial meltwaters. However, despite hydrogen sulphide appearing an initially promising candidate as a subglacial geothermal indicator, Kristmannsdóttir et al. (2002b) point out that both hydrogen sulphide and mercury will be rapidly oxidised once in free contact with the atmosphere.

A thorough chemical investigation into two major jökulhlaups from the Vatnajokull ice cap was carried out by Galeczka et al. (2014) who identified three parameters that affect the

chemical composition of glacial meltwaters that undergo interaction with geothermal or volcanic fluids:

1. Heat and gas supply
2. Overburden pressure and its subsequent effect on gas solubility
3. Interaction with the local geology.

In addition, Galeczka et al. (2014) demonstrate a chemical distinction between waters affected by geothermal activity and those derived from a sub-glacial eruption. Specifically, an increase in SO_4^{2-}, Cl^- and F^- during volcanic eruptions is noted. Of particular interest to this study is the increase in chorine concentrations. As river chlorine concentrations in Iceland have been relatively constant since 1972 (Gislason and Torssander, 2006) any deviation above the norm is likely to be indicative of sub-glacial volcanic activity.

1.4.5.1 Isotopic Signals of Anoxic Conditions

The equations presented thus far have assumed that the subglacial meltwaters have had free access to atmospheric oxygen. Bottrell and Tranter (2002) point out that this is unlikely to always be the case and therefore other oxidising agents must be present. It is suggested that iron will successfully oxidise sulphate under anoxic conditions (Equation 9):

Equation 9: Sulphide Oxidation under Anoxic Conditions

$$FeS_2 + 14Fe^{3+} + 8H_2O \rightarrow 2SO_4^{2-} + 15Fe^{2+}\ 16H^+$$

When sulphate is produced under oxic conditions (Equation 4) 3.5 out of the 4 oxygen molecules will come from free atmospheric oxygen. However, when the sulphate ion is produced under anoxic conditions the oxygen molecules will be exclusively from water (Wynn et al., 2006). These two sources are isotopically distinct with atmospheric oxygen being strongly enriched in ^{18}O at +23.7‰ whereas oxygen derived from water molecules will have a negative isotopic signature (Bottrell and Tranter, 2002). When atoms from free atmospheric oxygen are incorporated into sulphate there is an additional fractionation of -8.7‰ but this does not have an effect great enough to make the two sources of oxygen indistinguishable (Bottrell and Tranter, 2002).

However, the intermediary reaction between sulphide and sulphate produces sulphoxy ions (SO_3^{2-}) which will undergo isotopic exchange with water in such a way that the original signal is obscured (Bottrell and Tranter, 2002). This problem is resolved by only analysing the final oxygen atom on the sulphate ion (Wynn et al., 2006). Thus if the less than 25% of the oxygen ions are sourced from free atmospheric oxygen anoxic conditions must have been present (Bottrell and Tranter, 2002).

This was applied to the case of an Icelandic glacier by Wynn et al. (2015) who postulated that seasonal variations in the isotopic signature to sulphate molecules reflect subglacial geothermal activity. By utilising the technique described above, Wynn et al. (2015) show that anoxic conditions prevail in summer which is when a fully oxidised quick flow drainage system should dominate. This is interpreted as representing the influx of reduced geothermal gases into the system. The fully oxygenated waters in winter are explained due to the persistence of low altitude melting and the continued presence of a channelized system at the snout of the glacier during the winter months.

1.5 The Role of Noble Gases in the Cryosphere

Noble gases occupy group 18 in the periodic table and are characterised by their low chemical reactivity. This allows them to be widely employed as geochemical tracers as they are generally independent of biological or chemical influence (Ito et al., 2011). Perhaps the most profound use of the noble gases in the earth sciences was using the ratio of helium-3 to helium-4 to show the influence of magmatic fluids on different tectonic settings (Lupton and Craig, 1981; O'Nions and Oxburgh, 1988; Oxburgh and O'Nions, 1987) which had profound implications for theories on the formation of continental crust. Recently, noble gases have been employed to understand processes in the cryosphere as conventional proxies such as water isotopes have been shown to vary on a local scale (Jouzel et al., 1997; Winckler and Severinghaus, 2013). Although still in its infancy, isotopic analysis of noble gases from ice cores has been successfully employed in reconstructing paleotemperatures (Craig and Wiens, 1996); dating ice cores (Buizert et al., 2014) and understanding hydrothermal interaction at the glacier bed (Jean-Baptiste et al., 2001).

1.5.1 Reconstructing Paleotemperatures

Water isotopes are the primary method by which past temperature is reconstructed in ice cores (Petit et al., 1999) despite the fact that they have been shown to underestimate paleotemperatures by up to a factor of two (Winckler and Severinghaus, 2013). Furthermore, present day correlation between water isotopes and temperature does not necessarily imply that this can be extrapolated back in geologic time (Jouzel et al., 1997). Moreover, it has been demonstrated that isotopic exchange between the atmosphere and cryosphere has varied both temporally and spatially (Jouzel et al., 1997). However, Winckler and Severinghaus (2013) state that these variations can be overcome by using the noble gases to analyse past temperatures. This is due to the fact the noble gases are unreactive and therefore will not be affected by any biological process or chemical reaction.

Paleothermometry from ice cores by noble gas analysis can be acquired in one of two ways (Winckler and Severinghaus, 2013):

1. Thermal fractionation of noble gases in the firn layer.
2. Temperature dependent solubility of noble gases in seawater.

1.5.2 Paleothermometry from Thermal Fractionation

The stratigraphy of a glacier is typically composed of four layers: Snow; granular ice; firn and glacial ice. The granular ice and firn layer represent the metamorphism of snow into ice with a typical base of 50-100m (Winckler and Severinghaus, 2013). Thermal fractionation of noble gases occurs in the firn layer such that heavier isotopes preferentially occupy colder regions. Furthermore, gases diffuse in firn an order of magnitude quicker than heat and therefore the isotopic composition of the firn will always reach equilibrium with the firn temperature (Winckler and Severinghaus, 2013). Therefore, by studying the isotopic ratio of noble gases in bubbles trapped in ice the paleotemperature of the firn layer can be established. Craig and Wiens (1996) provide a different approach by using the ratio of krypton to argon to understand the thickness of the firn layer in ice. Noble gases and their isotopes are gravitationally fractionated in a snowpack depending on their atomic weight and the thickness of the firn. Therefore, the concentration of heavier isotopes will be elevated in glacial ice to a greater extent than lighter isotopes, with respect to atmospheric values. The thickness of the firn layer will be governed by mean annual temperature and therefore fractionation of isotopes relative to atmospheric concentrations will give an indication of the temperature at the time of deposition (Craig and Wiens, 1996). This technique is still in its infancy (Winckler and Severinghaus, 2013) but with further research could provide a more reliable record of past temperature than current isotopic techniques.

1.5.3 Paleothermometry from Solubility of Noble Gases in Seawater

The heavier noble gases (xenon and krypton) are highly soluble in water with a strong temperature dependence (Headly, 2008). Assuming that the atmospheric-ocean inventory of noble gases is constant then the dissolved component of xenon and krypton in ice cores will represent the atmospheric component of noble gases at that time (Ritz et al., 2011). Therefore, it can be assumed the remainder is present as the dissolved component in seawater and thus can give a quantitative estimate of past ocean temperature. The assumption that the ocean-atmosphere noble gas inventory is constant is adhered to by the majority of workers (Ritz et al., 2011; Winckler and Severinghaus, 2013) except for argon-40 which is constantly degassed from the Earth's mantle (Bender et al., 2008). At present this technique is only theoretical (Ritz et al., 2011) and certain complications such as the effect of convection in the firn layer have to be considered (Winckler and Severinghaus, 2013). Despite this Winckler and Severinghaus (2013) conclude that this method remains the most promising candidate for deep ocean temperature throughout geologic time.

1.5.4 Argon Degassing through Time Recorded in Noble Gas Concentrations in Ice Cores

Argon is the most abundant noble gas in the Earth's atmosphere due to radiogenic ^{40}Ar being produced by the decay of ^{40}K (Winckler and Severinghaus, 2013). This is in contrast to most noble gases which have a constant inventory on a timescale of 10^5 to 10^6 years. The current atmospheric inventory of ^{40}Ar is equal to the total ^{40}Ar degassing over Earth history (Bender et al., 2008) and therefore understanding the rate of degassing will have important implications for geodynamics and crustal formation. Recent work has analysed argon in hydrothermal quartz (Pujol et al., 2013) to establish the composition of the atmosphere in the Archean. However, this does not provide a continuous record and therefore very little can be inferred about the fluctuations of argon degassing throughout Earth history. Ice cores, by contrast, provide an accurate record of atmospheric composition for the last 800kyr. This was utilised by Bender et al. (2008) who showed that the atmospheric composition of argon has been increasing by $1.1 \pm 0.1 \times 10^8$ mol/yr. In addition, Bender et al. (2008) argues that this rate has been relatively constant and can therefore be used in the dating of ice of unknown age. Furthermore, ice cores will not be affected by in situ radiogenic decay of ^{40}K as in the lithosphere and can therefore provide an accurate history of argon degassing through the Quaternary.

1.5.5 Distinguishing Cosmic and Terrestrial Dust

Ice cores contain dust particles that have a lithogenic or cosmic origin. Noble gases provide a unique insight into understanding the provenance of cryospheric dust particles and how their flux has varied over time. Cosmic dust is enriched with helium-3 due to interaction with the solar wind whereas the terrigenous component is typically enriched in helium-4 (Winckler and Severinghaus, 2013). Muller and MacDonald (1997) suggested that Quaternary glacial cycles were being driven by fluctuations in cosmic dust to Earth due to the continued changing of the Earth's inclination. Analysis of ice cores has shown that cosmic dust flux has varied over the past 30,000 years (Winckler and Fischer, 2006) but not in accordance with glacial cycles, thus disproving the theory of (Muller and MacDonald, 1997) which was well received at the time. Finally, analysis of noble gases has the potential to infer the provenance of terrestrial dust particles by comparing the measured ratio of helium to a constant crustal proxy. Winckler and Severinghaus (2013) suggest Ca or ^{232}Th and compare with the local geology.

1.5.6 The Potential of Helium isotopes as Geothermal Indicators

Helium is the second most abundant element in the solar system but due to the formation mechanisms of the terrestrial planets, it remains relatively rare on Earth (Oxburgh and O'Nions, 1987). Helium-3 and helium-4 comprise the two stable isotopes of helium of which helium-4 is vastly more abundant. However, the ratio of helium-3 to helium-4 is not constant across the lithosphere resulting in diagnostic crustal heterogeneities (Lupton and Craig, 1981). Specifically, isotopic composition is correlated with tectonic setting which is summarised by Torgersen and Jenkins (1982):

- Hotspots: 14-25Ra
- Mid-Ocean Ridge: 8Ra
- Destructive Plate Boundary: 2-8Ra
- Atmospheric: 1Ra
- Stable Continental Crust: 0.01-0.1Ra

Where Ra = $(^{3}He/^{4}He)_{atmosphere}$ (Winckler and Severinghaus, 2013)

The reason for such variation in helium isotope ratios becomes clear when the two terrestrial sources of helium-3 are considered:

1. Radioactive decay of uranium and thorium
2. The remnant of "primordial helium" that was incorporated into the Earth during its formation (O'Nions and Oxburgh, 1988).

Primordial helium has been shown to be outgassing at regions of crustal thinning or mantle upwelling (Lupton and Craig, 1981) resulting in higher concentrations of helium-3. Moreover, radiogenic $^{3}He/^{4}He$ ratios are typically four orders of magnitude smaller than

primordial helium and thus the signature of mantle derived primordial helium can be distinguished from that formed by radioactive decay (Oxburgh and O'Nions, 1987).

Currently, there is no anthropogenic source of helium-3 although atmospheric nuclear bomb tests during the cold war resulted in significant "fallout" of radiogenic isotopes, including helium-3. This has been used to date old (pre-cold war) and young (post-cold war) ice in glaciers situated in stable cratonic environments (Cecil et al., 1998). However, in areas of active mantle outgassing, anthropogenic input is considered negligible when compared with the mantle derived signal (Oxburgh and O'Nions, 1987).

(Lupton and Craig, 1981) were among the first to demonstrate elevated levels of helium-3 at a mid-ocean ridge setting. This was followed by Oxburgh and O'Nions (1987) who demonstrated that continental crust undergoing active extension also degasses primordial helium and that this has important implications for theories of continental formation (O'Nions and Oxburgh, 1988). This led to helium isotopes in geothermal and volcanic gases being measured by Welhan et al. (1988) who concluded that helium isotope ratios correlate with the presence of magma beneath a hydrothermal system and that coupled with a high heat signal (>200°C) are indicative of magma at depths of less than 10km. More recently, helium isotopes have been measured in geothermal systems and have been shown to have the potential to be a non-destructive indicator for sites of geothermal energy (Kennedy and van Soest, 2007). A regional study of the actively rifting Basin and Range province in the USA was carried out by Kennedy and van Soest (2007) who concluded that helium isotopes correlate with the severity of crustal deformation on a km scale. Finally, Jean-Baptiste et al. (2001) used helium isotopes in ice cores to resolve any geothermal input into a sub-glacial lake. Therefore, the use of helium isotopes is well documented in the analysis of mantle degassing at areas of crustal thinning and has been shown to correlate with areas of more intensive crustal thinning and geothermal activity (Kennedy and van Soest, 2007).

1.5.6.1 Potential for Helium Isotopes as a Sub-Glacial Geothermal Indicator in Iceland

It has already been demonstrated by Jean-Baptiste et al. (2001) that helium isotopes can be used to determine lithospheric-cryospheric interaction. Furthermore, helium isotopes are already widely used in geomorphology for surface cosmogenic dating (Blard et al., 2014; Cerling, 1990). In addition, Jean-Baptiste et al. (2001) state that any crustal contamination of helium will depend on the length of time the ice is in contact with the bedrock as well as the helium flux. Temperate Icelandic glaciers are continually in motion and therefore the length of time a particular section of ice is in contact with the bedrock will be minimal. Furthermore, Hoke et al. (2000) showed that although primordial helium can be stored in fluid inclusions in olivine it is typically three orders of magnitude less than the concentration of helium in geothermal waters. Therefore, given the demonstrated use of helium isotopes in determining geothermal activity, their proven relationship with shallow magma and their ability to influence the chemistry of overlying ice sheets, it seems plausible that measuring the helium isotopes of glacial meltwater will give an indication of the geothermal input at the bed of the glacier.

Chapter 2: Site Description

2.1 Vatnajokull Ice Cap

The Vatnajokull ice cap (Figure 4) is located in south east Iceland and is the largest ice mass in Europe (Gudmundsson et al., 1997) with a total area of 8100km^2 (Aðalgeirsdóttir et al., 2006). The ice sheet reached its maximum extent around 1890 but is currently in rapid retreat and could disappear in as little as 200 years (Aðalgeirsdóttir et al., 2006). In addition, the ice cap is underlain by active volcanoes many of which have erupted in the recent past (Gudmundsson et al., 1997). Furthermore, recent research has demonstrated a link between glacial retreat and increased magma production beneath the ice cap (Pagli and Sigmundsson, 2008). Vatnajokull is described by Aðalgeirsdóttir et al. (2006) as "one of the most sensitive glaciers in the world" making identifying any link between geothermal activity and glacial retreat even more vital.

2.2 Öræfajökull volcanic system

The study glacier, Virkisjökull is situated above the Öræfajökull volcanic system. Öræfajökull has erupted twice in recorded history (1362 and 1728) with the 1362 eruption being the largest and deadliest Icelandic plinian eruption in historical times (Guðmundsson et al., 2008). One of the principal dangers of an eruption at Öræfajökull is the potential for large scale glacial floods to ensue making a chemical method of quantifying ice-volcano interaction more pressing.

2.3 Virkisjökull Glacier

Virkisjökull is one of the outlet glaciers from the Vatnajokull ice cap (Figure 4) and is currently monitored by the British Geological Survey (BGS), but has received very limited attention in the published literature (Bradwell et al., 2013; Everest and Bradwell, 2003). It is known to be in rapid retreat (Bradwell et al., 2013) with a large section of the snout classified as "dead ice" that is no longer a part of the active glacier system (Everest and Bradwell, 2003). The glacier drains into a lake that is extremely variable in its water content depending on prevailing weather conditions. The lake is drained by the Virkisá river which is a coherent stream until it passes underneath the road bridge from where it forms an anastomosing series of channels that are continually in transition. In order to understand groundwater flow at Virkisjökull, BGS drilled a series of boreholes at various positions in the sandur (Figure 5). All boreholes were drilled to a depth of 15m except for L2 and L3 which were drilled to a depth of 9m. Together with samples from the bridge, lake outlet and a moraine groundwater spring termed "car park spring" these form the main sites for investigation.

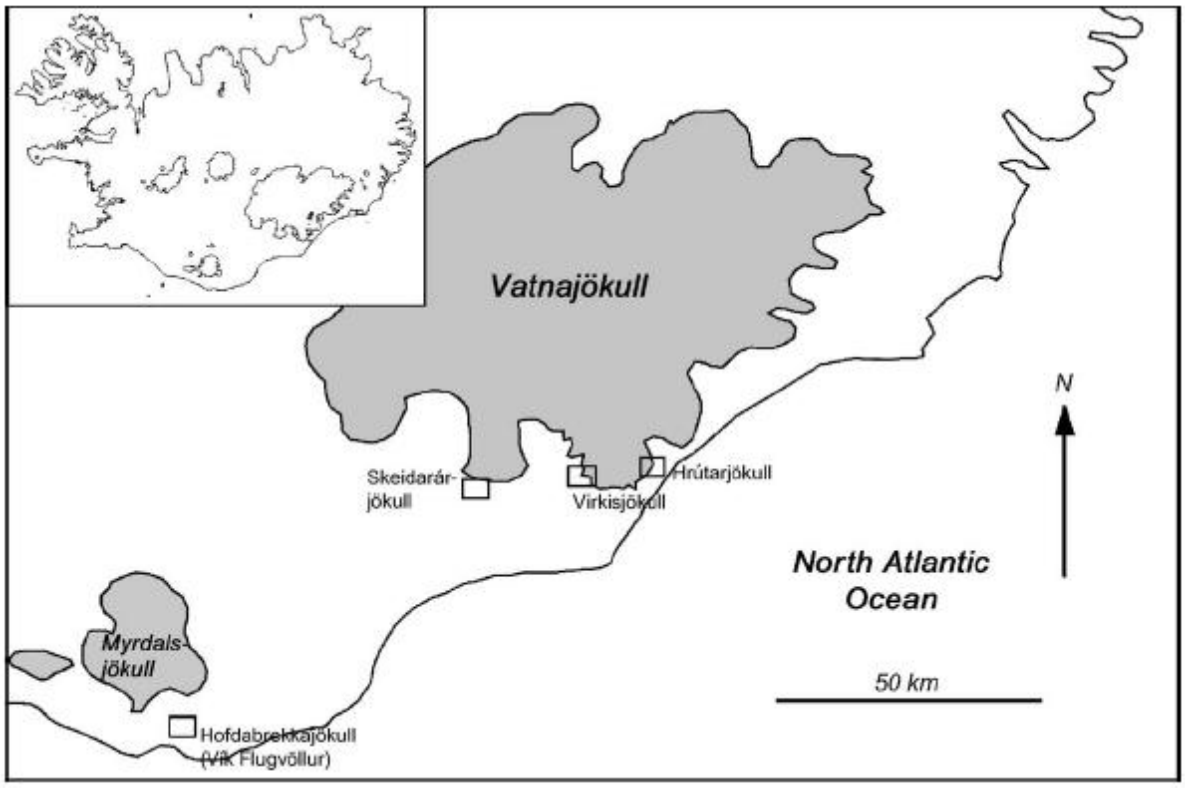

Figure 4: Map of the Vatnajokull and Myrdalsjokull ice caps in south-east Iceland showing the location of Virkisjökull glacier (Everest and Bradwell, 2003).

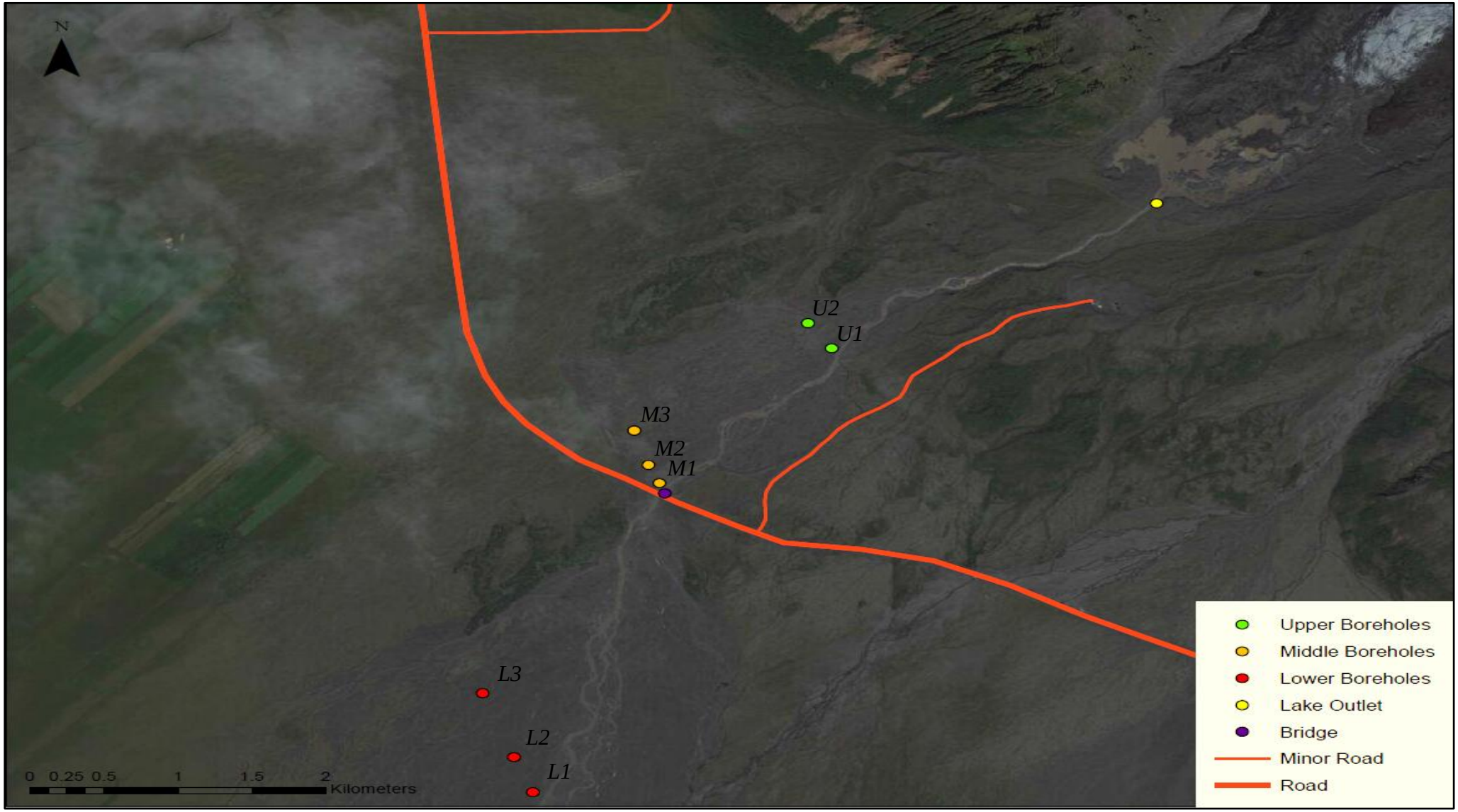

Figure 5: Map of all sample sites at Virkisjökull glacier. Henceforth prefix are used for Upper boreholes (U), Middle boreholes (M) and Lower boreholes (L). Boreholes are numbered from east to west. The snout of Virkisjökull is visible in the extreme north east with the Virkisá river trending north east to south west.

2.4 Hydrology of Virkisjökull catchment from the Virkisá River

Temperature measurements for the Virkisá River show a clear distinction between winter and summer with temperatures after April generally higher than during the winter months (Figure 6). This rapid increase in temperature is not reflected in the discharge until around the beginning of June where discharge suddenly increases and becomes more variable (Figure 7). This is likely to represent the time when subglacial cavities become connected to allow a subglacial channel system to transport the seasonally stored meltwater from higher up the glacier into the proglacial lake. Around mid-October river temperatures begin to decrease with an associated decrease in river discharge. Thus, river discharge and temperature measurements appear to operate in two distinct seasons: summer (June to October) and winter (November to May).

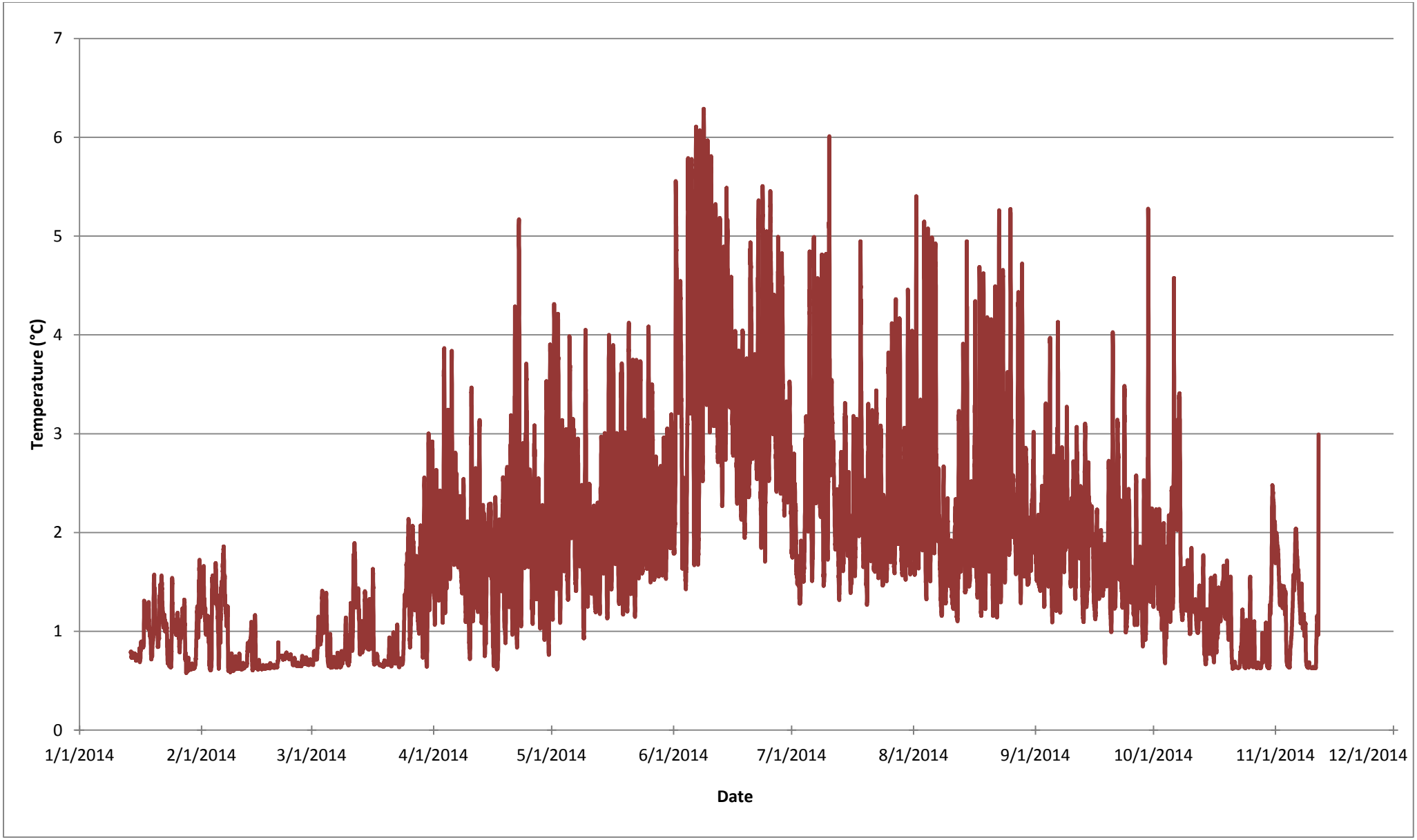

Figure 6: Temperature of the Virkisá River over the course of 2014. Data property of Dr Andrew Black of University of Dundee

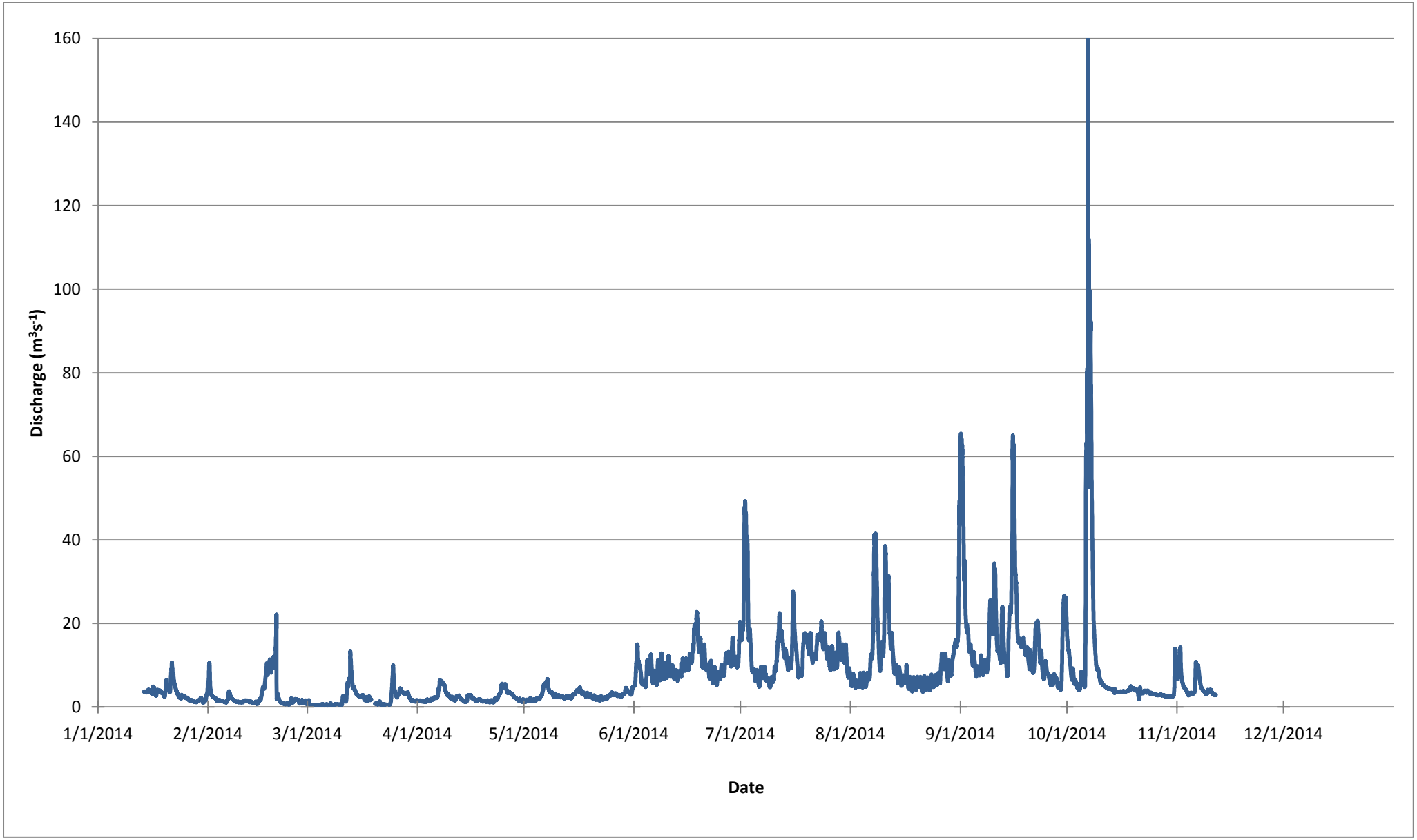

Figure 7: Discharge of the Virkisá River over the course of 2014. Data property of Dr Andrew Black of University of Dundee

Chapter 3: Methods

3.1 Additional Data

The main field campaign was carried out during spring 2015 between 26/03/15 and 1/04/15. A further two days of fieldwork was conducted at Sólheimajökull glacier between 3/04/15 and 4/04/15. These samples formed the primary basis for sulphate isotope analysis. In addition, to these samples BGS supplied data on major ion chemistry; trace metals, pH, conductivity, temperature and noble gas concentrations, collected between 2011 and 2015. Furthermore, three samples were collected from waters affected by the Bárðarbunga eruption. One sample was collected from waters upstream of the lava flow and two downstream from the lava flow. These will form an important end member as volcanically influenced waters.

3.2 Field Methods

In total 17 samples were collected from Virkisjökull glacier. Each site was measured for pH, conductivity and temperature using the WTW Mutli 340i pH-conductivity probe. This was calibrated for conductivity at the start of fieldwork and then once again on the 29/04/15. pH was calibrated every morning with the calibration fluids at a similar temperature to the waters being measured (0-5^{o}C). A one litre sample was taken from each site. The bottle used was washed out three times with the sample water prior to the final sample being taken. Each sample was then filtered through a 0.45µm cellulose nitrate membrane filter using a Nalgene filter unit and the flow regulated using a Nalgene hand pump. Again, this was flushed with sample water prior to the main bulk of sample being filtered. For each sample taken, 60ml of filtered water was set aside for bulk chemical analysis and 8ml for oxygen-deuterium isotopes.

3.2.1 Sulphate Isotope Field Collection

Approximately 1litre of filtered water was passed through a 1ml volume of cation and 1ml volume anion ion exchange resin. All resins were pre-conditioned with 1M HCl. Water was passed through the 50W-X8 cation resin first. This resulted in the removal of cations from solution, replaced by the H^+ counter-ion on the resin. The availability of H^+ ions also serves to neutralise any bicarbonate in the waters. This water is then directed into the anion resin (AG2-X8) onto which any sulphate becomes attached (Figure 8). Because of the dilute nature of precipitation and glacial ice, 5ml resin volumes were used for these sample types to allow sufficient water (up to 6l) to be processed. This allowed a measurable concentration of sulphate to be obtained whilst preventing resin over-load (and thereby 'self-elution') with the ion composition in such a large sample.

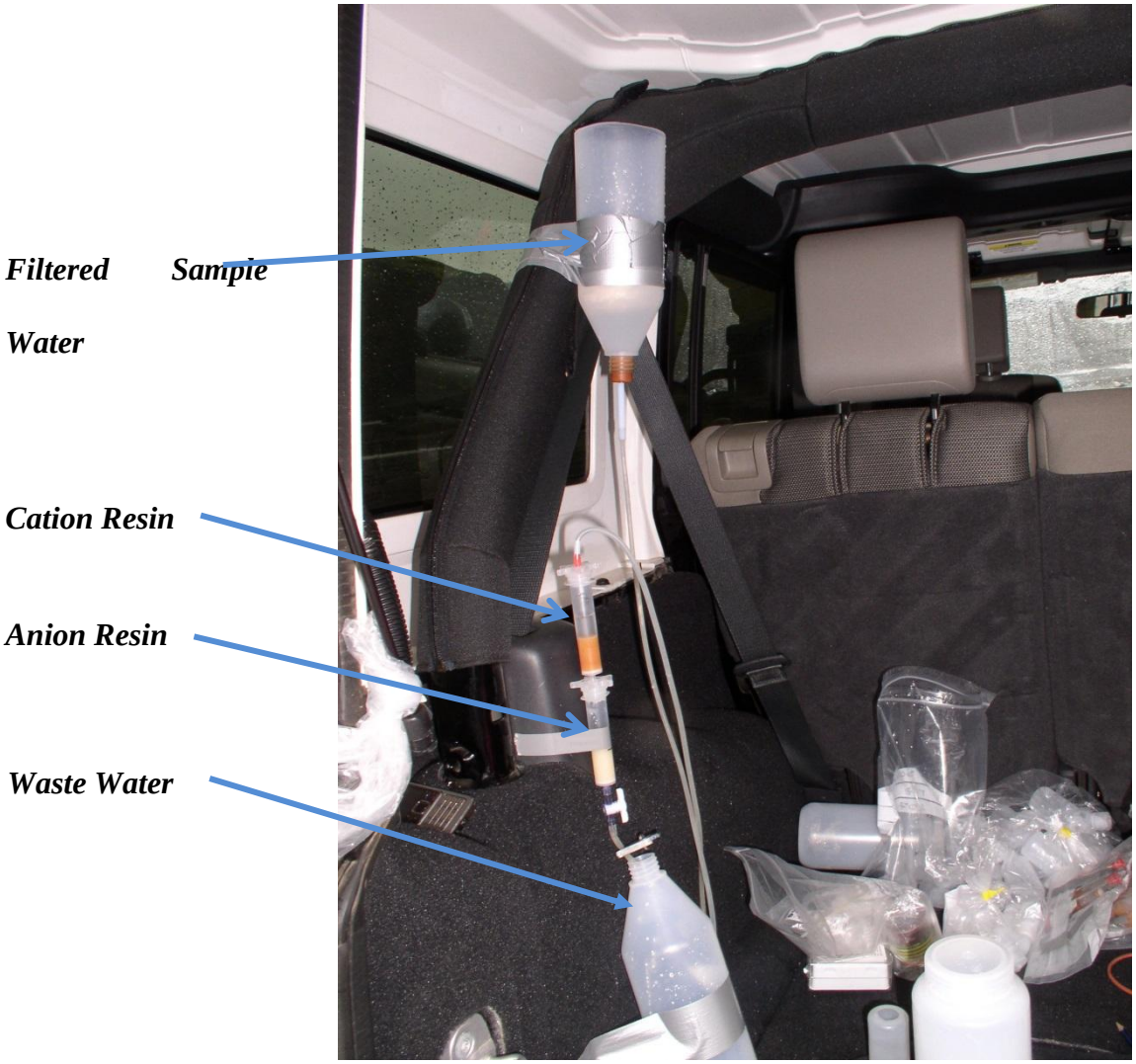

Figure 8: Field set up of cation and anion exchange resins to elute sulphate. The sample water is loaded into the reservoir and then allowed to flow through plastic tubing into the resins. Waste water is collected at the base.

3.2.2 Noble gas sampling

Four samples for noble gases were collected during spring 2015. Water from the sample site was allowed to pass through a copper tube for approximately 1 minute. The down flow end of the copper tube was then sealed shut first by crushing the end of the copper tube. Once the downstream end was sealed shut, the upstream end of the copper tube was crushed. This is to minimize any mixing with atmospheric air. Noble gas samples were also collected by BGS during summer 2011, 2013 and winter 2012 using the same method.

3.3 Laboratory Analysis

3.3.1 Major Anions

Major anions (Cl^-, SO_4^{2-}, F^- and NO_3^-) were measured using the Dionex ICS4000 in the centre for sustainable water management laboratories at Lancaster University. Six calibration standards were run at the beginning of the analysis for concentrations between those shown in Table 2 and limits of detection were calculated at three times the standard deviation. Calibration standards return to within 18% of the expected value for lowest calibration and to within 0.5% for the highest calibration.

Table 2: Low and high calibration standards for major anion analysis

Calibration	Fluorine (ppm)	Chlorine (ppm)	Sulphur (ppm)	Nitrogen (ppm)
Low Calibration	0.25	2	1	1
High Calibration	5	50	25	10

3.3.2 Major Cations

Major cations, were measured on the ICP-OES at Lancaster University. Samples were acidified using 0.1M nitric acid and then transferred into 15ml centrifuge tubes. The limit of detection was calculated as three times the standard deviation of the blank analyses (0.1M nitric acid). A check standard, calibration standard and blank was run after every nine samples. Five calibration standards were run at the beginning of the analysis within range of the expected concentrations (0ppm to 25ppm for Na^+, K^+ and Mg^{2+} and 0ppm to 80ppm for Ca^{2+}). Final results were extracted in counts per second and manually converted to concentration.

3.3.3 Trace Metals

Trace metals, were measured on the ICP-OES at Lancaster University. Samples were acidified using 0.1M nitric acid and transferred into 15ml centrifuge tubes. The limit of detection was calculated as three times the standard deviation of the blank analyses (0.1M nitric acid). A check standard, calibration standard and blank was run after every nine samples. Five calibration standards were run at the beginning of the analysis between 0ppb and 1000ppb for all trace metals except strontium were calibrations were run between 0ppb and 300ppb. Final results were extracted in counts per second and manually converted to concentration.

3.3.4 Sulphate Isotope Preparation

In order to extract the sulphate from the anion resins, each was flushed three times with 0.5ml 1M ultrapure HCl. The eluent was collected in a 1.5ml micro-centrifuge tube. 0.2ml of 1M $BaCl_2$ was added to the acidified samples and allowed to crystallise in the refrigerator for approximately 48 hours. The samples were then centrifuged at 3500rpm for twenty minutes, and then washed with milliQ water. This process was repeated 3 times. The samples were then left to dry in the heating cupboard and transferred to a desiccator until analysis.

3.3.4.1 Sulphate Isotope Analysis

Both $^{34}S/^{32}S$ and $^{18}O/^{16}O$ of the barium sulphate were measured using an Elementar Pyrocube elemental analyser connected to an Isoprime 100 mass spectrometer at the University of Lancaster. To measure the sulphur isotope composition 400µg ±20µg was measured into a tin capsule. Approximately 600µg of vanadium pentoxide was added into each capsule. The capsules were then sealed shut and pressed to ensure all air was extracted. Each sample was dropped into the elemental analyser furnace at 1050°C to ensure complete combustion to SO_4. To measure $^{18}O/^{16}O$ ratios, 400µg ±20µg of barium sulphate was measured out into a silver capsule. Approximately 600µg of carbon black was then added to each capsule. Finally, these samples were left to dry in the oven at 40°C overnight to ensure no excess moisture. Pyrolysis at 1450°C produced CO from which $^{18}O/^{16}O$ ratios were measured. Sulphur isotopic ratios were corrected to VCDT using international standards NBS-127 and SO6 ($\delta^{34}S$ +21.1‰ and 0.5‰ respectively) and oxygen isotopic ratios were corrected to VSMOW using NBS-127 and SO6 ($\delta^{18}O$ +9.3‰ and -11.3‰ respectively). An in house standard, MLSG, was run throughout to ensure precision ($\delta^{34}S$ +16.1‰ $\delta^{18}O$ -7.8‰). Finally, oxygen isotopes were blank subtracted to remove background values. The oxic/anoxic threshold was then calculated for each sample individually according to the equation laid out by Bottrell and Tranter (2002) as:

$$\delta^{18}O_{Threshold} = (23.7\text{-}8.7) \times 0.25 + (0.75 \times \delta^{18}O_{Water}) \qquad \textit{Equation 10}$$

3.3.5 Oxygen-Deuterium Isotope Analysis

Water isotopes (δD and $\delta^{18}O$) were measured using the Elementar Pyrocube elemental analyser connected to the Isoprime 100 mass spectrometer. $\delta^{18}O$ was measured using pyrolysis over glassy carbon beads at 1450°C. Deuterium-hydrogen concentrations were measured by the reduction of hydrogen at 1050°C over a chromium catalyst. Lab tap water was measured repeated throughout to ensure precision (δD -39.15‰, $\delta^{18}O$ -6.25‰). For oxygen analysis, standards had a precision of ±0.5‰ and deuterium analysis precision was ±1‰.

Chapter 4: Oxygen Deuterium Isotopes: Results and Discussion

4.1 Introduction

Oxygen and deuterium isotopes are used in an effort to isolate the major hydrological inputs into the Virkisjökull catchment. This is done with the primary focus of identifying sites dominated by glacial meltwater and sites dominated by precipitation. Classifying sites in this way provides a focus when attempting to resolve any subglacial geothermal input.

4.2 Results

Figure **5** shows the location of each sample site. Samples were classed as either: ice, lake outlet, car park spring, glacial meltwater, bridge, shallow sandur groundwater, upper boreholes, middle boreholes, lower boreholes and precipitation. Samples termed glacial meltwater cover a wide range of localities but predominantly involve supraglacial streams, glacial snout meltwater and ice-marginal streams that all appear to originate from melting ice. Furthermore, samples termed shallow sandur groundwater cover a large area but are formed of springs and groundwater fed rivers in the outwash sandur. These springs are continually changing location and therefore no consistent sample site could be identified.

Figure 9 shows all deuterium-oxygen isotopic data collected by the BGS and Lancaster University between 2011-2015. Samples have an isotopic composition ranging from -16‰ to -7‰ for $\delta^{18}O$ values and -130‰ to -50‰ for δD values. Samples plot close to the local meteoric water line according to data from GNIP (2015). The complete dataset from the BGS can be found in Appendix 2 in an excel spreadsheet. Oxygen-deuterium results from waters analysed at Lancaster University can be found in Appendix 1 in table form or on the original excel spreadsheet in Appendix 2.

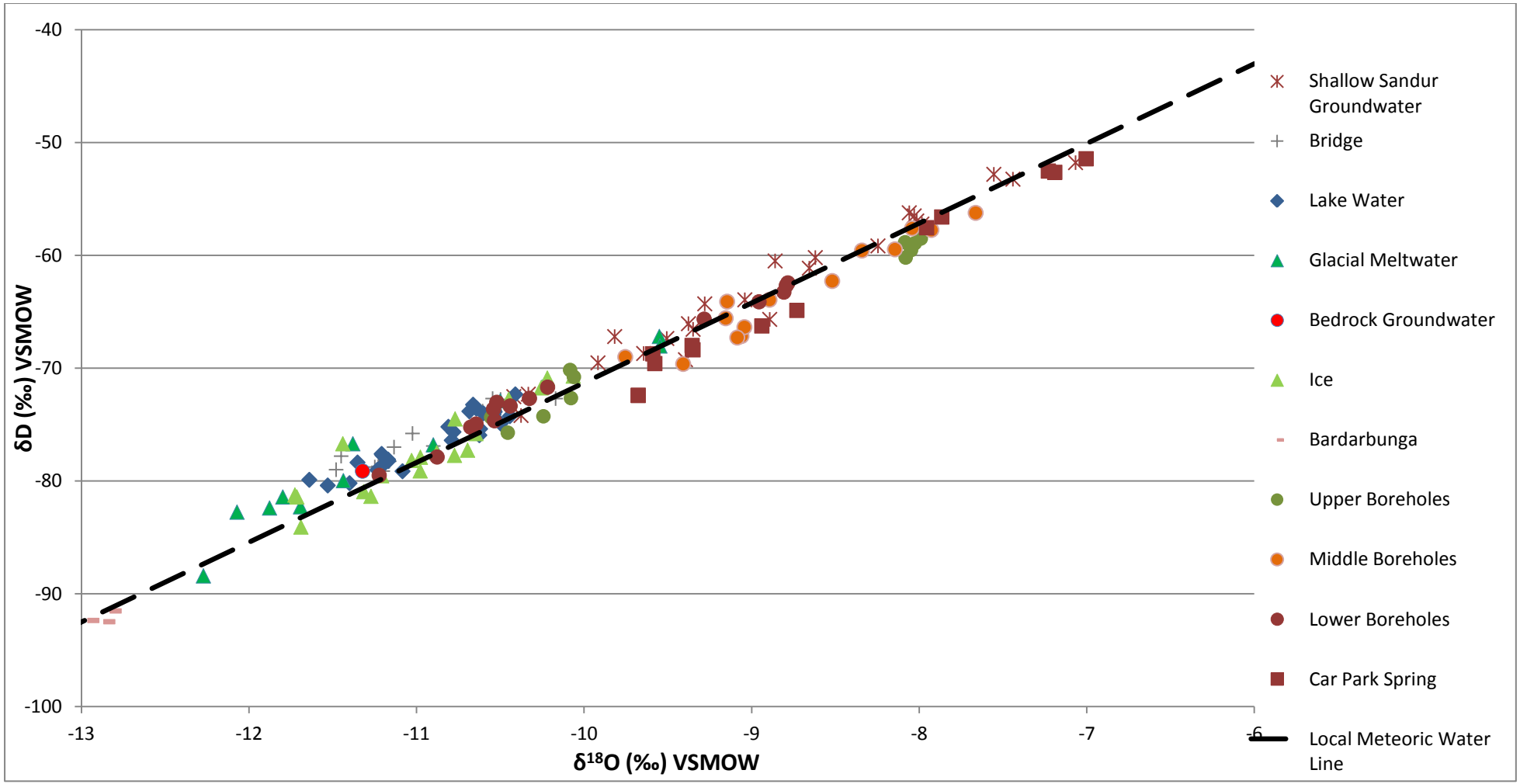

Figure 9: All data collected at Virkisjökull glacier from 2012-2015 by BGS and Lancaster University. Water collected from near the 2014 Bárðarbunga eruption is also displayed.

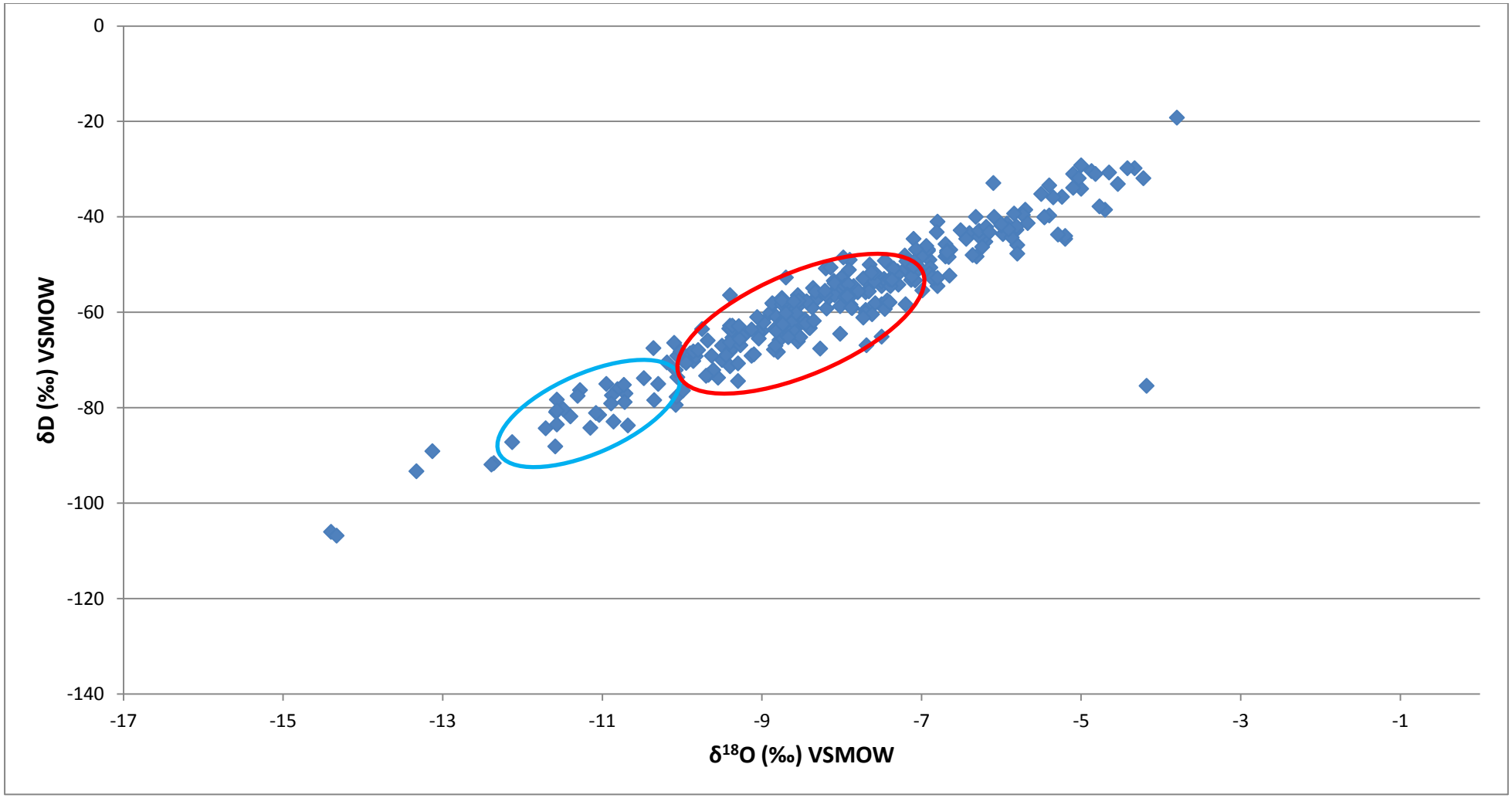

Figure 10: Oxygen deuterium data from precipitation at Reykjavik (GNIP). Red circle highlights range of data for groundwaters and blue circle highlights range of data for glacial meltwater from Figure 9.

4.3 Discussion

Samples appear to be portioned into two distinct groups. Samples with relatively low $\delta^{18}O$ and δD values tend to be those heavily influenced by glacial meltwater. Samples that have a relatively heavier isotopic signal are groundwaters with the exception of the deep groundwater borehole (termed bedrock groundwater on Figure 9) which was drilled to a depth of 156m into bedrock. Without incorporating dating techniques it is impossible to determine the age of this groundwater with any degree of certainty. Therefore, although it plots within the range of glacial values it is possible that other past processes were responsible for this shift and therefore it is excluded from this discussion. The remaining samples are divided into the two groups: groundwaters and glacial waters and analysed for seasonal trends and variations within sites. Finally, weekly trends in the isotopic composition of the car park spring and lagoon outlet are analysed from spring 2015 data.

4.3.1 Seasonal Variations in Groundwater

Figure 11 shows the variation in deuterium oxygen isotope composition with season for groundwaters. The sites measured on the sandur (all boreholes and shallow sandur groundwater) show significant variation but this appears to have no correlation with season. The car park spring however, does show variation with season (Figure 12). The lack of a seasonal relationship in the sandur groundwaters suggests that most of these sites are derived from a well-mixed precipitation fed aquifer. This is reinforced by the fact that the majority of groundwater values lie in the inter-quartile range of precipitation values: -6.93‰,-49.05‰ and -9.30‰,-66.25‰ (data from GNIP Reykjavik). Those with lighter values are therefore suggested to have a significant input from glacial meltwater. Upper boreholes with a lighter isotopic composition are exclusively derived from borehole U1. This borehole is situated adjacent to the river draining the proglacial lake and therefore is likely to have a substantial component from glacial meltwater. Borehole U2 is located 100m from the river and shows a heavier isotopic signature with little seasonal variation which suggests it is derived from a well-mixed deep aquifer. A significant number of the lower boreholes also show lighter values than would be expected if they were entirely precipitation derived. This is surprising given their location over 4km from the glacial front in the sandur. It is likely that this is a reflection of the braided nature of the proglacial river at this point on the sandur allowing glacial meltwater to percolate through a large area. In addition, this explains the lack of glacial water observed in the middle boreholes which are located further upstream where the river is still more tightly constrained to a single channel flow regime. The car park spring however, does show seasonal variation and its location adjacent to the lake outlet should reveal more about the distribution of glacial meltwater in the proglacial moraines.

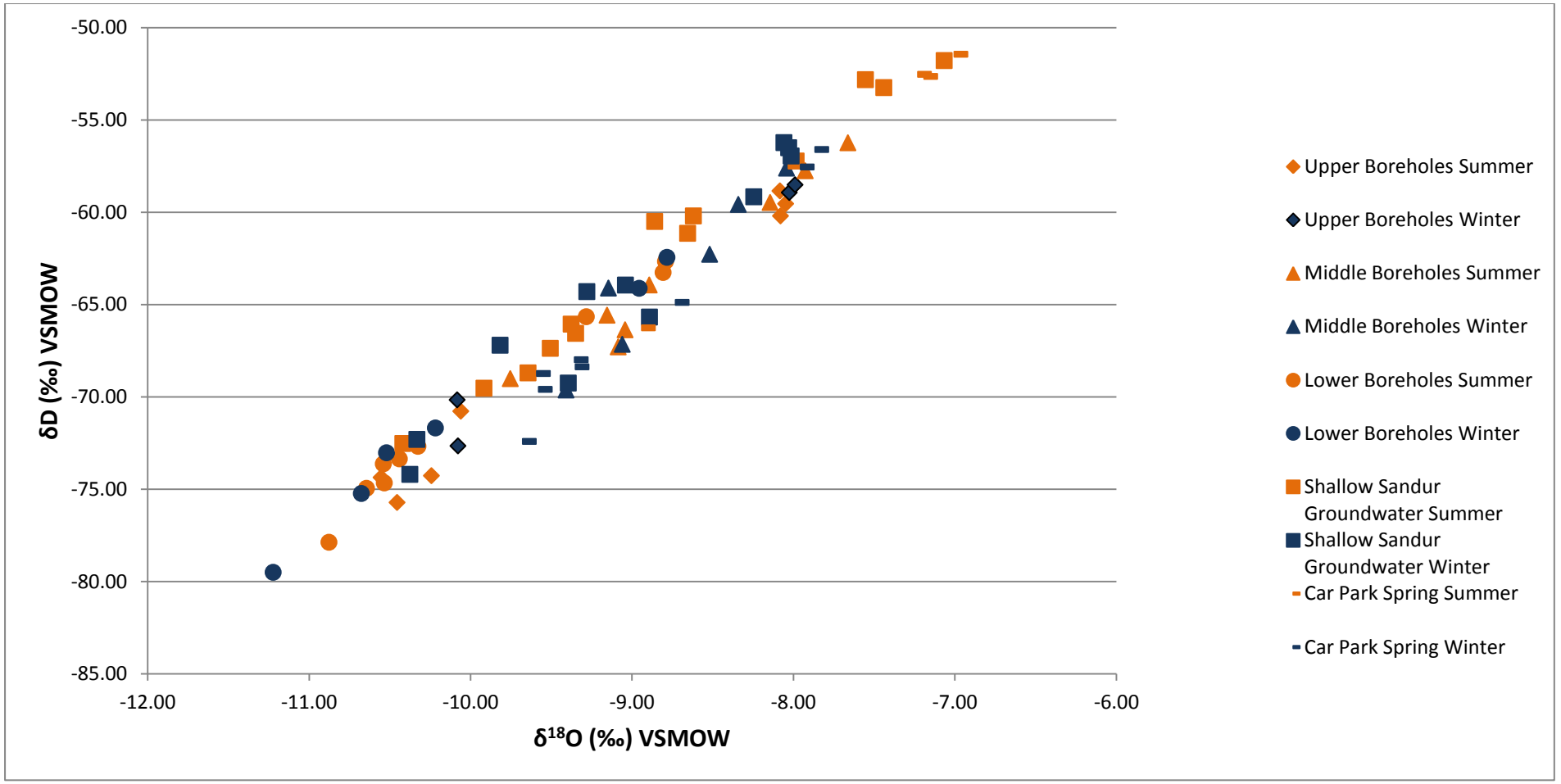

Figure 11: Deuterium-oxygen isotope values for groundwater sites separated by season.

4.3.1.1 Seasonal Variation in the Car Park Spring

Figure 12 shows the variation in the deuterium-oxygen isotopic composition of the car park spring over two and a half years. The isotopic composition of the water shows a clear distinction with season with the heaviest values occurring in summer and the lightest values in winter. This is likely a reflection of the dominant input in summer being rain, whereas in winter it will be seasonal snowmelt from the tundra surface. Why the other groundwater fed sites do not show such a clear seasonal variation is a reflection of the different geographies of the sites. All other groundwater measurements occurred on the sandur which will contain water sourced from a very large area and therefore not be as susceptible to changes in precipitation type.

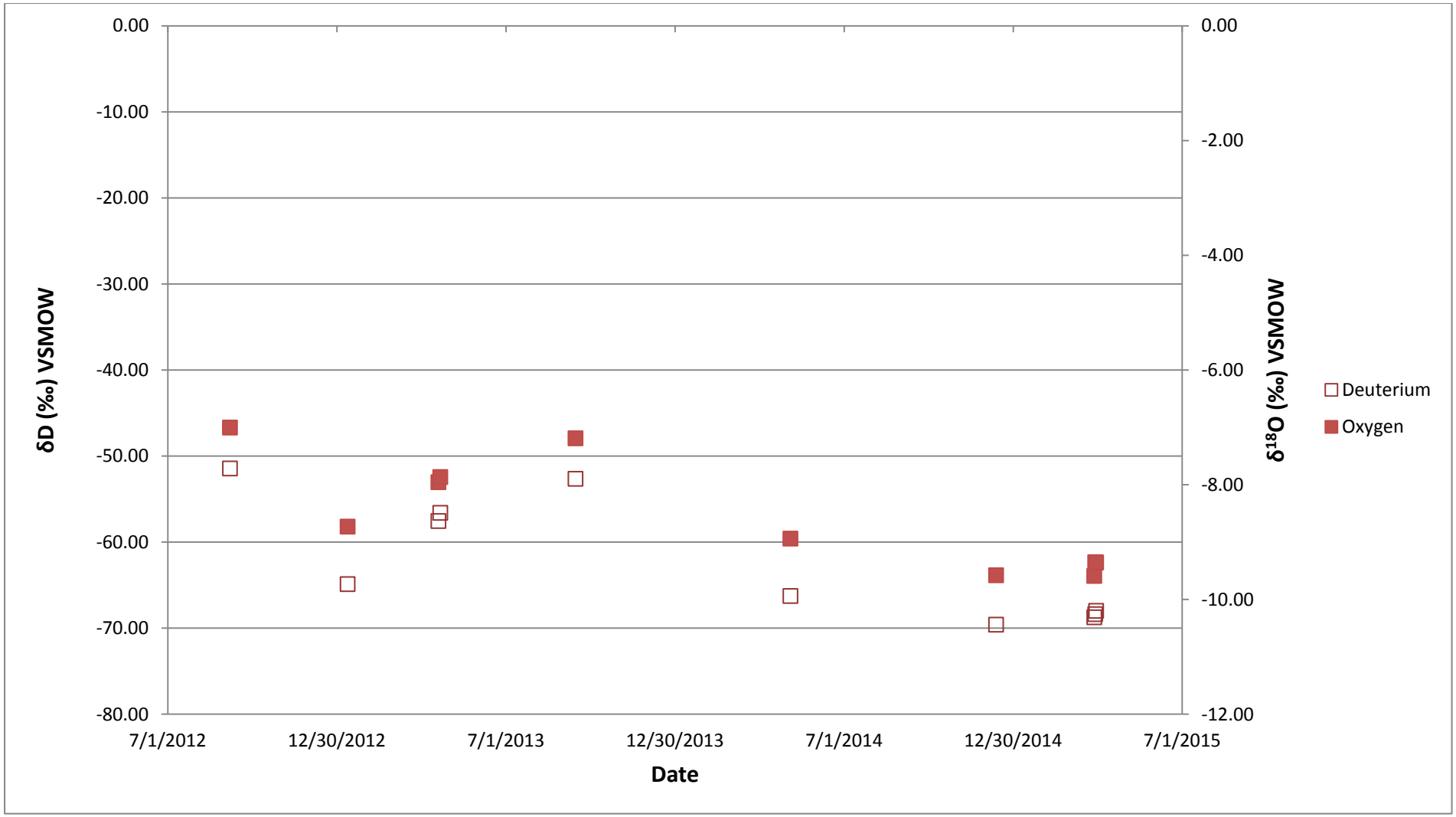

Figure 12: Variation in the isotopic composition of the car park spring with date over a 2.5 year period.

4.3.2 Seasonal Variation in Glacial Waters

Figure 13 shows the variation of surficial waters and ice with season. Overall, summer values show relatively lower concentrations of ^{18}O and deuterium than winter measurements. This could be interpreted in one of two ways. The most likely scenario would be that increased summer temperatures cause the melting of ice and snow from higher up the glacier which will have relatively lower oxygen deuterium values due to the altitude effect. This is reinforced by the fact that glacial samples collected during spring 2015 have values very similar to those of groundwaters samples, reflecting the lack of glacial melt due to the cold conditions. Thus summer glacial meltwater samples have isotopically lighter values than winter. It could also be argued, as it has been by Wynn et al. (2015) at Sólheimajökull glacier, that the relative decrease in $\delta^{18}O$ and δD values in summer is a reflection of increased geothermal activity during the summer months causing rapid melting of higher altitude snow and ice. The former mechanism appears the more likely candidate given the lack of any obvious geothermal signals although minor geothermal effects on oxygen-deuterium data alone cannot be ruled out.

4.3.2.1 Seasonal Variation in Ice

The isotopic composition of ice varies considerably which is to be expected given that all samples were taken from below the ice fall where the ice will be a well-mixed amalgamation of different aged sources. Thus, no obvious correlation between sample altitude and the isotopic composition of the ice was noted.

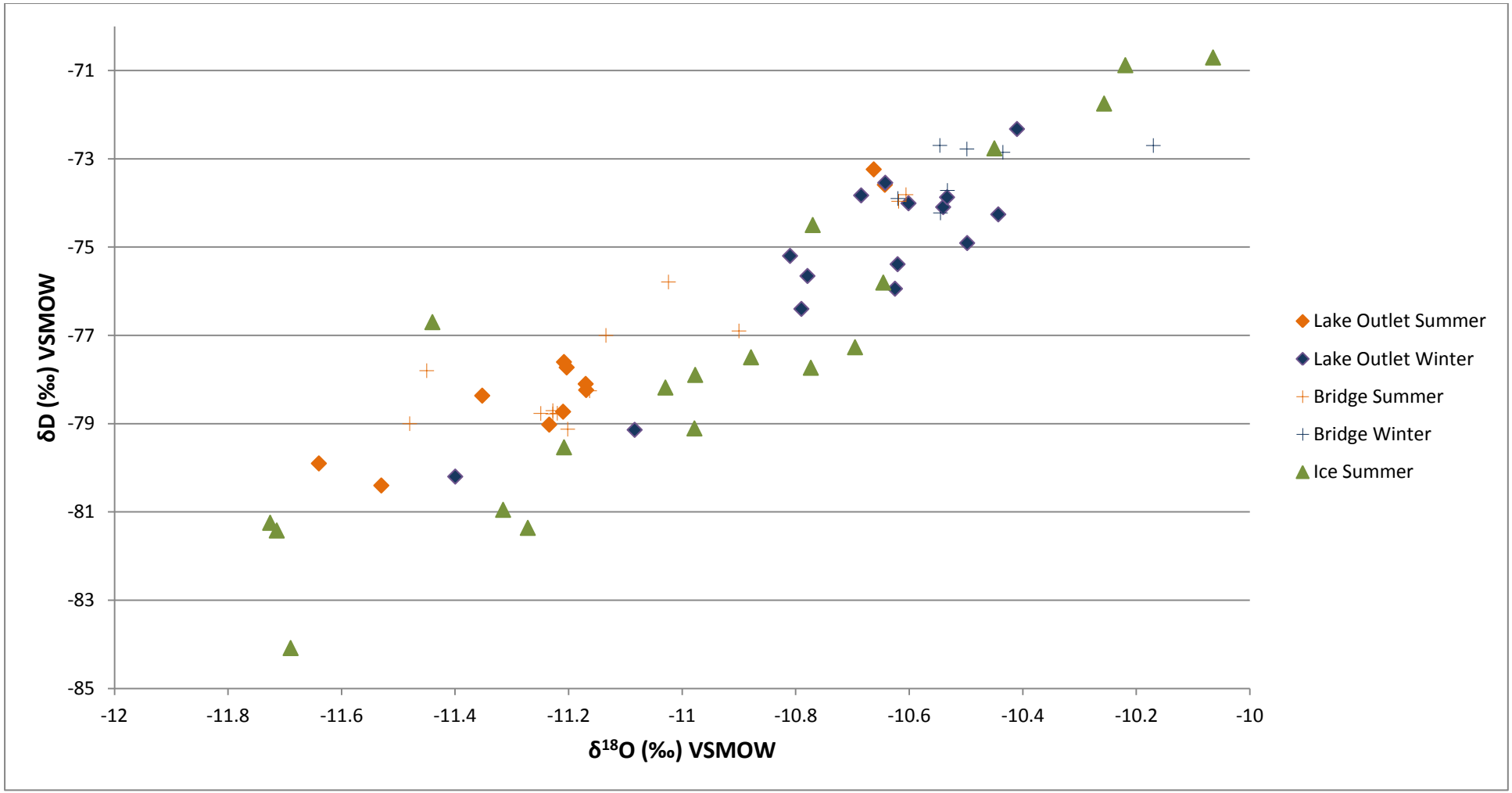

Figure 13: Isotopic composition of surficial waters and ice by season

4.3.2.2 Isotopic Variation in the Lake Outlet (Spring 2015)

The lake outlet was measured continuously during the field campaign of spring 2015 (Figure 14). Overall, a trend towards isotopically lighter values is observed, albeit a very slight one: change in $\delta^{18}O$ = -0.19‰ and δD = -1.68‰. These values lie very close to the limit of detection for the mass spectrometer and therefore most likely represent a constant sourcing during the sampling period. This is interpreted as being the result of the intensely cold period during spring 2015 restricting inputs into the proglacial lake to basal ice melt.

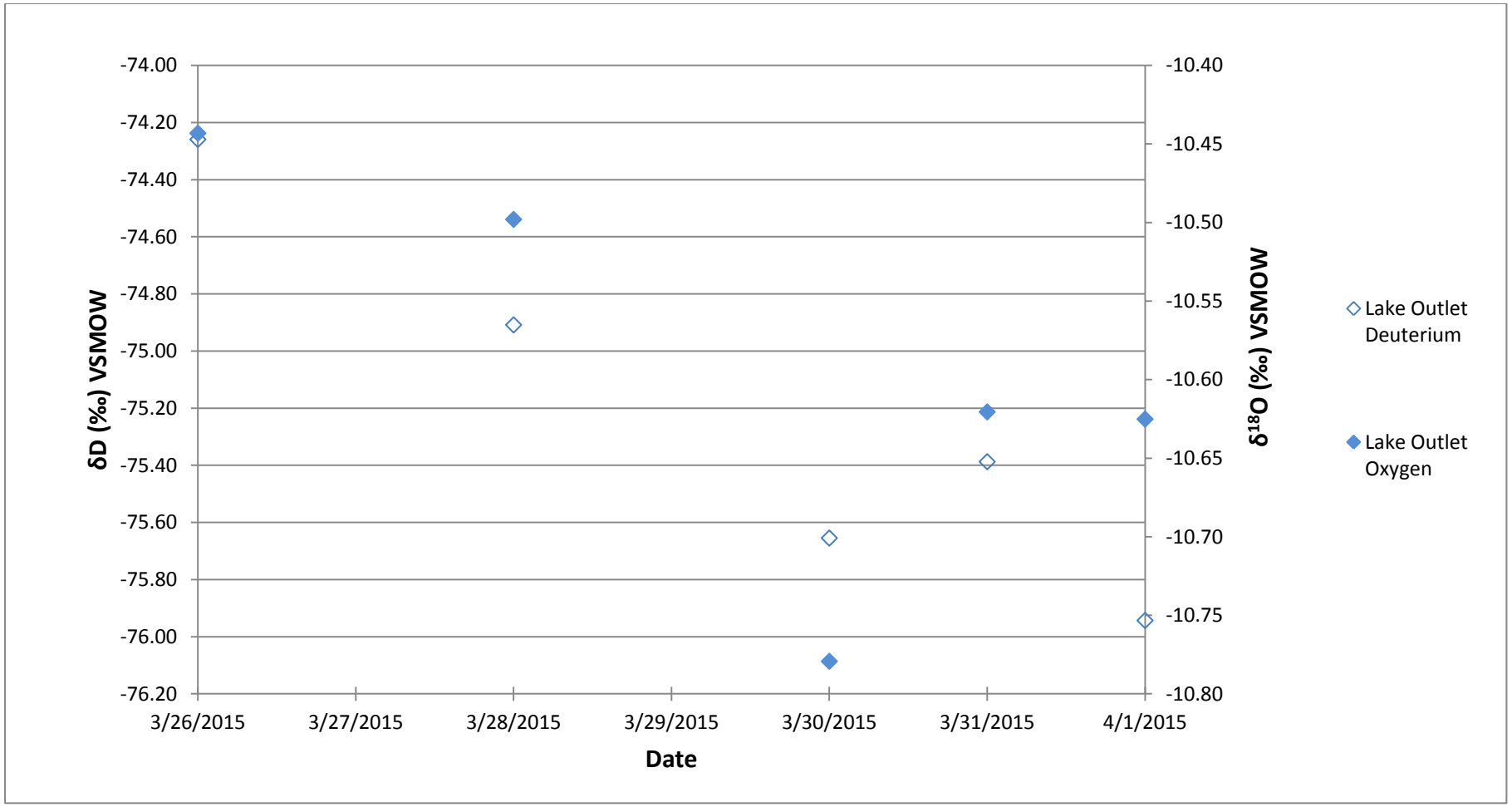

Figure 14: Variation in oxygen and deuterium isotope concentration by date for the lake outlet sample site.

4.4 Summary

1. Samples can be divided into two distinct groups by their oxygen-deuterium isotopic composition: Glacial meltwater samples occupying the isotopically lighter end of the samples measured and groundwater samples occupying the heavier end.
2. Groundwater samples with the exception of the car park spring show no seasonality suggesting that they are fed from a well-mixed aquifer.
3. The car park spring does show seasonality which is suggested as being a reflection of the main input in summer being rainwater and surface snowmelt in winter. This suggested the car park spring is a locally fed groundwater spring.
4. Glacial meltwater samples (lake outlet and bridge) do show seasonality with isotopically light waters occurring in summer. This is suggested to be due to increased summer melting of glacial ice and snow from a higher altitude which will have a relatively lighter isotopic composition.
5. Oxygen deuterium isotope data leaves open the possibility of a geothermal regime operating underneath Virkisjökull but does not actively support this conclusion. In order to better understand whether a subglacial geothermal regime is in operation in Virkisjökull we need to analyse chemistry that is diagnostic of geothermal activity. Sulphur isotopes were successfully employed by Wynn et al. (2015) as a subglacial geothermal indicator and shall form the focus of the next chapter.

Chapter 5: Sulphur Isotopes: Results and Discussion

5.1 Introduction

Oxygen-deuterium isotopes have provided an insight into the hydrological system operating at Virkisjökull and have demonstrated the partitioning of sites into two major groups: precipitation fed groundwater and glacial meltwater. Sulphur isotopes provide a means of resolving the major chemical inputs into these waters and thus providing a more complete hydrological model of the Virkisjökull area. Moreover, they have the potential to isolate a subglacial geothermal source. Identifying the sites most likely to hold a chemical signature of subglacial geothermal activity will be guided by the oxygen-deuterium analysis.

5.2 Sulphur Isotopes Results

Sulphate concentrations were measured for all sites sampled during spring 2015 and for selected sites sampled by BGS between summer 2011 and winter 2014. Sulphur isotopes were only measured for a selected group of sites including all those sampled during spring 2015, three from winter 2014 (borehole U1, borehole M3 and bridge), two from summer 2014 (lake outlet and bridge) and three from winter 2014 (car park spring, lake outlet and bridge). In addition, six sulphur isotope samples were measured from Sólheimajökull glacier during spring 2015 and 3 from the Bárðarbunga eruption site. Figure 15 shows sulphate concentrations vs the sulphur isotopic ratio for Virkisjökull. SO_4 concentrations range in value between 4.5ppm for the bridge sample collected in winter 2014 to less than 0.5ppm for ice and precipitation. There is significant variation in the sulphate isotopic ratio of Virkisjökull samples from 17.27‰ for precipitation to 3.6‰ for borehole U1 collected during winter 2014. Not plotted on this diagram are samples collected from the Bárðarbunga eruption. These have the highest sulphate concentrations measured of 15ppm and the lowest

sulphate isotope composition at -1.24‰. All data can be found in table form in Appendix 1 or as an excel spreadsheet in Appendix 2.

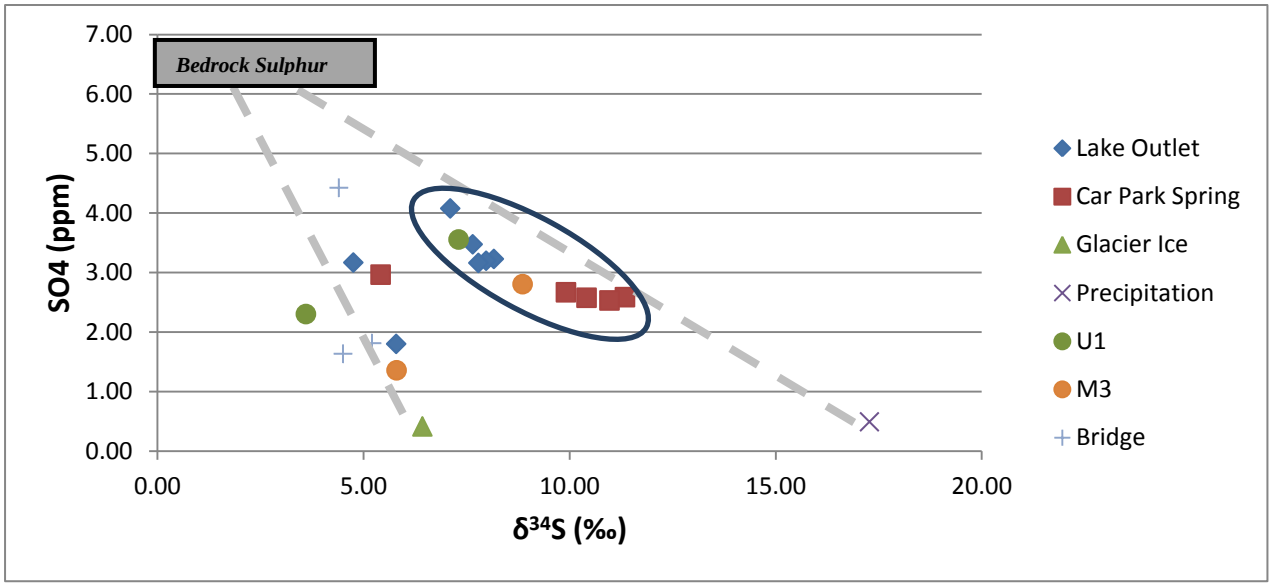

Figure 15: Selected Virkisjökull sites sampled between summer 2014 and spring 2015 comparing sulphate concentration to sulphur isotope composition. Circled are samples collected during spring 2015 (excluding "ice" and "precipitation") and dashed lines highlight the proposed mixing between chemical endmembers. Bedrock sulphur values taken from Wynn et al. (2015).

5.3 Sulphur Isotopes: Discussion

5.3.1 Mixing between Meteoric and Bedrock Sources (Spring 2015)

There are three possible major inputs into the Virkisjökull sulphate budget: Atmospheric sulphur, bedrock sulphur and geothermal sulphur. Atmospheric marine sulphate is relatively fixed at a +21‰ (Rees et al., 1978) and this is reflected in the sulphur isotope composition of the precipitation measured during spring 2015 at + 17.3‰ (Figure 15). This is to be expected given Virkisjökull's coastal location. Virkisjökull is situated above predominantly basalt terrain and which in Iceland has a sulphur signature of −2 to +0.4‰ (Torssander, 1989). Therefore, (with the exception of ice) samples collected during spring 2015 appear to represent a binary mixing between a bedrock sulphate signature and precipitation sulphate signature (Figure 15). This binary mixing was also observed in the oxygen-deuterium isotopes. The car park spring values plot closest to the precipitation endmember as this is a locally precipitation fed spring that will have undergone relatively little contact with the local geology. Plotting slightly more towards the bedrock endmember is the borehole M3 which is derived from a well-mixed precipitation fed aquifer; based on oxygen-deuterium data. Water from this site will have had a longer contact time with the local geology than the car park spring and therefore shows a slightly more bedrock based signature. Finally, the lake outlet and upper borehole U1 plot closest to the bedrock endmember reflecting the large input of glacial meltwater into these sites that has undergone significant contact with the country rock in a subglacial setting. There is therefore a clear distinction in sulphate isotopic signature of the various sites sampled during spring 2015 which appears to reflect the relative inputs of bedrock and precipitation sulphate into each site. Glacier ice collected during the spring 2015 field campaign shows relatively lighter sulphur isotope values. This reflects the exposure of glacier ice to atmospheric sulphur inputs that will cause a trend towards lighter values than precipitation. These inputs include deposition of aerosols from anthropogenic

pollution, volcanic aerosols and deposition of ash particulates. Therefore, the temporal exposure of glacial ice to these inputs relative to precipitation results in a lighter sulphur isotope signature.

5.3.2 Mixing between Meteoric and Bedrock Sources (Winter 2014 – Spring 2015)

Other sites shown on Figure 15 were measured at different times of the year and all show significantly lighter isotopic values than those collected in spring 2015. There are three possible explanations for this isotopic variability:

1. Excessive ice melting at other times of the year compared to spring 2015.
2. Variation in the sulphate content of precipitation.
3. Sub-glacial input of geothermal gases interacting with the glacier hydrological system.

5.3.3 Sulphur Isotope Signature of Ice Melt

Ice melt forms an endmember to a second binary mixing trend between bedrock and ice sulphate signatures. Due to the temperate nature of the southern Icelandic climate, ice melt makes a significant contribution to the hydrological system throughout the year. However, during spring 2015 continuous sub-zero temperatures ensured that ice melt contribution was very small and thus precipitation dominated as an endmember. This pendulum effect between meteoric endmembers of the binary mixing trends is entirely governed by the prevailing weather conditions.

5.3.4 Isotopic Variation in Precipitation Fed Sites

For sample sites devoid of any glacial melt input (borehole M3 and car park spring), variation in the isotopic signatures between seasons can be explained by deviations in the sulphur isotope composition of precipitation throughout the year (Figure 15). The sulphate isotopic composition of precipitation has been shown to vary significantly depending on relative inputs of marine aerosols, volcanic aerosols, anthropogenic emissions and continental biogenic emissions (Jenkins and Bao, 2006). Inputs from volcanic aerosols will likely have been more significant for samples taken after summer 2014 due to the eruption at Bárðarbunga. This appears the most likely mechanism which has likely caused a single car park spring value to show a significantly lighter isotopic composition than those measured in spring 2015. Borehole M3 which also shows significantly lighter isotope values than those measured in spring 2015 was collected prior to the eruption of Bárðarbunga and therefore it is likely that this was caused by a combination of variation in precipitation sulphate and water-rock contact time.

5.3.5 Geothermal Indicators

The isotopic signature of geothermal sulphate is poorly constrained but current estimates vary between +4.2‰ for H_2S (Robinson et al., 2009b; Wynn et al., 2015) and 0‰ for magmatic sulphur (Nielsen et al., 1991). Isotopic values from volcanically influenced waters at Bárðarbunga showed a sulphur isotope ratio of 0‰ (this study). These isotopic values lie close to the bedrock endmember, thus rendering source discrimination difficult. However, identifying a geothermal signal from sulphate has been approached in at least three separate ways:

1. Comparing sulphate equivalence to major univalent and divalent cations respectively (Robinson et al., 2009b).
2. Comparing sulphate: chlorine ratios to the sulphur isotope composition (Robinson and Bottrell, 1997).
3. Using sulphate oxygen isotopes to determine the anoxic/oxic regime operating in the glacial hydrological system to determine whether geothermal gases are being oxidised in an open channelized system (Wynn et al., 2015).

Robinson et al. (2009b) identified that geothermal waters will have relatively elevated values of sulphate compared to calcium and magnesium. In addition, Robinson et al. (2009b) show that if weathering of carbonates and sulphides is the only input of major cations and sulphur then coupled sulphide oxidation and carbonate dissolution must be occurring. This will produce a Ca + Mg: SO4 ratio of 2:1 (Figure 16). Thus, deviation from this line suggests a system with multiple inputs.

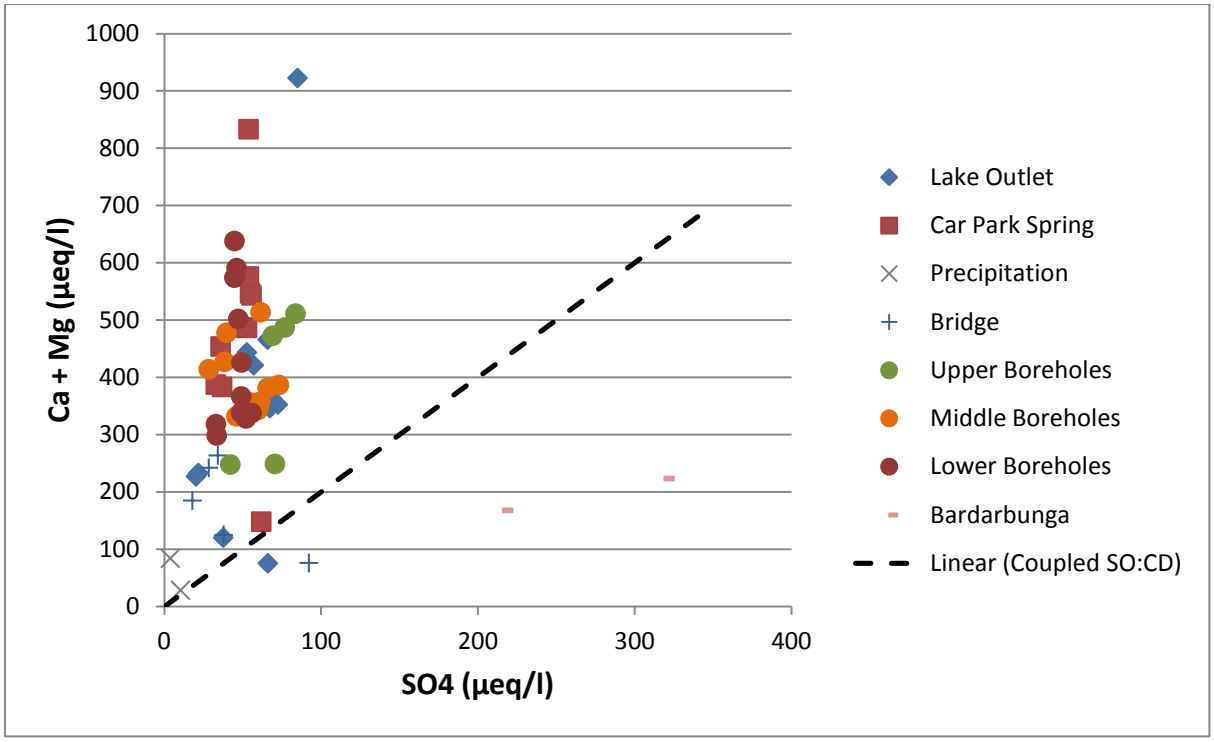

Figure 16: Comparing Ca +Mg equivalence to sulphate equivalence for selected Virkisjökull sites. Dashed line represents coupled sulphide oxidation and carbonate dissolution (hereafter referred to as coupled SO-CD).

Data presented in Figure 16 shows significant excess in calcium and magnesium at nearly all sites than would be expected if purely coupled SO-CD is occurring. The apparent excess in calcium and magnesium is most readily explained by the weathering of calcium silicates. Samples that were directly affected by the eruption at Bárðarbunga show significant excess of sulphate. This was also observed in geothermally influenced waters by Robinson et al. (2009b). All but two samples collected at Virkisjökull show the opposite trend to that expected if there was a dominant geothermal influence. In addition, there is no clear distinction between precipitation derived sites (such as the car park spring) and glacial meltwater sites (such as the lake outlet). This implies that there is no extra (geothermal) sulphate component being supplied to subglacial waters that is not already present in precipitation fed waters. However, two samples collected during spring 2014 show more

sulphate that would be expected given the concentration of divalent cations. These samples are primarily derived from glacial meltwater which is where a geothermal signal is most likely to be present. However, these samples were collected during the height of the Bárðarbunga eruption in the north west of Vatnajokull. Moreover, the precipitation fed car park spring waters sampled during this period also plot very close to the boundary line. Therefore, these samples have likely had a heightened influence from volcanic aerosols and ash deposition.

Another approach adopted by Robinson and Bottrell (1997) suggests comparing sulphate/ sulphate + chlorine to the sulphur isotope ratio (Figure 17). Using this technique Robinson and Bottrell (1997) successfully demonstrated that precipitation, volcanic rocks and geothermal fluids all plot in distinct zones. Results from Bárðarbunga agree with Robinson and Bottrell (1997) by having a sulphate/ sulphate + chlorine ratio of close to 1. Given the lack of data on volcanic rocks it can only be assumed that the basaltic geology has a similar isotope composition as described by Torssander (1989) of 0‰. Sulphate chlorine ratios are taken from Clarke 1967 and are assumed to be around average for igneous rocks and basalts. Using this data gives a sulphate to sulphate +chlorine ratio of between 0.75 and 0.90. Thus, Figure 17 reinforces the binary mixing described by Figure 15 as no samples appear to be being "pulled" towards the geothermal endmember. This is further backed up by Figure 18 which shows the variation in fluorine with respect to sulphate.

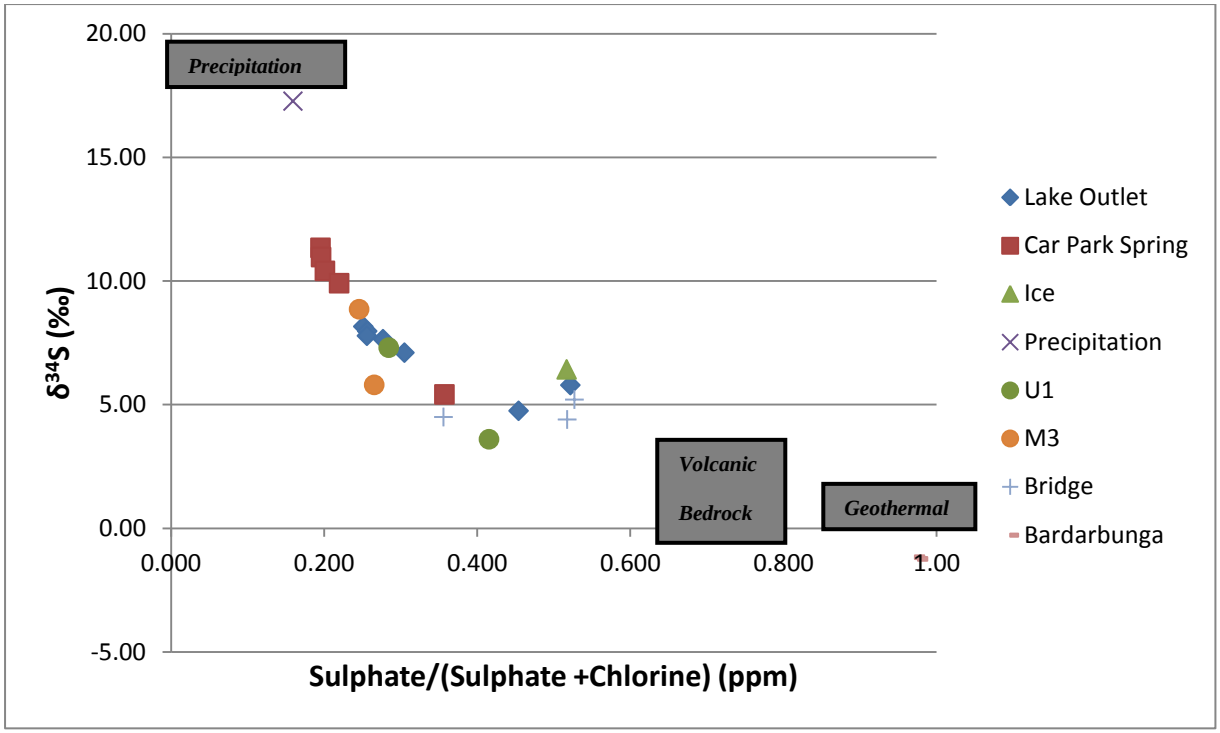

Figure 17: Sulphur isotope ratios vs sulphate/sulphate + chlorine ratios for all Virkisjökull and Bárðarbunga sites. Boxes highlight approximate positions of various endmembers (based on Robinson and Bottrell, 1997).

Fluorine is primarily derived from a geothermal or volcanic input and the lack of distinction between precipitation fed sites (car park spring and borehole M3) and glacial water fed sites (lake outlet, bridge and borehole U1) reinforces the argument for very little geothermal activity occurring underneath Virkisjökull (Figure 18). The minor quantities of fluorine found in these waters are likely to be the result of a combination of aerosol deposition and bedrock weathering. Therefore, analysis of sulphur isotopes coupled with bulk chemistry suggests that there is very little geothermal activity occurring underneath the Virkisjökull glacier. The final technique applied was using sulphate isotopes to identify any signals of anoxia that may result from oxidation of geothermal gases as outlined by Wynn et al. (2015).

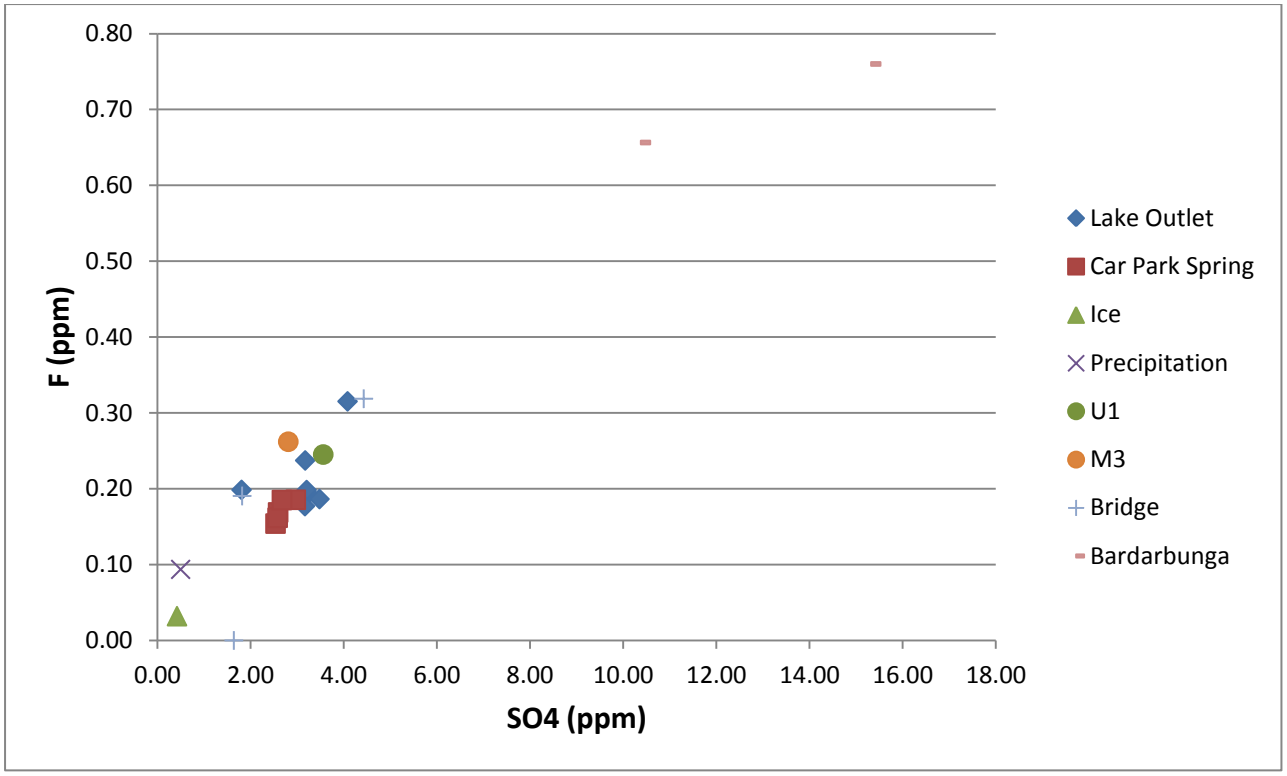

Figure 18: Showing fluorine and sulphate concentrations from all Virkisjökull and Bárðarbunga sites.

5.4 Summary

1. Samples collected from Virkisjökull can be represented as a three way mixing between endmembers of "ice", "precipitation" and "bedrock" sulphate sources. During spring 2015 when very little ice melt occurred, due to unseasonably low temperatures, an apparent binary mixing occurred between precipitation and bedrock. At other times of the year when temperatures are higher, ice melt dominates as an endmember. The governance of this model is prevailing weather conditions which will dictate the relative inputs of ice melt and precipitation into the hydrological system.

2. Samples collected during spring 2015 show a clear distinction by site which is interpreted as representing the relative contact time with the country rock. The car park spring plots closest to the precipitation endmember reflecting its situation as a locally sourced moraine spring. This is in agreement with oxygen-deuterium isotopes which show the car park spring to be a predominantly precipitation fed site with little input from long term residence groundwater. The lake outlet sites and borehole U1 plot towards the bedrock end member. This is interpreted as reflecting the input of glacial meltwater into these sites which has undergone significant contact time with the country rock. Finally, borehole M3 plots between the car park spring and lake outlet. This is interpreted as reflecting its sourcing from a well-mixed aquifer source with very little input from glacial meltwater.

3. Analysis of sulphur isotopes and concentrations coupled with other major chemistry has shown there to be a very weak or non-existent geothermal source operating underneath the Virkisjökull glacier. All but two samples plotted to the left of the coupled SO:CD line suggesting that there was very little extra input of sulphate. This was reinforced by analysis of $SO_4/(SO_4 + Cl)$ ratios which again demonstrated Virkisjökull samples to plot significantly apart from the volcanically influenced Bárðarbunga samples. Finally, analysis of fluorine

concentrations, which can only be derived in significant concentrations from volcanic sources shows a significant disparity between Virkisjökull and Bárðarbunga sites.

Chapter 6: Geochemical Signals of Anoxia

6.1 Introduction

Although sulphur isotopes failed to provide any evidence of a geothermal heat source underneath Virkisjökull, they successfully identified the chemical composition of waters in the catchment being derived from a three way mixing between ice melt, precipitation and bedrock. How great an influence bedrock weathering exerts on the chemistry of the waters is related to their residence time. Therefore, samples that showed more of a bedrock signal should also demonstrate chemical signals of longer residence times. Analysis of oxygen isotopes of sulphate provides a geochemical method to resolve whether conditions of anoxia are present at the time the sulphate was incorporated into the waters. In the absence of any external reducing agents (e.g. geothermal gases) this provides a way of partitioning waters by their relative residence times. However, as demonstrated by Wynn et al. (2015) they can also provide a means of identifying geothermal gases influencing the redox conditions at the glacier bed.

6.2 Geochemical Signals of Anoxia: Results

Samples analysed for SO_4 oxygen isotopes are shown in Figure 19 plotted against their anoxic threshold value. Values range from +8.51‰ (precipitation) to -4.66‰ for borehole U1 sampled during winter 2014. Ice was not measured for sulphate oxygen isotopes due to a lack of barium sulphate precipitate. This is likely a reflection of the low sulphate concentration in this sample. The anoxic-oxic threshold is represented by the dotted line on Figure 19. Only water from sample U1 collected during winter 2014 can be described as anoxic. All other waters plot in the oxic regime. Data can be found in table form in Appendix 1 or on an excel spreadsheet in Appendix 2.

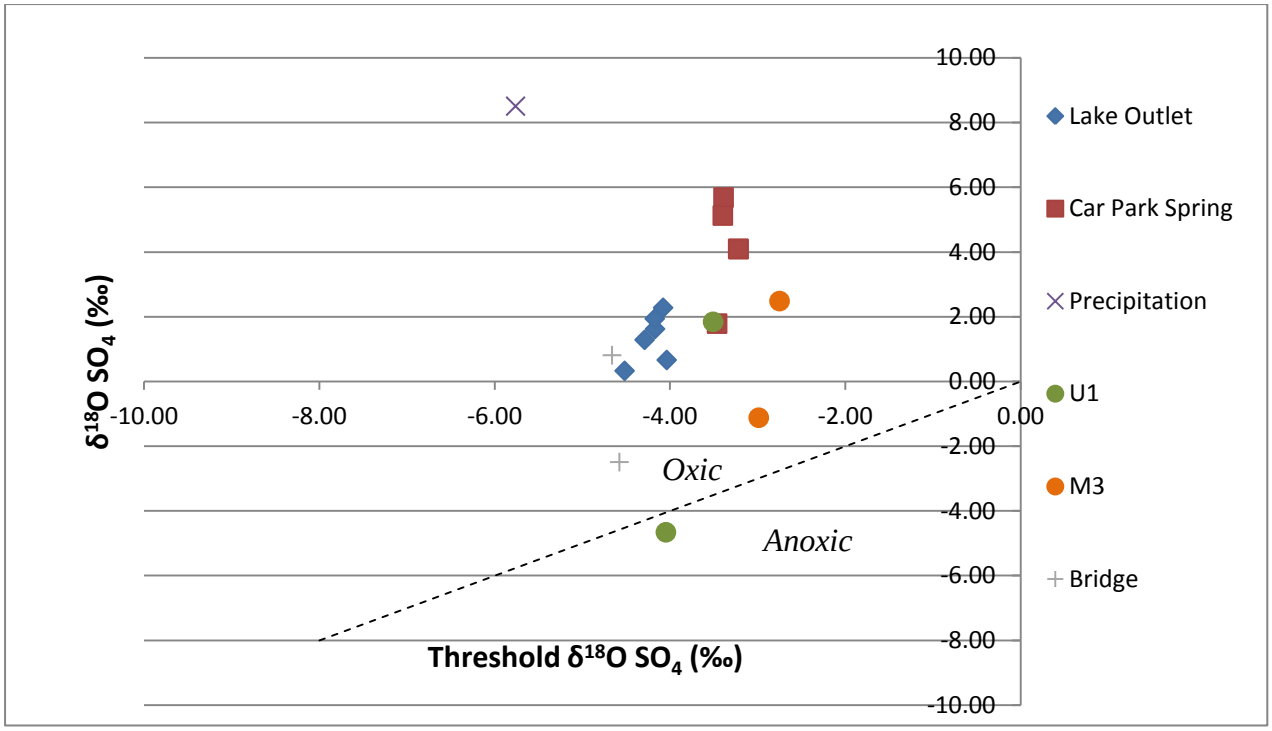

Figure 19: Oxygen isotope composition of sulphate vs the calculated anoxic-oxic threshold value (calculated using technique outlined by Bottrell and Tranter (2002)) for all Virkisjökull samples.

6.3 Geochemical Signals of Anoxia: Discussion

With the exception of U1 (winter 2014) all samples plot in the oxic regime, where oxic implies greater than 75% of oxygen on the sulphate ion are derived from atmospheric oxygen. However, within this there is variability between samples. There appears to be a trend between the car park spring and lake outlet samples such that the latter plot closer to the anoxic/oxic boundary. This suggests that there is a greater proportion of free atmospheric oxygen available to waters in the car park spring than lake outlet. This is most likely a reflection of the relative water-rock contact time of the respective waters. The precipitation derived car park spring will have undergone relatively little contact with the local geology and thus plots closest to the precipitation endmember. Water from the lake outlet will have undergone significant residence times underneath the glacier and thus more oxygen will be used up in water-rock weathering reactions. This agrees with sulphur isotope data that showed glacial derived waters to have a greater affiliation with a bedrock chemical signature.

6.3.1 Variation in Redox Conditions in Groundwaters

There appears to be significant variation in the redox state of groundwaters in the proglacial sandur. Borehole M3 was concluded to be derived from a well-mixed aquifer. Therefore, the seasonal variation in borehole M3 is most likely a reflection of the seasonal variation in groundwater residence time. The one anoxic sample was taken from borehole U1 in winter 2014. This borehole is situated adjacent to the Virkisá river and from oxygen-deuterium analysis it was concluded that this borehole was fed from a mixture of glacial meltwater and local groundwater. Therefore, anoxic waters must be derived from either glacial meltwater or local groundwater. The fact that all samples taken from Virkisá river (bridge and lake outlet) plot in the oxic regime suggest that water of glacial origin is oxic. Therefore, the anoxic source is likely to be derived from local groundwater and unlikely to be geothermally influenced.

6.3.2 Seasonal Variation in Redox Conditions

Figure 20 highlights the variation in the sulphate isotopic composition of all Virkisjökull sites with season. Both spring 2014 and spring 2015 samples appear to plot on a mixing line between precipitation and glacial influenced groundwater. This is suggested to be the result of:

1. Increased water rock contact time downstream from the glacier pulling samples down towards the sulphur bedrock signature of 0‰.
2. Increasing mixing with groundwater that will have undergone significant water rock interaction and thus display a mildly anoxic signature as in U1 (spring 2014).

Alternatively, a mixing between geothermal waters and precipitation would also explain this trend. However, waters that show a similar sulphate oxygen signature to Bárðarbunga have a significantly different sulphur isotope signature. In addition, no mixing with a geothermal source was noted in the analysis of sulphate concentrations (Figure 17), which reinforces the case for the sulphate being derived from a bedrock rather than geothermal source.

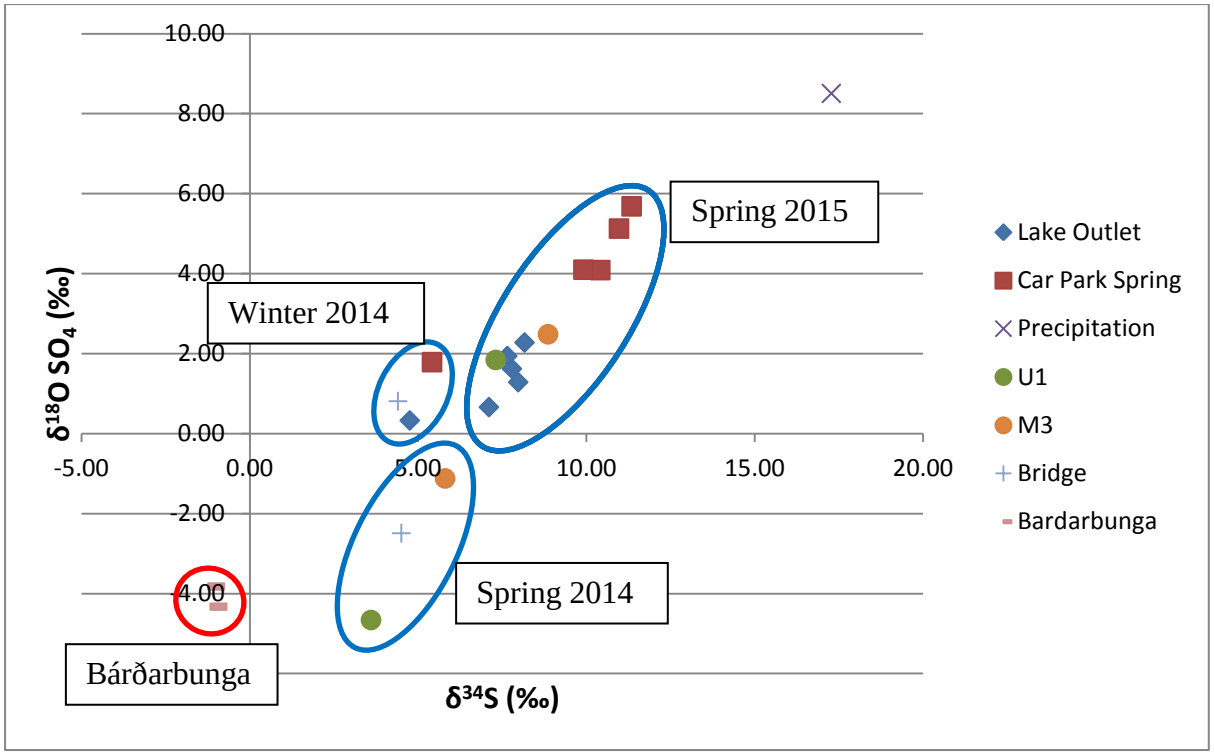

Figure 20: Isotopic composition of all Virkisjökull sites and Bárðarbunga sites. Blue circles highlight when samples were taken at Virkisjökull. Red circle highlights the Bárðarbunga sites.

Winter 2014 samples appear to have a lighter sulphur isotope composition than the spring 2014 samples and thus do not plot on the same mixing line. As discussed in the sulphur chapter, this could be down to a number of factors including anthropogenic emissions, volcanic aerosols or geothermal input. Sulphate oxygen isotope data supports a combination of the first two as the waters are still oxic and therefore it is unlikely that any geothermal gases in significant volumes are interacting with the waters. In addition, the clustering of samples during winter 2014 is not noted during other times of the year, suggesting a common input into each sample site. This is surprising given that the car park spring is predominantly precipitation derived and the bridge and lake outlet are predominately glacial water and groundwater derived. Therefore, any sulphate source causing this similarity must be able to interact with each of these water types. Given that the winter 2014 samples were taken at the

height of the Bárðarbunga eruption it is suggested that volcanic aerosols and ash deposition interacting with the glacier meltwater and precipitation resulted in a general overall decrease in the sulphur isotope composition at each site.

6.4 Seasonal Variations in Redox Conditions

Work on the redox state of glacial meltwaters was first advanced by Tranter et al. (2002b) and Bottrell and Tranter (2002) who demonstrated that conditions of anoxia appear to vary by season. In alpine systems, it was concluded that anoxic conditions prevail in the winter months when the hydrological system becomes isolated from atmospheric oxygen. This is a result of the winter hydrological system in alpine glaciers being composed of a series of sub-glacial cavities that are isolated from the atmosphere. In summer, increased temperatures result in an oxidised and channelized hydrological system whereby sub-glacial water has access to free atmospheric oxygen (Bottrell and Tranter, 2002). This was expanded on by Wynn et al. (2006) who showed the same relationship also operated in polar glaciers and that the transition from anoxic winter conditions to oxic summer conditions was very rapid. In Icelandic glaciers, Wynn et al. (2015) identified seasonality in the redox state of sub-glacial waters but found the opposite relationship than that observed in polar and alpine systems. This inverse alpine relationship was interpreted as the result of the continuous melting of the glacier front during winter due to the temperate climate of Iceland allowing for a well-connected hydrological regime to operate all year round. However, in the summer months melting higher up the glacier tapped into the geothermal fields of the Katla volcanic system which resulted in reducing geothermal gases using up all the free atmospheric oxygen in the sub-glacial hydrological system. Thus anoxic conditions prevailed in the summer.

At Virkisjökull a third case appears to be occurring with oxic conditions all year round. Using the Wynn et al. (2015) model for Icelandic glaciers this would suggest that melting is occurring in all seasons allowing for a well-connected, oxidised hydrological system to be operating. This is in agreement with observations at other Icelandic glaciers (Björnsson and Pálsson, 2008; Wynn et al., 2015). Therefore, the presence of an oxic signal in the summer suggests that reducing geothermal gases are not present in sufficient quantity to cause anoxia

in the sub-glacial environment. Thus, sulphate oxygen isotopes suggest that Virkisjökull has a well-connected sub-glacial hydrological system that is in operation all year round. Furthermore, oxygen isotopes are in agreement with sulphur isotopes and major chemistry data that point towards a weak to non-existent level of sub-glacial geothermal activity.

6.5 Summary

1. All samples except borehole U1 (spring 2014) plot in the oxic regime (Figure 19). Variation in the oxygen isotope signature of the sulphate is interpreted as representing the relative water-rock contact time of the respective samples. This explains why the lake outlet samples plot closer to the anoxic/oxic boundary than the car park spring samples. This is in agreement with sulphur and oxygen-deuterium isotope analysis.

2. There is significant seasonal variation between sites (Figure 20). It is suggested that this is the result of variation in the water-rock contact time of the various sites and seasonal changes in groundwater residence time. A geothermal source was excluded based on the oxic nature of nearly all samples and the difference in $\delta^{34}S$ between the geothermally influenced Bárðarbunga waters and all Virkisjökull samples.

3. Polar and Alpine subglacial waters are known to switch rapidly between oxic conditions in the summer and anoxic conditions in the winter (Wynn et al., 2015). In a geothermally influenced glacier the opposite is found to be true with anoxic conditions in the summer and oxic conditions during the winter (Wynn et al., 2015). Virkisjökull appears to represent a third endmember such that oxic conditions prevail all year round. This is suggested to be the result of the temperate nature of Icelandic glaciers allowing a fully oxidised subglacial hydrological system to operate all year round.

Chapter 7: Noble Gases: Results and Discussion

7.1 Introduction

Oxygen-deuterium isotopes demonstrated how the Virkisjökull catchment is dominated by two endmembers: precipitation fed groundwater and glacial water. This was followed by sulphur isotopes demonstrating the major chemical inputs into the catchment waters to be precipitation, ice melt and bedrock weathering and that this was strongly influenced by weather conditions. Sulphate oxygen isotopes complimented this by identifying the variation in relative water-rock contact time at different sites, which was in agreement with the relative contribution of bedrock weathering described by sulphur isotopes. In addition, a fully oxic, subglacial channelized system was suggested to be in operation all year round at Virkisjökull. The final geochemical tool applied to the Virkisjökull glacier and catchment is the noble gases. Although a relatively new field for glaciologists, their potential is immense. Of particular interest to this study is their ability to distinguish basal ice melt from englacial ice melt (firn) and supraglacial melt. It is expected therefore, that noble gases will be able to not only identify the presence of ice melt but also its stratigraphic origin from within the glacier. This provides a method for further focusing more conservative tracers of geothermal activity as well as the potential to resolve the hydrological pathways of basal ice melt compared to englacial and supraglacial melt. It should be noted that basal ice is not referred to in the strict glaciological sense but as ice below the firn interface.

7.2 Fractionation of Noble Gases in the Cryosphere

Noble gases trapped as air bubbles in glacial ice vary in their concentration stratigraphically through the glacier (Weißbach, 2014). This fractionation is caused by three processes:

1. Gravitational fractionation.
2. Thermal fractionation.
3. Preferentially degassing of neon and argon at firn-ice interface (Huber et al., 2006; Severinghaus and Battle, 2006).

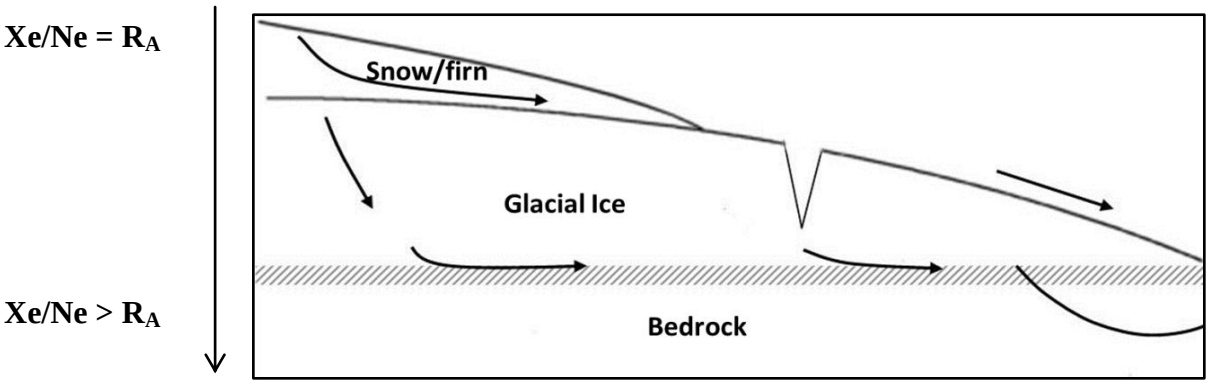

Figure 21: The stratigraphy of noble gases in a glacier. If the atmospheric ratio of Xe/Ne is R_A then it can be inferred that some increase in the Xe/Ne ratio is to be expected down the glacier relative to atmospheric ratios.

Therefore, it is suggested that basal meltwater will have a different noble gas signature compared to supraglacial and englacial (firn) melt. The diurnal and seasonal variation of the atmospheric noble gas concentration is not expected to affect the model suggested here as once the noble gases are enclosed in the firn layer they will be equilibrated with the temperature of the firn and therefore fractionation effects will be occurring from the same inventory of noble gases.

In terms of identifying a geothermal signal, the above model is very appealing given its ability to distinguish surface melt from potentially geothermally derived basal melt. The

above model has been used successfully by Weißbach (2014) as a geochemical signal for Pleistocene ice melt in an Estonian aquifer. However, to the author's knowledge this is the first time such a technique has been applied to a modern glacier to resolve the various components of ice melt in the proglacial sandur. Although not a standalone signal of geothermal activity, noble gases can identify the sites that contain proportionally the greatest volume of basal ice melt and thus give a focus for more standard geochemical signals of geothermal activity (e.g. sulphate and fluorine concentrations).

7.3 Using Noble Gases to Quantify Basal Ice Melt

In order to quantify the relative contribution of basal ice melt, the total concentration of each noble gas must be resolved into its major inputs. These are termed: atmosphere, excess air and basal ice melt. The concentration of noble gases present at equilibrium with the atmosphere in a non-saline water body at low temperatures are taken from Kipfer et al. (2002) and are shown in Table 3.

Table 3: Equilibrium concentrations for Ne, Ar, Kr and Xe. Concentrations were measured at 4°C and at 458m above sea level (Kipfer et al., 2002).

Ne (cm^3 $STPg^{-1}$)	**Ar (cm^3 $STPg^{-1}$)**	**Kr (cm^3 $STPg^{-1}$)**	**Xe (cm^3 $STPg^{-1}$)**
$2.03x10^{-7}$	$4.23x10^{-4}$	$1.03x10^{-7}$	$1.55x10^{-8}$

Therefore, the noble gas concentration of each site, if in equilibrium, should be the concentrations shown in the table above. The fact that all concentrations plot above this value is primarily due to the component termed “excess air.”

7.3.1 Excess Air

Excess air is ubiquitous in groundwaters and is believed to be the result of small pockets of air trapped in the soil and subsurface interacting with recharging waters and causing them to exhibit noble gas concentrations in excess of equilibrium (Kipfer et al., 2002). Although still not fully understood (Aeschbach-Hertig et al., 2000), three major models have been proposed to explain excess air and allow a quantitative analysis of the relative contribution to each noble gas:

1. Unfractionated excess air model (UA) (Heaton and Vogel, 1981)
2. Partial re-equilibrium model (PR) (Stute et al., 1995)
3. Closed equilibrium model (CE) (Aeschbach-Hertig et al., 2000)

Each of these models makes a prediction of the relative input of each noble gas to the excess air component (Figure 22-Figure 24).

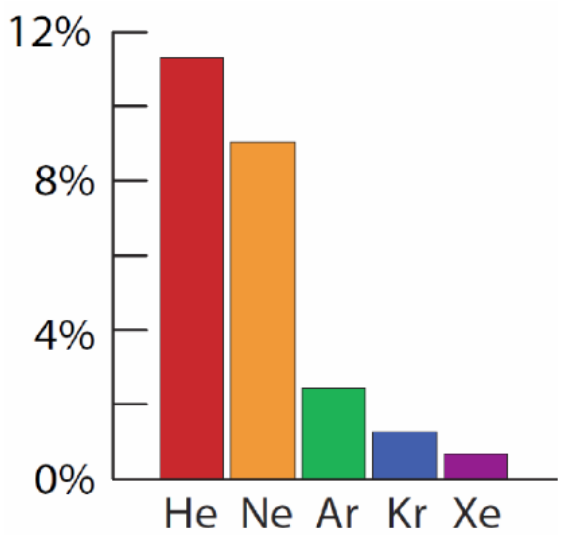

Figure 22: Relative contribution of each noble gas to "excess air" according to the UA model.

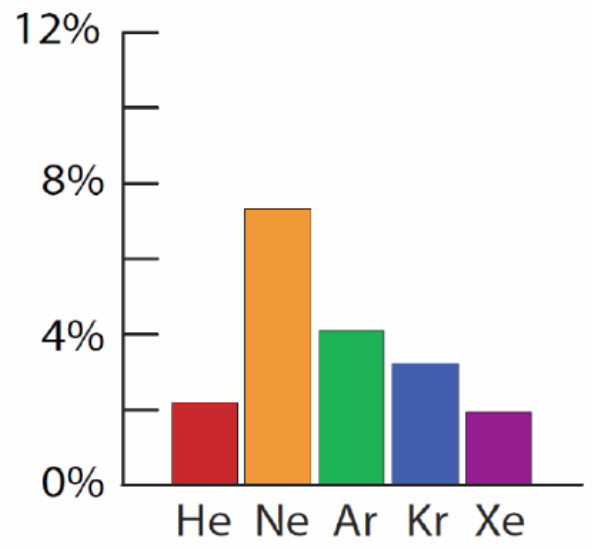

Figure 23: Relative contribution of each noble gas to "excess air" according to the PR model.

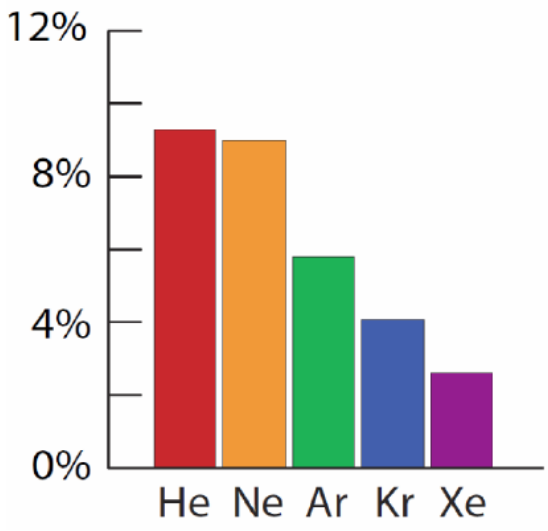

Figure 24: Relative contribution of each noble gas to "excess air" according to the CE model.

In the current literature the CE model is the most commonly employed (Kipfer et al., 2002). Furthermore, Weißbach (2014) used the CE model when calculating the relative input of glacial ice to groundwater and therefore it will be the model used to calculate excess air in this study.

7.3.2 Calculating Basal Ice Melt Contribution

The contribution of glacier ice to the total concentration of a noble gas (X) can be described in the following equation:

$$X_{Ice\ Melt} = X_{Measured} - (X_{Equilibrium} + X_{Excess\ Air}) \qquad \textit{Equation 11}$$

In order to allow an absolute value for excess air to be calculated, neon is assumed to have no ice melt component. To a first order approximation this is valid given that neon is depleted in basal ice given the mechanisms outlined in (Section 7.2) and that excess air has a much larger effect on neon than the heavier noble gases Figure 24. Therefore for neon the equation becomes:

$$Ne_{Excess\ Air} = Ne_{Measured} - Ne_{Equilibrium} \qquad \textit{Equation 12}$$

This value for excess air in neon is calculated as a percentage of the measured value and this allows the excess air component for the heavier noble gases to be scaled proportionally according to the CE model (Figure 24):

$$X_{Excess\ Air} = X(Ne_{Excess\ Air}/Ne_{CE\ Model}) \qquad \textit{Equation 13}$$

Finally, using this scaled value for excess air, Equation 11 can be employed and the relative contribution of ice melt calculated. In order to isolate the percentage contribution of basal ice melt, xenon is used given that it is likely to be the most elevated at the glacier bed compared to atmospheric values according to the mechanisms laid out in Section 7.2.

7.4 Noble Gases: Results

Table 4 shows the measured concentrations of noble gases collected by BGS between September 2011 and April 2013 and the percentage difference between equilibrium and measured concentrations as predicted by the CE model. The majority of concentration measurements show elevated values of neon compared to equilibrium and less of a disparity for the heavier gases. Using these values the contribution of ice melt to this "extra" noble gas was calculated (Table 5). As expected, argon shows very little contribution from ice melt whereas the heavier noble gases do. The ice melt contribution to the inventory of xenon is particularly high although values are variable, ranging from 0% (lake outlet and M3) to 14% (L1). Based on the fractionation effects described in Section 7.2 xenon should show the most elevated values of ice melt. Therefore, proportions of ice melt according to xenon concentrations will form the basis for quantifying ice melt and attempting to resolve a geothermal signal. Raw data can be found in Appendix 2 along with an excel spreadsheet for calculations of basal melt contribution.

Table 4: The measured concentrations of noble gases Ne, Ar, Kr and Xe along with the percentage above equilibrium according to Kipfer et al. (2002). It is postulated that the excess noble gases will be a combination of ice melt and excess air.

Date	Sample site	[Neon] cm^3STP/g	Ne Above Equilibrium (%)	[Argon] cm^3STP/g	Ar Above Equilibrium (%)	[Krypton] cm^3STP/g	Krypton Above Equilibrium (%)	[Xenon] cm^3STP/g	Xenon Above Equilibrium (%)
Sep-11	Lake Outlet	2.84E-07	28.54	4.93E-04	14.17	1.14E-07	9.32	1.75E-08	11.21
Sep-11	Lake Outlet	2.76E-07	26.33	4.74E-04	10.83	1.11E-07	6.89	1.68E-08	7.48
Apr-12	Bridge	2.32E-07	12.56	4.76E-04	11.15	1.17E-07	11.94	1.85E-08	16.00
Apr-12	Bridge	2.28E-07	10.81	4.73E-04	10.64	1.14E-07	9.29	1.83E-08	15.29
Sep-12	U1	2.89E-07	29.64	5.20E-04	18.65	1.25E-07	17.53	1.94E-08	19.98
Sep-12	U2	2.72E-07	25.40	4.86E-04	12.97	1.21E-07	14.87	1.92E-08	19.35
Sep-12	M1	2.86E-07	29.00	4.84E-04	12.64	1.23E-07	16.46	1.99E-08	22.00
Sep-12	M2	3.96E-07	48.77	5.31E-04	20.28	1.17E-07	11.72	1.87E-08	17.08
Sep-12	L1	2.64E-07	23.21	4.91E-04	13.88	1.26E-07	18.05	1.95E-08	20.36
Sep-12	L2	3.61E-07	43.76	5.42E-04	21.89	1.24E-07	17.02	1.92E-08	19.13
Sep-12	L3	2.93E-07	30.63	4.99E-04	15.18	1.25E-07	17.68	1.97E-08	21.38
Apr-13	U1	2.63E-07	22.70	5.03E-04	15.95	1.26E-07	18.19	1.82E-08	14.87
Apr-13	M3	2.42E-07	16.01	4.30E-04	1.56	1.03E-07	-0.15	1.49E-08	-4.06
Apr-13	L3	2.20E-07	7.88	4.47E-04	5.33	1.11E-07	6.96	1.69E-08	8.18

Table 5: Calculated contribution of basal ice melt for Ar, Kr and Xe

Date	Sample site	Ar Ice (%)	Kr Ice (%)	Xe Ice (%)
Sep-11	Lake Outlet	0	0	3
Sep-11	Lake Outlet	0	0	0
Apr-12	Bridge	3	6	12
Apr-12	Bridge	4	4	12
Sep-12	U1	0	4	11
Sep-12	U2	0	4	12
Sep-12	M1	0	4	13
Sep-12	M2	0	0	3
Sep-12	L1	0	8	14
Sep-12	L2	0	0	6
Sep-12	L3	0	4	13
Apr-13	U1	1	8	8
Apr-13	M3	0	0	0
Apr-13	L3	0	3	6

7.5 Noble Gases: Discussion

Results for the contribution of ice melt to each site are shown schematically for both winter and summer in Figure 25 and Figure 26 respectively.

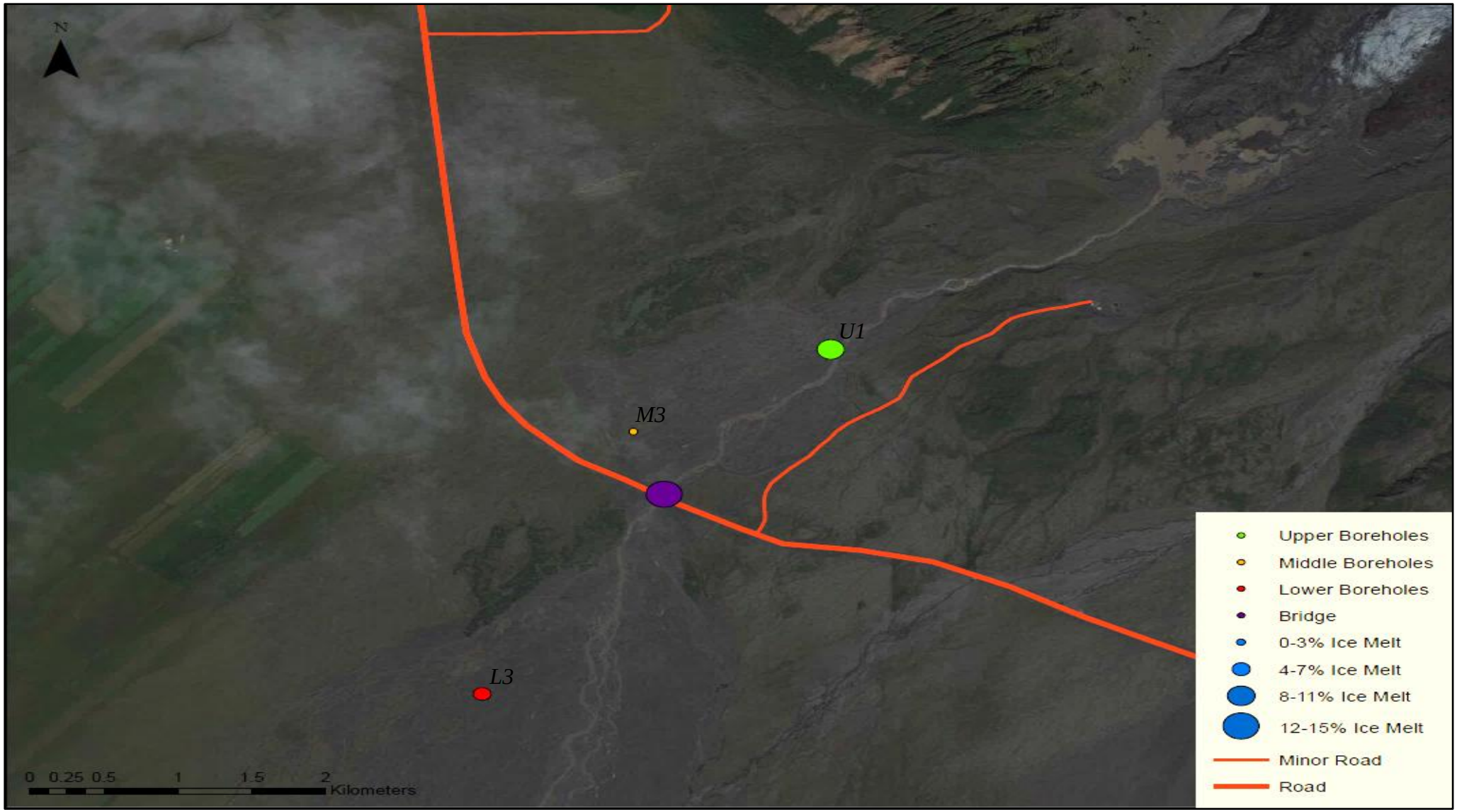

Figure 25: Sites sampled for noble gases during April 2012 and April 2013. Size of circles represents the relative contribution of basal ice melt according to concentrations of Xe.

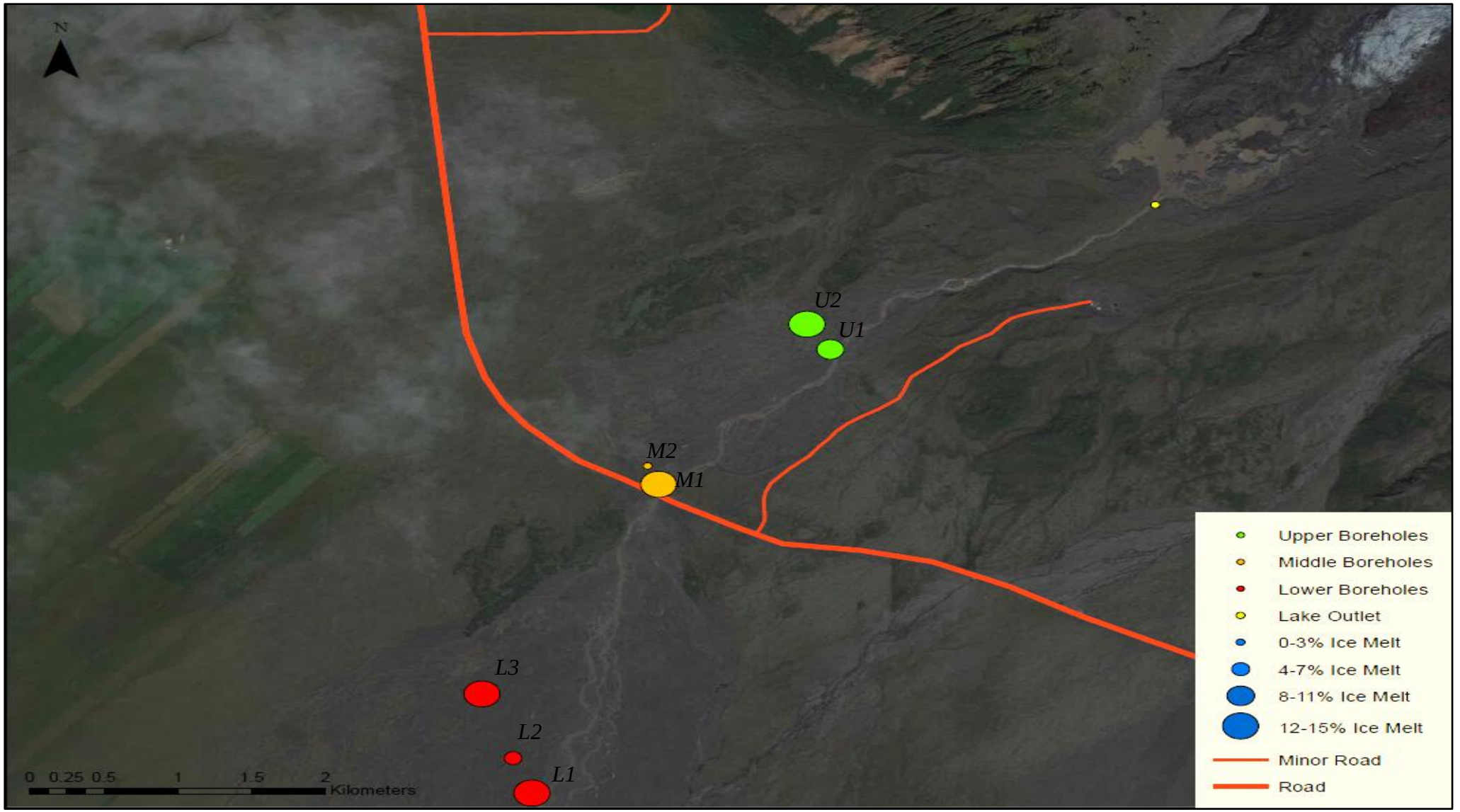

Figure 26: Sites sampled for noble gases during September 2011 and September 2012. Size of circles represents the relative contribution of basal ice melt according to concentrations of Xe.

7.5.1 Contribution of Basal Ice Melt to Proglacial Melt Waters

Proglacial discharge waters (lake outlet and bridge sites) show a distinct seasonal contrast in basal melt input. Given that the bridge site drains from the lake outlet, their hydrological inputs are likely to be similar. The lake outlet was sampled in summer and noble gases suggest that, proportionally, very little basal ice melt was contributing to the lake's noble gas inventory. This seems unlikely given that the glacier drains into the lake itself. However, two reasons are suggested to explain this apparent paradox:

1. In the summer months the major hydrological input into the lake outlet will be surface melt from the winter snowpack and surface runoff from precipitation. This will significantly dilute any noble gas signature of basal ice melt.
2. The permeable nature of the proglacial sandur (MacDonald et al., 2012) will allow for a significant volume of basal meltwater to be transported as groundwater and not mix in the lake itself.

Thus, analysis of noble gases concludes that although the lake has a significant component of ice melt (from water isotope analysis) the relative contribution of basal ice during the summer months is minimal.

The bridge site was measured during winter 2012 and shows a significant component of basal ice melt. Given the reasons outlined above this suggests that surface melt is at a minimum during the winter months and therefore the relative contribution of basal melt is at an annual maximum. The lack of surface melt diluting any basal melt signature stands to reason given the colder temperatures in the winter months. Furthermore, given the distance between the lake outlet and bridge sites (3km) some interaction with glacial groundwater with a basal meltwater component is likely.

Therefore, noble gases have demonstrated that a significant component of basal meltwater is transported by groundwater rather than surface flow. If this is the case then a significant component of glacial meltwater should be observed in many of the borehole sites.

7.5.2 Contribution of Basal Ice Melt to Sandur Groundwater

Groundwater in the proglacial sandur is measured by the three sets of boreholes (Upper, Middle and Lower) which, with one exception, show an input from basal meltwater. Taking each set in turn reveals spatial and seasonal variation in the contribution of basal ice melt.

7.5.2.1 Contribution of Basal Ice Melt to the Upper Boreholes

Water isotopes demonstrated a strong glacial signal for borehole U1 but suggested borehole U2 was predominantly fed by precipitation. However, noble gases indicate that the upper boreholes (U1 and U2) have a significant component of basal ice melt throughout the year. Borehole U1 was measured during both summer and winter and shows more of an input from basal meltwater during the summer. Noble gases also suggest a component of basal meltwater to borehole U2. Water isotope analysis ruled out a large glacial component for this borehole. However, this apparent discrepancy demonstrates the potential power of the noble gas technique in that it cannot only distinguish basal melt from bulk ice melt but can also resolve signals of glacial meltwater that are too dilute for water isotopes to display. Therefore, noble gases suggest a year round flow of groundwater derived from basal melt in the region of the upper boreholes.

7.5.2.2 Contribution of Basal Ice Melt to the Middle Boreholes

The middle boreholes do not show the same similarity as the upper boreholes in terms of basal melt contribution. Borehole M1 shows a significant component of glacier meltwater, most likely reflecting its proximity to the river. Boreholes to the east M2 and M3 show decreasing volumes of basal meltwater with distance from the river with borehole M3 showing no basal melt input at all. This is in agreement with water isotopes which demonstrated that M2 and M3 were most likely derived from a precipitation fed aquifer. However, water isotopes also demonstrated that M1 had minimal glacial input. It is suggested that this is again the result of water isotopes not being able to distinguish a signal of glacial meltwater to the level of detail that the noble gases can. Therefore, noble gas analysis at the middle boreholes suggests that basal glacial meltwater is strongly confined to the area around the river channel in agreement with work done at other glaciers in Iceland (Robinson et al., 2009a).

7.5.2.3 Contribution of Basal Ice Melt to the Lower Boreholes

Finally, lower boreholes all show a contribution of glacial melt regardless of season. Borehole L3 was measured twice and as was observed in the upper boreholes it shows increased basal melt during the summer months. The fact that all lower boreholes show a signal of basal ice melt suggests that it is no longer confined to the main channel. Again, this is in agreement with water isotopes that demonstrated significant variation in the isotopic composition of the lower boreholes, suggesting glacial input. This was put down to the braided nature of the river in the area around the lower boreholes. Furthermore, the river in the vicinity of the lower boreholes has been shown to be seasonally variable in its lateral extent (O'Dochartaigh et al., 2012). Thus, the distribution of glacial meltwater in the region around the lower boreholes will vary with the position of the main river channels.

7.5.3 Signals of Geothermal Activity

Noble gases have provided a way of identifying the proportions of basal ice melt into each site. This does not by itself demonstrate geothermal activity but does give a focus for where more conservative tracers of geothermal activity can be applied. This is done in Figure 27 where concentrations of fluorine which is primarily derived from a volcanic or geothermal source are plotted against basal ice melt contribution.

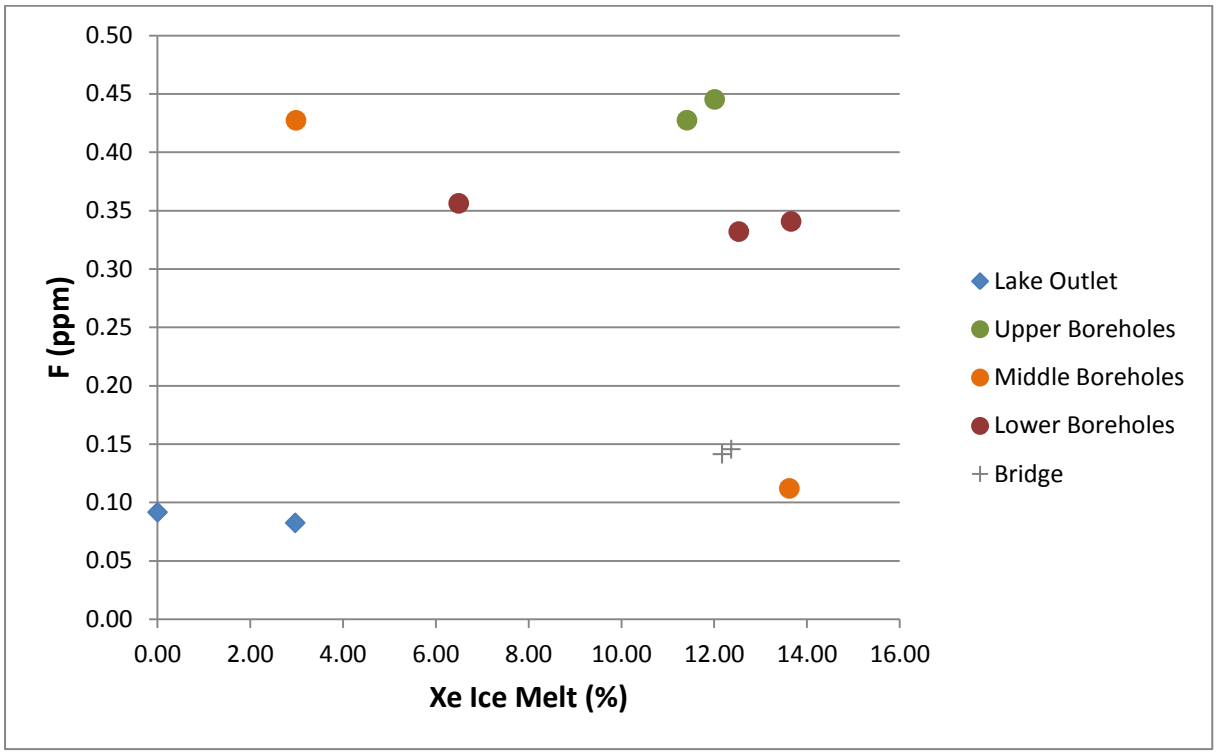

Figure 27: Concentrations of fluorine vs the percentage of basal ice melt according to xenon concentrations.

If a geothermal signal were present, a linear relationship would be expected between basal ice melt contribution and chemical indicators of volcanic activity. Figure 27 demonstrates that this is not the case. On the contrary, the relationship between fluorine concentrations and basal ice melt input suggests that there is no direct link between them. Therefore, using noble gases to isolate sites dominated by basal ice melt would conclude, alongside sulphur and

sulphate oxygen analysis, that there is a very weak to non-existent geothermal regime operating underneath the Virkisjökull glacier.

7.6 Summary

Quantifying basal ice melt from direct measurement has proved elusive to glaciologists with most studies focusing on modelling of airborne or satellite data (Depoorter et al., 2013; Fahnestock et al., 2001; Pritchard et al., 2012). Noble gases however, have demonstrated their potential to do just that and provide a focus for chemical studies of subglacial geothermal activity. The main findings are:

1. Sites that have been measured in summer and winter show an increase in the contribution of basal ice melt during the summer months.
2. Basal ice melt is only a very small contributor to the proglacial lake. Given that oxygen deuterium isotopes pointed at a strong glacial signal in the proglacial lake there must still be a significant component of glacial ice melt. This suggests that the lake is primarily fed by supraglacial runoff, precipitation and melting of englacial ice rather than basal ice melt. However, further sampling would be needed to confirm this.
3. Basal ice melt is extracted from the glacier via groundwater flow as well as surface flow. This explains the lack of ice melt in the proglacial lake and its dominance in the sandur groundwater and the Virkisá river.
4. In agreement with Robinson et al. (2009a) ice melt appears confined to the main channel until the river becomes braided where the spatial extent increases.
5. There appears to be no correlation with distance from the glacier snout and a decreasing ice melt contribution to the groundwater as observed in other glacier groundwater systems (Robinson et al., 2009a). This is in agreement with water isotopes that demonstrated a glacial signal in the lower boreholes but not in the middle boreholes.
6. Alongside sulphur and sulphate oxygen analysis noble gases do not provide any evidence for the presence of a geothermal regime operating underneath the Virkisjökull glacier.

Chapter 8: Conceptual Hydrological Model

Figure 29 summarises the hydrological regime operating in the Virkisjokull catchment. Oxygen-deuterium isotopes revealed a glacial catchment dominant by two endmembers: precipitation and glacial ice melt with ice melt proving to be the dominant input into the proglacial lake and sites directly influenced by the Virkisá River. Oxygen deuterium isotopes demonstrated that north of the bridge, only one borehole (U1) was influenced by bulk glacial meltwater (). This suggests that the Virkisá River is the main mechanism by which ice melt is removed from Virkisjökull. Once the river passes under the bridge it becomes braided and this is reflected in the oxygen-deuterium isotopes recording an ice melt signature in all the lower boreholes. However, the river channels are in a continuous state of change in the region of the lower boreholes and thus depending on their position at the time of sampling an ice melt signature may or may not be picked up. Oxygen-deuterium isotopes also revealed a seasonality in proglacial discharge waters which was interpreted as reflecting increased melting from higher up the glacier during the summer months.

Due to fractionation effects during the compression of firn to ice, noble gases provide a method of quantifying the relative proportion of basal ice melt in the system. This revealed basal ice melt to be a relatively weak component in the lake outlet but making up greater than 10% in both upper boreholes and M1. Although water isotope data suggested both U2 and M1 to be precipitation fed the sensitivity of noble gases to basal ice melt suggests a weak glacial input that was too small to be identified by water isotopes. This suggests that although a large amount of ice melt is removed via the lake as demonstrated by oxygen-deuterium isotopes, a proportion of basal ice melt is removed by groundwater flow and mixes with the Virkisá River further

downstream. In addition, both oxygen-deuterium isotopes and noble gases show the lower boreholes to have a strong glacial melt signature which suggests it is the dominant hydrological input even 8km from the glacier snout. Only the car park spring and boreholes M2 and M3 revealed no glacial input reflecting the confinement of glacial meltwater to the Virkiá River. The middle boreholes (M2 and M3) showed no seasonality in their oxygen-deuterium isotope composition which is interpreted as representing their derivation from a well-mixed precipitation fed aquifer. The car park spring did show a variation in its isotope composition with season which reflects its origin from local precipitation. All sites demonstrated that their chemistry is derived from the mixing of three sources: bedrock weathering, ice melt and precipitation. The variation between sites reflects the difference in water-rock contact time such that glacial meltwaters show an increased bedrock signal compared to precipitation fed sites. Furthermore, the seasonal variation in water chemistry can be explained by the fluctuating inputs of ice melt and precipitation, a process that is entirely governed by the prevailing weather conditions.

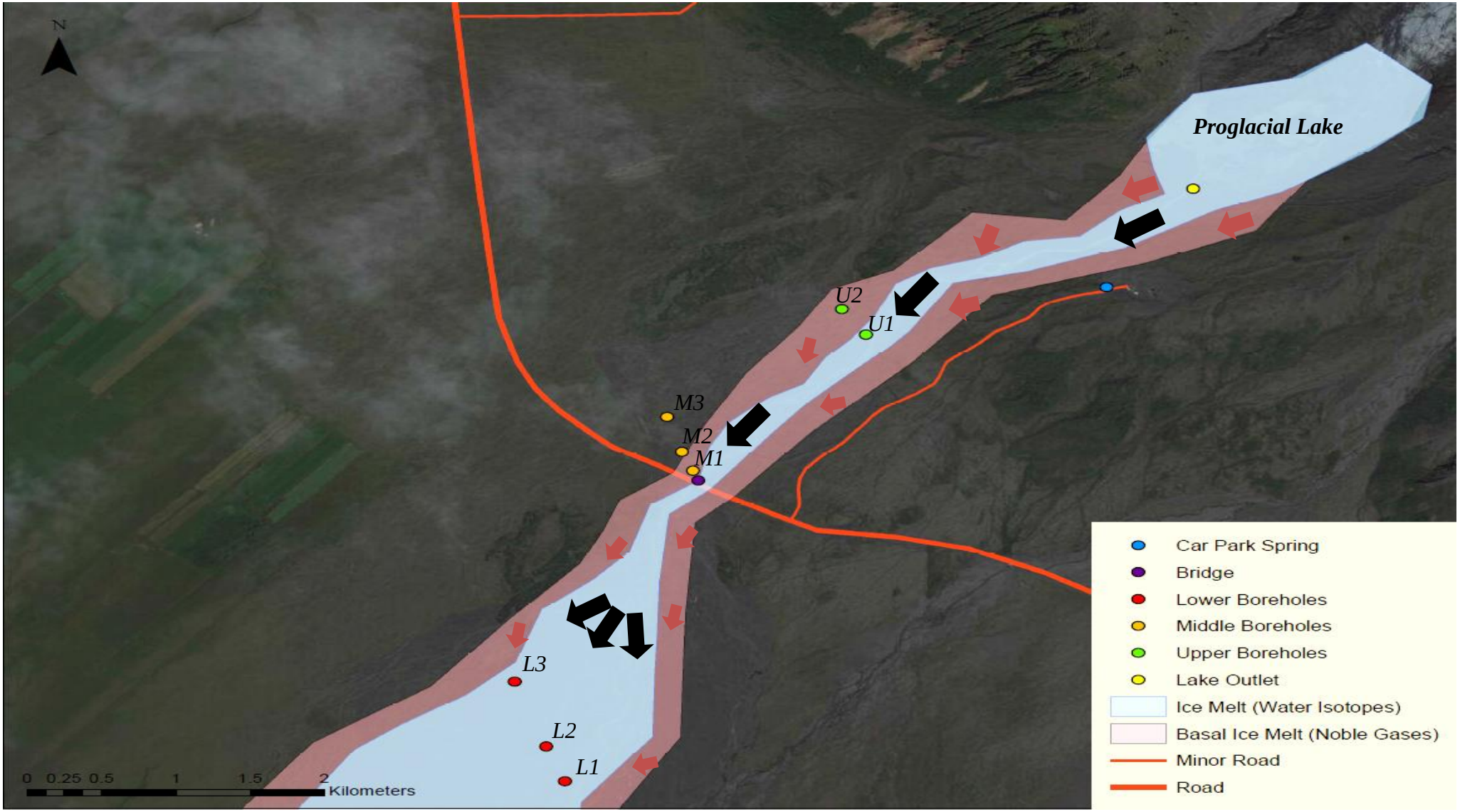

Figure 28: Highlighting approximate distribution of ice melt in the Virkisjökull catchment based on oxygen-deuterium isotopes and the more sensitive noble gases. Arrows indicate the direction of water flow with the size of the arrow representing the relative proportion of ice melt. Red arrows indicate basal ice melt as predicted by noble gases and black arrows indicate bulk ice melt as described by water isotopes.

Chapter 9: Conclusions

Using a suite of chemical analyses alongside field observations, the hydrochemical regime operating in the Virkisjökull region has been investigated with emphasis on resolving any geothermal activity occurring underneath the glacier. Oxygen-deuterium isotopes demonstrated a hydrological system that is dominated by two endmembers: precipitation fed groundwater and glacial meltwater. Seasonality in glacial meltwater samples suggested increased melting from higher up the glacier associated with increased summer temperatures whereas a lack of seasonality in all sandur groundwater sites hinted at the presence of a well-mixed aquifer in the proglacial sandur. Seasonality was observed in moraine groundwaters next to the glacier (car park spring) suggesting that these moraine groundwaters are more sensitive to precipitation. Sulphate isotopes demonstrated that the sulphate signature of waters in the Virkisjökull region is a product of a three way mixing between precipitation, ice melt and bedrock. The dominant input during the spring 2015 campaign was precipitation due to the unseasonably cold temperatures reducing ice melt to a minimum. This mixing process is related directly to the prevailing weather conditions. Analysis of sulphate isotopes suggested that an oxic regime operates in the Virkisjökull glacier all year around. This is contrary to that observed by Wynn et al. (2015) at Sólheimajökull glacier and to the seasonality observed in Alpine and Polar glaciers (Tranter et al., 2002b; Wynn et al., 2006). Finally, noble gases have demonstrated their potential as a geochemical signature of basal ice melt. Analysis of the xenon concentrations provided a tool for quantifying the input of basal ice melt to each site which demonstrated that the majority of basal meltwater is removed via groundwater rather than through the proglacial bulk meltwater channels. This provides a powerful new tool to the field of glaciology that will allow for a more complete understanding of the melting processes in glaciers. Taken together these geochemical tools

revealed no obvious signal of geothermal activity underneath the Virkisjökull glacier and thus it must be concluded that any geothermal activity associated with the Öræfajökull volcanic system is either spatially distinct or exerting a weak to non-existent influence on the hydrochemical regime of the Virkisjökull glacier.

9.1 Future Work

The relationship between glaciers and geothermal activity remains an exciting and understudied area of the earth sciences. To enable further understanding in this area, the following steps should be taken:

1. Measuring helium isotopes in glacial meltwaters remains the most promising candidate for identifying a subglacial geothermal signal. A comparative study between a glacier that is known to be geothermally influenced (e.g. Sólheimajökull) and a glacier that lies above stable continental crust (Alpine or Polar glacier) would determine the validity of the technique.
2. Utilizing noble gases to determine the proportion of basal ice melt in proglacial waters has demonstrated a new and novel technique to understand the distribution of glacial meltwater in the sandur. Furthermore, its ability to distinguish basal from bulk ice melt allows a far more complete model for ice melt to be constructed than previously demonstrated. This technique should be employed at other glaciers in order to develop it further and to increase understanding of basal melting.
3. It is possible that due to Virkisjökull's small size, any geothermal regime is not operating at a large enough spatial extent to affect its meltwater chemistry. Therefore, a similar chemical study of neighbouring glaciers would confirm whether this is the case. Furthermore, an expanded study would allow for a more complete understanding of interactions between the lithosphere and cryosphere in the southern portion of the Vatnajokull ice cap.

References

Aðalgeirsdóttir, G., Jóhannesson, T., Björnsson, H., Pálsson, F., and Sigurðsson, O., 2006, Response of Hofsjökull and southern Vatnajökull, Iceland, to climate change: Journal of Geophysical Research: Earth Surface, v. 111, no. F3, p. F03001.

Aeschbach-Hertig, W., Peeters, F., Beyerle, U., and Kipfer, R., 2000, Palaeotemperature reconstruction from noble gases in ground water taking into account equilibration with entrapped air: Nature, v. 405, no. 6790, p. 1040-1044.

Allen, C., 1980, Icelandic Subglacial Volcanism: Thermal and Physical Studies: The Journal of Geology, v. 88, no. 1, p. 108-117.

Bao, H., Fairchild, I. J., Wynn, P. M., and Spötl, C., 2009, Stretching the Envelope of Past Surface Environments: Neoproterozoic Glacial Lakes from Svalbard: Science, v. 323, no. 5910, p. 119-122.

Bender, M. L., Barnett, B., Dreyfus, G., Jouzel, J., and Porcelli, D., 2008, The contemporary degassing rate of 40Ar from the solid Earth: Proceedings of the National Academy of Sciences of the United States of America, v. 105, no. 24, p. 8232-8237.

Björnsson, H., and Pálsson, F., 2008, Icelandic glaciers: Jökull, no. 58, p. 365–386.

Blankenship, D. D., Bell, R. E., Hodge, S. M., Brozena, J. M., Behrendt, J. C., and Finn, C. A., 1993, Active volcanism beneath the West Antarctic ice sheet and implications for ice-sheet stability: Nature, v. 361, no. 6412, p. 526-529.

Blard, P. H., Lave, J., Farley, K. A., Ramirez, V., Jimenez, N., Martin, L. C. P., Charreau, J., Tibari, B., and Fornari, M., 2014, Progressive glacial retreat in the Southern Altiplano (Uturuncu volcano, 22 degrees S) between 65 and 14 ka constrained by cosmogenic He-3 dating: Quaternary Research, v. 82, no. 1, p. 209-221.

Bottrell, S. H., and Tranter, M., 2002, Sulphide oxidation under partially anoxic conditions at the bed of the Haut Glacier d'Arolla, Switzerland: Hydrological Processes, v. 16, no. 12, p. 2363-2368.

Bourgeois, O., Dauteuil, O., and Van Vliet-Lanoë, B., 1998, Pleistocene subglacial volcanism in Iceland: tectonic implications: Earth and Planetary Science Letters, v. 164, no. 1–2, p. 165-178.

Bradwell, T., 2004, Lichenometric Dating in Southeast Iceland: The Size-Frequency Approach: Geografiska Annaler. Series A, Physical Geography, v. 86, no. 1, p. 31-41.

Bradwell, T., Sigurđsson, O., and Everest, J., 2013, Recent, very rapid retreat of a temperate glacier in SE Iceland: Boreas, v. 42, no. 4, p. 959-973.

Buizert, C., Baggenstos, D., Jiang, W., Purtschert, R., Petrenko, V. V., Lu, Z.-T., Müller, P., Kuhl, T., Lee, J., Severinghaus, J. P., and Brook, E. J., 2014, Radiometric 81Kr dating identifies 120,000-year-old ice at Taylor Glacier, Antarctica: Proceedings of the National Academy of Sciences, v. 111, no. 19, p. 6876-6881.

Cecil, L. D., Green, J. R., Vogt, S., Michel, R., and Cottrell, G., 1998, Isotopic composition of ice cores and meltwater from upper fremont glacier and Galena Creek rock glacier, Wyoming: Geografiska Annaler Series a-Physical Geography, v. 80A, no. 3-4, p. 287-292.

Cerling, T. E., 1990, Dating geomorphologic surfaces using cosmogenic 3He: Quaternary Research, v. 33, no. 2, p. 148-156.

Clark, I., and Fritz, P., 1997, Environmental Isotopes in Hydrogeology, CRC-Press.

Clark, P. U., Dyke, A. S., Shakun, J. D., Carlson, A. E., Clark, J., Wohlfarth, B., Mitrovica, J. X., Hostetler, S. W., and McCabe, A. M., 2009, The Last Glacial Maximum: Science, v. 325, no. 5941, p. 710-714.

Collins, D. N., 1977, Hydrology of an alpine glacier as indicated by the chemical composition of meltwater: Zeitschrift für Gletscherkunde und Glazialgeologie, v. 13, p. 219-238.

Corr, H. F. J., and Vaughan, D. G., 2008, A recent volcanic eruption beneath the West Antarctic ice sheet: Nature Geosci, v. 1, no. 2, p. 122-125.

Craig, H., 1961, Isotopic Variations in Meteoric Waters: Science, v. 133, no. 3465, p. 1702-1703.

Craig, H., and Wiens, R. C., 1996, Gravitational Enrichment of 84Kr/36Ar Ratios in Polar Ice Caps: A Measure of Firn Thickness and Accumulation Temperature: Science, v. 271, no. 5256, p. 1708-1710.

Dansgaard, W., 1964, Stable isotopes in precipitation: Tellus, v. 16, no. 4, p. 436-468.

Depoorter, M. A., Bamber, J. L., Griggs, J. A., Lenaerts, J. T. M., Ligtenberg, S. R. M., van den Broeke, M. R., and Moholdt, G., 2013, Calving fluxes and basal melt rates of Antarctic ice shelves: Nature, v. 502, no. 7469, p. 89-92.

Dyurgerov, M. B., and Meier, M. F., 2000, Twentieth century climate change: Evidence from small glaciers: Proceedings of the National Academy of Sciences of the United States of America, v. 97, no. 4, p. 1406-1411.

Einarsson, T., 1961, Pollenanalytische Untersuchungen fur spat- und postglazialen Klimatgeschichte Islands.: Siinderveroffentichungen des Geologischen Institutes der Universitat Koln., no. 6.

-, 1967, Zu der Ausdehung der weichselzeitlichen vereisung Nordislands.: Sdnderiiffentlichungen des Geologischen Institutes der Universitat Koln, no. 1, p. 167-173.

Einarsson, T., and Albertsson, K. J., 1988, The Glacial History of Iceland During the Past Three Million Years: Philosophical Transactions of the Royal Society B: Biological Sciences, v. 318, no. 1191, p. 637-644.

Elefsen, S., Snorrason, Á., Haraldsson, H., Gislason, S. R., and Kristmannsdóttir, H. K., Real-time monitoring of glacial rivers in Iceland, *in* Proceedings The Extremes of the Extremes: Extraordinary Floods, Reykjavik, 2002, IAHS Publication, p. 199-204.

Everest, J., and Bradwell, T., 2003, Buried glacier ice in southern Iceland and its wider significance: Geomorphology, v. 52, no. 3-4, p. 347-358.

Fahnestock, M., Abdalati, W., Joughin, I., Brozena, J., and Gogineni, P., 2001, High Geothermal Heat Flow, Basal Melt, and the Origin of Rapid Ice Flow in Central Greenland: Science, v. 294, no. 5550, p. 2338-2342.

Foulger, G. R., 2006, Older crust underlies Iceland: Geophysical Journal International, v. 165, no. 2, p. 672-676.

Foulger, G. R., 2010, Plates vs. plumes [electronic resource] : a geological controversy, Hoboken, N.J., Hoboken, N.J. : Wiley-Blackwell.

Froehlich, K., Gibson, J., and Aggarwal, P., Deuterium excess in precipitation and its climatological significance, *in* Proceedings Study of Environmental Change Using Isotope Techniques, Vienna, Austria., 2002, Volume 13, International Atomic Energy Agency, p. 54–65.

Galeczka, I., Oelkers, E. H., and Gislason, S. R., 2014, The chemistry and element fluxes of the July 2011 Múlakvísl and Kaldakvísl glacial floods, Iceland: Journal of Volcanology and Geothermal Research, v. 273, no. 0, p. 41-57.

Geirsdóttir, Á., Hardardóttir, J., and Eiríksson, J., 1997, The Depositional History of the Younger Dryas-Preboreal Búdi Moraines in South-Central Iceland: Arctic and Alpine Research, v. 29, no. 1, p. 13-23.

Geirsdóttir, Á., Miller, G. H., Axford, Y., and Sædís, Ó., 2009, Holocene and latest Pleistocene climate and glacier fluctuations in Iceland: Quaternary Science Reviews, v. 28, no. 21-22, p. 2107-2118.

Gislason, S. R., and Torssander, P., 2006, Response of sulfate concentration and isotope composition in Icelandic rivers to the decline in global atmospheric SO2 emissions into the North Atlantic Region: Environ Sci Technol, v. 40, no. 3, p. 680-686.

GNIP, 2015, Water Isotope System for Data Analysis, Visualization and Electronic Retrieval, Volume 2015.

Gudmundsson, H. J., 1997, A review of the holocene environmental history of Iceland: Quaternary Science Reviews, v. 16, no. 1, p. 81-92.

Guðmundsson, M. T., Larsen, G., Höskuldsson, Á., and Gylfason, Á. G., 2008, Volcanic hazards in Iceland: Jökull, no. 58, p. 251–268.

Gudmundsson, M. T., Sigmundsson, F., and Bjornsson, H., 1997, Ice-volcano interaction of the 1996 Gjalp subglacial eruption, Vatnajokull, Iceland: Nature, v. 389, no. 6654, p. 954-957.

Hardarson, B. S., and Fitton, J. G., 1991, Increased mantle melting beneath Snaefellsjokull volcano during Late Pleistocene deglaciation: Nature, v. 353, no. 6339, p. 62-64.

Headly, M. A., 2008, Krypton and xenon in air trapped in polar ice cores : paleo-atmospheric measurements for estimating past mean ocean temperature and summer snowmelt frequency. Ph.D Thesis University of California, San Diego.

Heaton, T. H. E., and Vogel, J. C., 1981, “Excess air” in groundwater: Journal of Hydrology, v. 50, p. 201-216.

Helmberger, D. V., Wen, L., and Ding, X., 1998, Seismic evidence that the source of the Iceland hotspot lies at the core-mantle boundary: Nature, v. 396, no. 6708, p. 251-255.

Hodson, A., Tranter, M., Gurnell, A., Clark, M., and Hagen, J. O., 2002, The hydrochemistry of Bayelva, a high Arctic proglacial stream in Svalbard: Journal of Hydrology, v. 257, no. 1–4, p. 91-114.

Hodson, A., Tranter, M., and Vatne, G., 2000, Contemporary rates of chemical denudation and atmospheric CO2 sequestration in glacier basins: an Arctic perspective: Earth Surface Processes and Landforms, v. 25, no. 13, p. 1447-1471.

Hoke, L., Lamb, S., Hilton, D. R., and Poreda, R. J., 2000, Southern limit of mantle-derived geothermal helium emissions in Tibet: implications for lithospheric structure: Earth and Planetary Science Letters, v. 180, no. 3–4, p. 297-308.

Huber, C., Beyerle, U., Leuenberger, M., Schwander, J., Kipfer, R., Spahni, R., Severinghaus, J. P., and Weiler, K., 2006, Evidence for molecular size dependent gas fractionation in firn air derived from noble gases, oxygen, and nitrogen measurements: Earth and Planetary Science Letters, v. 243, no. 1–2, p. 61-73.

Huybers, P., and Langmuir, C., 2009, Feedback between deglaciation, volcanism, and atmospheric CO2: Earth and Planetary Science Letters, v. 286, no. 3-4, p. 479-491.

Ingólfsson, Ó., 1985, Late Weichselian Glacial Geology of the Lower Borgarfjördur Region, Western Iceland: a Preliminary Report: Arctic; Vol 38, No 3 (1985): September: 167–260.

Ito, G., Shen, Y., Hirth, G., and Wolfe, C. J., 1999, Mantle flow, melting, and dehydration of the Iceland mantle plume: Earth and Planetary Science Letters, v. 165, no. 1, p. 81-96.

Ito, T., Hamme, R. C., and Emerson, S., 2011, Temporal and spatial variability of noble gas tracers in the North Pacific: Journal of Geophysical Research, v. 116, no. C8.

Jean-Baptiste, P., Petit, J.-R., Lipenkov, V. Y., Raynaud, D., and Barkov, N. I., 2001, Constraints on hydrothermal processes and water exchange in Lake Vostok from helium isotopes: Nature, v. 411, no. 6836, p. 460-462.

Jenkins, K. A., and Bao, H., 2006, Multiple oxygen and sulfur isotope compositions of atmospheric sulfate in Baton Rouge, LA, USA: Atmospheric Environment, v. 40, no. 24, p. 4528-4537.

Jóhannesson, H., and Sæmundsson, K., 1998, Geological map of Iceland: Tectonics.

Jouzel, J., Alley, R. B., Cuffey, K. M., Dansgaard, W., Grootes, P., Hoffmann, G., Johnsen, S. J., Koster, R. D., Peel, D., Shuman, C. A., Stievenard, M., Stuiver, M., and White, J., 1997, Validity of the temperature reconstruction from water isotopes in ice cores: Journal of Geophysical Research: Oceans, v. 102, no. C12, p. 26471-26487.

Kennedy, B. M., and van Soest, M. C., 2007, Flow of Mantle Fluids Through the Ductile Lower Crust: Helium Isotope Trends: Science, v. 318, no. 5855, p. 1433-1436.

Kipfer, R., Aeschbach-Hertig, W., Peeters, F., and Stute, M., 2002, Noble Gases in Lakes and Ground Waters: Reviews in Mineralogy and Geochemistry, v. 47, no. 1, p. 615-700.

Knight, P., 2013, Glaciers, Routledge.

Kristmannsdóttir, H., Gislason, S., Snorrason, Á., Haraldsson, H., Hauksdottir, S., and Gunnarsson, A., Seasonal variation in the chemistry of glacial-fed rivers in Iceland, *in* Proceedings The Extremes of the Extremes: Extraordinary Floods, Reykjavik, 2002a, IAHS Publication, p. 223-229.

Kristmannsdóttir, H., Sigurgeirsson, M., Ármannsson, H., Hjartarson, H., and Ólafsson, M., 2000, Sulfur gas emissions from geothermal power plants in Iceland: Geothermics, v. 29, no. 4–5, p. 525-538.

Kristmannsdóttir, H., Snorrason, Â., Gislason, S., Haraldsson, H., Gunnarsson, A., Hauksdottir, S., and Elefsen, S., Geochemical warning for subglacial eruptions - background and history, *in* Proceedings The Extremes of the Extremes: Extraordinary Floods, Reykjavik, 2002b, IAHS Publication, p. 231-236.

Lawler, D. M., BjÖRnsson, H., and Dolan, M., 1996, Impact of subglacial geothermal activity on meltwater quality in the Jökulsá á Sólheimasandi system, southern Iceland: Hydrological Processes, v. 10, no. 4, p. 557-577.

Lawver, L. A., and Muller, R. D., 1994, Iceland hotspot track: Geology, v. 22, no. 4, p. 311-314.

Lupton, J. E., and Craig, H., 1981, A Major Helium-3 Source at 15{degrees}S on the East Pacific Rise: Science, v. 214, no. 4516, p. 13-18.

MacDonald, A. M., Everest, J. D., Black, A. R., O Dochartaigh, B. E. O., Bonsor, H. C., Darling, W. G., and Gooddy, D., 2012, Glacial meltwater and groundwater interactions : evidence from the Virkisjokull observatory in Iceland, 39th IAH Conference: Niagara Canada.

Maclennan, J., Jull, M., McKenzie, D., Slater, L., and Grönvold, K., 2002, The link between volcanism and deglaciation in Iceland: Geochemistry, Geophysics, Geosystems, v. 3, no. 11, p. 1-25.

Mandeville, C. W., 2010, Sulfur: A Ubiquitous and Useful Tracer in Earth and Planetary Sciences: Elements, v. 6, no. 2, p. 75-80.

McDougall, I., Kristjansson, L., and Saemundsson, K., 1984, Magnetostratigraphy and geochronology of northwest Iceland: Journal of Geophysical Research, v. 89, no. B8, p. 7029.

Moorbath, S., Sigurdsson, H., and Goodwin, R., 1968, KAr ages of the oldest exposed rocks in Iceland: Earth and Planetary Science Letters, v. 4, no. 3, p. 197-205.

Muller, R. A., and MacDonald, G. J., 1997, Glacial Cycles and Astronomical Forcing: Science, v. 277, no. 5323, p. 215-218.

Muntean, J. L., Cline, J. S., Simon, A. C., and Longo, A. A., 2011, Magmatic-hydrothermal origin of Nevada/'s Carlin-type gold deposits: Nature Geosci, v. 4, no. 2, p. 122-127.

Nielsen, H., Pilot, J., Grinenko, L. N., Lein, Y., Smith, J. W., and Pankina, R. G., 1991, Lithospheric Sources of Sulphur, *in* Krouse, H. R., and Grinenko, V. A., eds., Stable isotopes: natural and anthropogenic sulphur in the environment.: New York, SCOPE 43 Wiley, p. 65-132.

O'Dochartaigh, B. E., MacDonald, A. M., Wilson, P. R., and Bonsor, H., 2012, Groundwater investigations at Virkisjokull, Iceland : data report 2012: British Geological Survey.

O'Nions, R. K., and Oxburgh, E. R., 1988, Helium, volatile fluxes and the development of continental crust: Earth and Planetary Science Letters, v. 90, no. 3, p. 331-347.

Oxburgh, E. R., and O'Nions, R. K., 1987, Helium Loss, Tectonics, and the Terrestrial Heat Budget: Science, v. 237, no. 4822, p. 1583-1588.

Pagli, C., and Sigmundsson, F., 2008, Will present day glacier retreat increase volcanic activity? Stress induced by recent glacier retreat and its effect on magmatism at the Vatnajökull ice cap, Iceland: Geophysical Research Letters, v. 35, no. 9.

Petit, J. R., Jouzel, J., Raynaud, D., Barkov, N. I., Barnola, J. M., Basile, I., Bender, M., Chappellaz, J., Davis, M., Delaygue, G., Delmotte, M., Kotlyakov, V. M., Legrand, M., Lipenkov, V. Y., Lorius, C., Pepin, L., Ritz, C., Saltzman, E., and Stievenard, M., 1999, Climate and atmospheric history of the past 420,000 years from the Vostok ice core, Antarctica: Nature, v. 399, no. 6735, p. 429-436.

Petit, J. R., White, J. W. C., Young, N. W., Jouzel, J., and Korotkevich, Y. S., 1991, Deuterium excess in recent Antarctic snow: Journal of Geophysical Research: Atmospheres, v. 96, no. D3, p. 5113-5122.

Pritchard, H. D., Ligtenberg, S. R. M., Fricker, H. A., Vaughan, D. G., van den Broeke, M. R., and Padman, L., 2012, Antarctic ice-sheet loss driven by basal melting of ice shelves: Nature, v. 484, no. 7395, p. 502-505.

Pujol, M., Marty, B., Burgess, R., Turner, G., and Philippot, P., 2013, Argon isotopic composition of Archaean atmosphere probes early Earth geodynamics: Nature, v. 498, no. 7452, p. 87-90.

Rees, C. E., Jenkins, W. J., and Monster, J., 1978, The sulphur isotopic composition of ocean water sulphate: Geochimica et Cosmochimica Acta, v. 42, no. 4, p. 377-381.

Rignot, E., Bamber, J. L., Van Den Broeke, M. R., Davis, C., Li, Y. H., Van De Berg, W. J., and Van Meijgaard, E., 2008, Recent Antarctic ice mass loss from radar interferometry and regional climate modelling: Nature Geoscience, v. 1, no. 2, p. 106-110.

Ritz, S. P., Stocker, T. F., and Severinghaus, J. P., 2011, Noble gases as proxies of mean ocean temperature: sensitivity studies using a climate model of reduced complexity: Quaternary Science Reviews, v. 30, no. 25-26, p. 3728-3741.

Robinson, B. W., and Bottrell, S. H., 1997, Discrimination of sulfur sources in pristine and polluted New Zealand river catchments using stable isotopes: Applied Geochemistry, v. 12, no. 3, p. 305-319.

Robinson, Z. P., Fairchild, I. J., and Arrowsmith, C., 2009a, Stable isotope tracers of shallow groundwater recharge dynamics and mixing within an Icelandic sandur, Skeiðarrasandur., *in* Marks D., Hock R., Lehning M., Hayashi M., and R, G., eds., Hydrology in Mountain Regions: Observations, Processes and Dynamics, Volume 326: Perugia, IAHS, p. 119–125.

Robinson, Z. P., Fairchild, I. J., and Spiro, B., 2009b, The sulphur isotope and hydrochemical characteristics of Skeiðarársandur, Iceland: identification of solute sources and implications for weathering processes: Hydrological Processes, v. 23, no. 15, p. 2212-2224.

Seal, R. R., 2006, Sulfur Isotope Geochemistry of Sulfide Minerals: Reviews in Mineralogy and Geochemistry, v. 61, no. 1, p. 633-677.

Serreze, M. C., Walsh, J. E., Chapin, F. S., Osterkamp, T., Dyurgerov, M., Romanovsky, V., Oechel, W. C., Morison, J., Zhang, T., and Barry, R. G., 2000, Observational evidence of recent change in the northern high-latitude environment: Climatic Change, v. 46, no. 1-2, p. 159-207.

Severinghaus, J. P., and Battle, M. O., 2006, Fractionation of gases in polar ice during bubble close-off: New constraints from firn air Ne, Kr and Xe observations: Earth and Planetary Science Letters, v. 244, p. 474-500.

Sigvaldason, G. E., 1963, Influence of Geothermal Activity on the Chemistry of three Glacier Rivers in Southern Iceland: Jökull, v. 13, p. 10.

Stute, M., Clark, J. F., Schlosser, P., Broecker, W. S., and Bonani, G., 1995, A 30,000 yr Continental Paleotemperature Record Derived from Noble Gases Dissolved in Groundwater from the San Juan Basin, New Mexico: Quaternary Research, v. 43, no. 2, p. 209-220.

Thompson, R. N., 1982, Magmatism of the British Tertiary Volcanic Province: Scottish Journal of Geology, v. 18, no. 1, p. 49-107.

Thordarson, T., and Hoskuldsson, A., 2002, Iceland, Harpenden, Harpenden : Terra.

Torgersen, T., and Jenkins, W. J., 1982, Helium isotopes in geothermal systems: Iceland, The Geysers, Raft River and Steamboat Springs: Geochimica et Cosmochimica Acta, v. 46, no. 5, p. 739-748.

Torssander, P., 1989, Sulfur isotope ratios of Icelandic rocks: Contributions to Mineralogy and Petrology, v. 102, no. 1, p. 18-23.

Tranter, M., Brown, G., Raiswell, R., Sharp, M., and Gurnell, A., 1993, A conceptual model of solute acquisition by Alpine glacial meltwaters: Journal ofGlaciology, v. 39, no. 133.

Tranter, M., Brown, G. H., Hodson, A. J., and Gurnell, A. M., 1996, Hydrochemistry as an indicator of subglacial drainage system structure: A comparison of alpine and sub-polar environments: Hydrological Processes, v. 10, no. 4, p. 541-556.

Tranter, M., Huybrechts, P., Munhoven, G., Sharp, M. J., Brown, G. H., Jones, I. W., Hodson, A. J., Hodgkins, R., and Wadham, J. L., 2002a, Direct effect of ice sheets on terrestrial bicarbonate, sulphate and base cation fluxes during the last glacial cycle: minimal impact on atmospheric CO2 concentrations: Chemical Geology, v. 190, no. 1–4, p. 33-44.

Tranter, M., Sharp, M. J., Brown, G. H., Willis, I. C., Hubbard, B. P., Nielsen, M. K., Smart, C. C., Gordon, S., Tulley, M., and Lamb, H. R., 1997, Variability in the chemical composition of in situ subglacial meltwaters: Hydrological Processes, v. 11, no. 1, p. 59-77.

Tranter, M., Sharp, M. J., Lamb, H. R., Brown, G. H., Hubbard, B. P., and Willis, I. C., 2002b, Geochemical weathering at the bed of Haut Glacier d'Arolla, Switzerland—a new model: Hydrological Processes, v. 16, no. 5, p. 959-993.

Tuffen, H., 2010, How will melting of ice affect volcanic hazards in the twenty-first century?: Philos Trans A Math Phys Eng Sci, v. 368, no. 1919, p. 2535-2558.

Weißbach, T., 2014, Noble gases in palaeogroundwater of glacial origin in the Cambrian - Vendian aquifer system, Estonia. Master's thesis]: Ruprecht-Karls-University, 116 p.

Welhan, J. A., Poredai, R. J., Rison, W., and Craig, H., 1988, Helium isotopes in geothermal and volcanic gases of the western United States, I. Regional variability and magmatic origin: Journal of Volcanology and Geothermal Research, v. 34, no. 3–4, p. 185-199.

Wilson, L., and Head, J. W., 2002, Heat transfer and melting in subglacial basaltic volcanic eruptions: implications for volcanic deposit morphology and meltwater volumes: Geological Society, London, Special Publications, v. 202, no. 1, p. 5-26.

Winckler, G., and Fischer, H., 2006, 30,000 Years of Cosmic Dust in Antarctic Ice: Science, v. 313, no. 5786, p. 491.

Winckler, G., and Severinghaus, J., 2013, Noble Gases in Ice Cores: Indicators of the Earth's Climate History, *in* Burnard, P., ed., The Noble Gases as Geochemical Tracers, Springer Berlin Heidelberg, p. 33-53.

Wolfe, C. J., Th. Bjarnason, I., VanDecar, J. C., and Solomon, S. C., 1997, Seismic structure of the Iceland mantle plume: Nature, v. 385, no. 6613, p. 245-247.

Wynn, P. M., Hodson, A., and Heaton, T., 2006, Chemical and Isotopic Switching within the Subglacial Environment of a High Arctic Glacier: Biogeochemistry, v. 78, no. 2, p. 173-193.

Wynn, P. M., Hodson, A. J., Heaton, T. H. E., and Chenery, S. R., 2007, Nitrate production beneath a High Arctic glacier, Svalbard: Chemical Geology, v. 244, no. 1-2, p. 88-102.

Wynn, P. M., Morrell, D. J., Tuffen, H., Barker, P., Tweed, F. S., and Burns, R., 2015, Seasonal release of anoxic geothermal meltwater from the Katla volcanic system at Sólheimajökull, Iceland: Chemical Geology, v. 396, no. 0, p. 228-238.

Appendix 1

Oxygen-Deuterium Results for Samples measured at Lancaster University

Spring 2014

Sample Code	Sample Site	Day	$\delta^{18}O$ (‰)	δD (‰)
U1	Borehole U1, ~10m from river.	03/05/2014	-10.46	-75.7
M3	Borehole M3, ~500m from river.	03/05/2014	-9.04	-66.4
River	Virkisá river by road bridge	03/05/2014	-11.16	-78.3

Summer 2014

Sample Code	Sample Site	Day	$\delta^{18}O$ (‰)	δD (‰)
Virkisá Road Bridge	Bridge	Unknown	-11.29	-79.40
Virkisá Lake Outflow	Lake Outlet	Unknown	-11.40	-80.20
14 Bar 010203	Bárðarbunga (Upstream from Magma)	Unknown	-12.83	-91.52
14 Bar 060708	Bárðarbunga (Downstream from Magma)	Unknown	-12.96	-92.37
14 Bar 121314	Bárðarbunga (Downstream from Magma)	Unknown	-12.87	-92.48

Winter 2014

Sample Code	Sample Site	Day	$\delta^{18}O$ (‰)	δD (‰)
Bridge	Bridge	12/12/2014	-11.27	-79.16
Sandur Spring	Sandur Spring	12/12/2014	-8.41	-61.95
Car Park Spring	Car Park Spring	12/12/2014	-9.68	-72.41
Lake Outlet	Lake Outlet	12/12/2014	-11.08	-79.14

Spring 2015

Sample Code	Sample Site	Day	$\delta^{18}O$ (‰)	δD (‰)
AMcD-Virkis 1.1	Ice-marginal Spring	26/03/2015	-10.34	-74.88
AMcD-Virkis 1.2	Snowmelt stream	26/03/2015	-10.39	-77.52
AMcD-Virkis 1.3	Lake Outlet	26/03/2015	-10.44	-74.26
AMcD-Virkis 2.1	Main Channel Sandur	27/03/2015	-10.47	-74.30
AMcD-Virkis 2.2	Groundwater Spring Sandur	27/03/2015	-8.75	-63.30
AMcD-Virkis 2.3	Precipitation	27/03/2015	-12.74	-85.16
AMcD-Virkis 3.1	Car Park Spring	28/03/2015	-9.58	-69.59
AMcD-Virkis 3.2	Lagoon Outlet	28/03/2015	-10.50	-74.91
AMcD-Virkis 4.1	Car Park Spring	29/03/2015	-9.59	-68.74
AMcD-Virkis 5.1	U1	30/03/2015	-9.74	-70.41
AMcD-Virkis 5.2	M3	30/03/2015	-8.73	-64.04
AMcD-Virkis 5.3	Car Park Spring	30/03/2015	-9.35	-68.37
AMcD-Virkis 5.4	Lake Outlet	30/03/2015	-10.78	-75.65
AMcD-Virkis 6.1	Glacier Ice	31/03/2015	-10.44	-74.73
AMcD-Virkis 6.2	Lake Outlet	31/03/2015	-10.62	-75.39
AMcD-Virkis 7.1	Lake Outlet	01/04/2015	-10.63	-75.94
AMcD-Virkis 7.2	Car Park Spring	01/04/2015	-9.36	-67.99
AMcD-Sol Bridge 93	Sólheimajökull Bridge	03/04/2015	-9.69	-66.30
AMcD-Sol MZ 93	Sólheimajökull Mixed Zone	03/04/2015	-9.89	-69.26
AMcD-Sol Lagoon Outlet 93	Sólheimajökull Lagoon Outlet	03/04/2015	-10.08	-67.36
AMcD-Sol Bridge 94	Sólheimajökull Bridge	04/04/2015	-10.03	-67.32
AMcD-Sol MZ 94	Sólheimajökull Mixed Zone	04/04/2015	-10.01	-68.41
AMcD-Sol Lagoon Outlet 94	Sólheimajökull Lagoon Outlet	04/04/2015	-10.03	-68.63

Sulphate Isotope Results for Samples measured at Lancaster University

Spring 2014

Sample Code	Sample Site	Day	$\delta^{34}S$ (‰)	SO_4 $\delta^{18}O$ (‰)	$\delta^{18}O$ Threshold (‰)	Anoxic?
U1	Borehole U1, ~10m from river.	03/05/2014	3.6	-4.66	-4.05	YES
M3	Borehole M3, ~500m from river.	03/05/2014	5.8	-1.12	-2.99	NO
River	Virkisá river by road bridge	03/05/2014	4.5	-2.49	-4.58	NO

Summer 2014

Sample Code	Sample Site	Day	$\delta^{34}S$ (‰)	SO_4 $\delta^{18}O$ (‰)	$\delta^{18}O$ Threshold (‰)	Anoxic?
Virkisá Road Bridge	Bridge		5.20		-4.67	NO
Virkisá Lake Outflow	Lake Outlet		5.79		-4.75	NO
14 Bar 010203	Bárðarbunga (Upstream from Magma)		2.47		-5.83	NO
14 Bar 060708	Bárðarbunga (Downstream from Magma)		-1.17	-4.33	-5.93	NO
14 Bar 121314	Bárðarbunga (Downstream from Magma)		-1.24	-3.82	-5.86	NO

Winter 2014

Sample Code	Sample Site	Day	$\delta^{34}S$ (‰)	SO_4 $\delta^{18}O$ (‰)	$\delta^{18}O$ Threshold (‰)	Anoxic?
Bridge	Bridge	12/12/2014	4.40	0.81	-4.66	NO

Sandur Spring	Sandur Spring	12/12/2014	5.90	6.45	-2.51	NO
Car Park Spring	Car Park Spring	12/12/2014	5.41	1.79	-3.46	NO
Lake Outlet	Lake Outlet	12/12/2014	4.75	0.33	-4.52	NO

Spring 2015

Sample Code	Sample Site	Day	$\delta^{34}S$ (‰)	SO_4 $\delta^{18}O$ (‰)	$\delta^{18}O$ Threshold (‰)	Anoxic?
AMcD-Virkis 1.1	Ice-marginal Spring	26/03/2015	10.04	5.08	-3.96	NO
AMcD-Virkis 1.2	Snowmelt stream	26/03/2015	9.81	5.94	-3.99	NO
AMcD-Virkis 1.3	Lake Outlet	26/03/2015	7.10	0.66	-4.04	NO
AMcD-Virkis 2.1	Main Channel Sandur	27/03/2015	8.19	2.48	-4.06	NO
AMcD-Virkis 2.2	Groundwater Spring Sandur	27/03/2015	10.68	6.37	-2.76	NO
AMcD-Virkis 2.3	Precipitation	27/03/2015	17.27	8.51	-5.76	NO
AMcD-Virkis 3.1	Car Park Spring	28/03/2015	11.34	5.68	-3.39	NO
AMcD-Virkis 3.2	Lagoon Outlet	28/03/2015	8.16	2.28	-4.08	NO
AMcD-Virkis 4.1	Car Park Spring	29/03/2015	10.97	5.13	-3.40	NO
AMcD-Virkis 5.1	U1	30/03/2015	7.30	1.84	-3.51	NO
AMcD-Virkis 5.2	M3	30/03/2015	8.86	2.48	-2.75	NO
AMcD-Virkis 5.3	Car Park Spring	30/03/2015	10.41	4.09	-3.22	NO

AMcD-Virkis 5.4	Lake Outlet	30/03/2015	7.97	1.29	-4.29	NO
AMcD-Virkis 6.1	Glacier Ice	31/03/2015	6.43			
AMcD-Virkis 6.2	Lake Outlet	31/03/2015	7.78	1.62	-4.17	NO
AMcD-Virkis 7.1	Lake Outlet	01/04/2015	7.65	1.94	-4.17	NO
AMcD-Virkis 7.2	Car Park Spring	01/04/2015	9.91	4.10	-3.22	NO
AMcD-Sol Bridge 93	Sólheimajökull Bridge	03/04/2015	6.64	0.93	-3.47	NO
AMcD-Sol MZ 93	Sólheimajökull Mixed Zone	03/04/2015	6.36	1.21	-3.63	NO
AMcD-Sol Lagoon Outlet 93	Sólheimajökull Lagoon Outlet	03/04/2015	6.57	1.08	-3.77	NO
AMcD-Sol Bridge 94	Sólheimajökull Bridge	04/04/2015	7.07	1.00	-3.73	NO
AMcD-Sol MZ 94	Sólheimajökull Mixed Zone	04/04/2015	6.25	-0.09	-3.71	NO
AMcD-Sol Lagoon Outlet 94	Sólheimajökull Lagoon Outlet	04/04/2015	6.74	-0.47	-3.73	NO